

INFORMATION TO USERS

This manuscript has been reproduced from the microfilm master. UMI films the text directly from the original or copy submitted. Thus, some thesis and dissertation copies are in typewriter face, while others may be from any type of computer printer.

The quality of this reproduction is dependent upon the quality of the copy submitted. Broken or indistinct print, colored or poor quality illustrations and photographs, print bleedthrough, substandard margins, and improper alignment can adversely affect reproduction.

In the unlikely event that the author did not send UMI a complete manuscript and there are missing pages, these will be noted. Also, if unauthorized copyright material had to be removed, a note will indicate the deletion.

Oversize materials (e.g., maps, drawings, charts) are reproduced by sectioning the original, beginning at the upper left-hand corner and continuing from left to right in equal sections with small overlaps. Each original is also photographed in one exposure and is included in reduced form at the back of the book.

Photographs included in the original manuscript have been reproduced xerographically in this copy. Higher quality 6" x 9" black and white photographic prints are available for any photographs or illustrations appearing in this copy for an additional charge. Contact UMI directly to order.

UMI

A Bell & Howell Information Company
300 North Zeeb Road, Ann Arbor MI 48106-1346 USA
313/761-4700 800/521-0600

A Morphometric and Chemostratigraphic Study of Upper Campanian
Baculitids from Punta San Jose, Baja California

by

David Hunt Backus

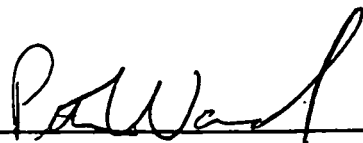
A dissertation submitted in partial fulfillment
of the requirements for the degree of

Doctor of Philosophy

University of Washington

1998

Approved by



Program Authorized
to Offer Degree

GEOLOGICAL SCIENCES

Date

2/23/98

UMI Number: 9826327

**Copyright 1998 by
Backus, David Hunt**

All rights reserved.

**UMI Microform 9826327
Copyright 1998, by UMI Company. All rights reserved.**

**This microform edition is protected against unauthorized
copying under Title 17, United States Code.**

UMI
300 North Zeeb Road
Ann Arbor, MI 48103

© Copyright 1998

David H. Backus

In presenting this dissertation in partial fulfillment of the requirements for the Doctoral degree at the University of Washington, I agree that the Library shall make its copies freely available for inspection. I further agree that extensive copying of this dissertation is allowable only for scholarly purposes, consisting with "fair use" as prescribed in the U.S. Copyright Law. Requests for copying or reproduction of this dissertation may be referred to University Microfilms, 1490 Eisenhower Place, P.O. Box 975, Ann Arbor, MI 48106, to whom the author has granted "the right to reproduce and sell (2) copies of the manuscript in microform and/or (b) printed copies of the manuscript made from microform."

Signature 

Date 2/20/98

University of Washington

Abstract

A Morphometric and Chemostratigraphic Study of Upper Campanian
Baculitids from Punta San Jose, Baja California

by David Hunt Backus

Chair of the Supervisory Committee: Professor Peter D. Ward
Geological Sciences

Campanian/Maastrichtian strata of the Pacific Coast region are difficult to place in a global chronostratigraphic framework. Most sections are tectonically complex, while current biozonal schemes are only regionally useful due to endemism. The rediscovered section at Punta San Jose, Baja California is highly fossiliferous and contains well preserved, biostratigraphically useful forms of the ammonite genus *Baculites*.

A review of species described from North America, in conjunction with a morphometric analysis of material from Punta San Jose and the Sucia Islands, Washington, suggests that morphologic characters used to describe baculitid species are suspect and in need of further study. In particular, 1) ribbing and keeling are not species-specific for baculitids; 2) cross-section form is plastic and can be modified during the repair of shell damage; and 3) simple shape characteristics of the septal suture are insufficient for the identification of Pacific coast species.

$^{87}\text{Sr}/^{86}\text{Sr}$ data place the Punta San Jose section in the Upper Campanian and support the placement of the *Baculites rex* ammonite zone within the upper Campanian by Ward (1978). The Sr isotopic data also place the top of the *Baculites inornatus* zone in the Upper Campanian. The structure of the data indicates that linear modeling of the Sr isotopic curve over long periods of time (>.5-3my) may not be appropriate. In addition, the structure of the Sr data and estimates of depositional rates for comparable shelf sequences suggest a time for deposition of 0.1my to 1.5my for the section. Deposition of this section in a short period of time is implied by the uniformity of the section and the lack of any depositional hiatus.

TABLE OF CONTENTS

	Page
List of Figures.....	iii
List of Tables.....	vi
List of Plates.....	vii
Chapter I: Introduction	1
Regional baculitid species concepts	4
Alternatives to biostratigraphy	6
Sr isotope stratigraphy	6
The section at Punta San Jose.....	10
Problems with species identification	14
Morphological characters of <i>Baculites</i>	14
Evolutionary pattern of baculitids	25
Hypotheses to be tested.....	28
Chapter II: Strontium Isotope Stratigraphy of Punta San Jose	30
Introduction to strontium analysis.....	30
Analytical methods & results	30
Discussion	33
Assessing error	36
Complications due to depositional history.....	38
Correlation with other sections	41
Depositional rates and sampling interval	45
Conclusions	46
Chapter III: Baculitid Morphometrics	48
Introduction to morphometrics	48
Previous morphometric studies	48
Cross-section	49
Cross-section shape analysis	63
Cluster analysis.....	64
Discussion of cluster analysis.....	65
Eigenshape analysis.....	69
Results of eigenshape analysis.....	71
Interpretation of data	75
Punta San Jose	75
Sucia Islands	82
Combined set..	85
Discussion of eigenshape analysis	90
Suture morphology and baculitid systematics	95
Suture analysis	96
Method of measuring suture element	98
Results of suture analysis.....	102
Discussion of suture data	103
Baculitid morphology and biostratigraphy	108
Baculitid evolution at Punta San Jose	110
Chapter IV: Conclusions	112
Cited References	114
Appendix A: Sorted Eigenshape Analysis Score.....	121
Correlations of Punta San Jose data set (n=154).....	121
Covariances of Punta San Jose data set (n=154).....	125
Correlations of Sucia Islands data set (n=37)	129
Covariances of Sucia Islands data set (n=37)	130

Correlations of Combined data set (n=191)	131
Covariances of Combined data set (n=191)	135
Covariances of Rerun Combined data set (n=144)	135
Appendix B: Statistics from Suture Analysis.....	142
Basic Statistics for U/L Suture Element Data	142
Correlation Matrix for U/L Suture Element Ratios.....	145
Frequency Table for Correlation Matrix.....	151

LIST OF FIGURES

Number	Page
1. Pacific Coast Baculitid Biozones	3
2. Western Interior fossil zones	5
3. Campanian magnetic polarity zones	7
4. Sr isotopic curve, Lagerdorf/Kronsmoor, Germany	9
5. Location Map for Punta San Jose	11
6. Section at Punta San Jose	12
7. Nanaimo Group formations	15
8. Examples of sutures from Punta San Jose	16
9. Examples of baculitid sutures	20
10. Sutures and cross-sections attributed to <i>Baculites occidentalis</i>	21
11. Histogram of specimens from Navasink Formation	23
12. Histogram of ribbed and keeled specimens from Punta San Jose	26
13. Sr isotopic data from Punta San Jose	34
14. Sr isotope data from Lagerdorf/Kronsmoor, Germany	37
15. Comparison of fossil zones for Norfolk, Enfland & Lagerdorf/Kronsmoor, Germany	40
16. Sr isotopic data from Norfolk, England	42
17. Sr Isotopic data from Clayton, NJ borehole	43
18. Sr isotopic data for Western Interior fossil zones	44
19. Diagram of cross-section measurements	51
20. Plot of Width/Height data against stratigraphic level at Punta San Jose	52
21. Plot of Max/Mid data against stratigraphic level at Punta San Jose	53
22. Plot of DW/VW data against stratigraphic level at Punta San Jose	54
23. Cross-sections showing the range of variation in shape of venters	55

24.	Cross-sections of four recut specimens	60
25.	Graphic output from Punta San Jose (n=154) cluster analysis	66
26.	Graphic output from Sucia Islands (n=37) cluster analysis	67
27.	Graphic output from Combined set (n=191) cluster analysis	68
28.	Comparison of eigenshapes from eigenshape analyses based on correlations & covariances for the principle data sets	72
29.	Eigenshapes and representative shapes for Punta San Jose data set (n=154)	73
30.	Eigenshapes and representative shapes for Sucia Islands data set (n=37).....	74
31.	Eigenshapes and representative shapes for Combined data set (n=191)	76
32.	Plots of scores from Punta San Jose data set on first 5 eigenvectors	78
33.	Plots of scores from Punta San Jose data set on various combinations of eigenvectors 2-5	79
34.	Plots of scores from the first 5 eigenvectors of the Punta San Jose data set vs. specimen size.....	80
35.	Plots of scores from the first 5 eigenvectors of the Punta San Jose data set vs. stratigraphic level	81
36.	Plots of scores from Sucia Islands data set on first 5 eigenvectors.....	83
37.	Plots of scores from Sucia Islands data set on various combinations of eigenvectors 2-5	84
38.	Plots of scores from Combined data set (n=191) on first 5 eigenvectors	87
39.	Plots of scores from Combined set (n=191) on various combinations of eigenvectors 2-5	88
40.	Eigenshapes and representative shapes from Combined data set (n=144)	89
41.	Plots of scores from Combined data set (n=144) on first 5 eigenvectors.....	91
42.	Plots of scores from rerun Combined set (n=144) on various combinations of eigenvectors 2-5	92
43.	Schematic diagram of U/L suture element showing measurement points	99

44.	Graphic output from cluster analysis of U/L suture element data	104
45.	Examples of U/L suture elements	105
46.	Range chart for Pacific Coast baculitids	109

LIST OF TABLES

Number		Page
1.	Isotopic and chemical data from Punta San Jose	32
2.	Ratios measured for U/L suture element	101

LIST OF PLATES

Number	Page
1a. Lateral view of UWB90036	17
1b. Oral view of UWB90036	17
1c. Lateral view of UWB78836	17
1d. Oral view of UWB78836	17
2a. Lateral view of UWB95130	24
2b. Lateral view of UCB: A/8580-6	24
2c. Lateral view of UWB94629 (small end)	24
2d. Lateral view of UWB94629 (large end)	24
2e. Lateral view of UWB78894	24
3a. Aboral view of UWB78718	56
3b. Ventral view of UWB78718	56
3c. Lateral view of UWB78718	56
3d. Oral view of UWB78718	56
3e. Aboral view of UWB78719	56
3f. Dorsal view of UWB78719	56
3g. Lateral view of UWB78719	56
3h. Oral view of UWB78719	56
4a. Aboral view of UWB95044	58
4b. Lateral view of UWB95044	58
4c. Dorsal view of UWB95044	58
4d. Oral view of UWB 95044	58
4e. Oral view of UWB78927	58
4f. Lateral view of UWB78927	58
4g. Flank view of UWB78927	58

4h.	Aboral view of UWB78927	58
5a.	Dorsal view of UWB90044	59
5b.	Aboral view of UWB90044	59
5c.	Oral view of UWB90044	59
5d.	Lateral view of UWB90044	59
5e.	Lateral view of UWB78722	59
5f.	Oral view of UWB78722	59
5g.	Aboral view of UWB78722	59
5h.	Oral view of UWB95064	59
5i.	Aboral view of UWB95064	59
5j.	Lateral view of UWB95064	59

ACKNOWLEDGMENTS

The work necessary to complete this dissertation could not have been done without the help and support of family, friends and colleagues. I am grateful to Alan Kohn, Bruce Nelson, Jody Bourgeois and Peter Ward for providing guidance, criticism and patience during the completion of this project. In particular, I am in debt to Jody Bourgeois for her thoughtful suggestions and editorial pen during the final stages of writing. I must also thank Peter Ward for allowing me to attempt this project under less than ideal circumstances. In addition, I owe a debt of gratitude to Steve Gould for his early support and encouragement of my academic pursuits.

Collecting trips to Sucia Island and to localities along the Pacific coast of Baja, California were particularly successful due to the enthusiastic participation, connections and keen eye of Bruce Crowley. I am also grateful to Joe Kirschvink for inclusion in, and his support of several trips onto the Baja peninsula.

Thank you to Bruce Nelson, John Rensberger, Hugh O'Brien, and Scott Kuehner for their technical support during the various stages of the Sr analysis. I am also thankful for the support and encouragement of the staff at the Burke Museum. In particular, Ron Eng and Liz Nesbitt have been unfailingly generous with their time and friendship. In addition, I am pleased to know Ken McCloud and Rob Thomas, who have been friends and colleagues in the truest sense during my time at the University of Washington. Special thanks must be given to Leon Sawyko and Carol Franck who provided a welcoming place to stay during my visits to Seattle.

Finally, I am sincerely grateful for the encouragement of my extensive, extended family. In particular, I could never have completed this dissertation without the patience, support, and encouragement of my partner, Wendy Raymond. An additional source of inspiration has been the presence of our son, Caleb, whether he knows it or not.

This project was funded by several grants from the National Science Foundation, The University of Washington's Graduate Research Fund (Geological Sciences), the Conchologists of America, and the Paleontological Society.

CHAPTER 1

INTRODUCTION

Measuring time is an essential component for any investigation of the oceanographic, biological, or tectonic changes recorded in sedimentary sequences. However, upper Cretaceous rock sequences of the Pacific Coast of North America are difficult to place in a global time-stratigraphic framework for several reasons. Biostratigraphic correlation with other Upper Cretaceous sections in the world has been problematic due to the extreme endemism exhibited by macrofauna collected from Pacific Coast sections (Jeletzky, 1971). This complication also stems, in part, from the diversity of depositional environments represented in Upper Cretaceous strata of the region. While ammonites and other mollusks have been used with some success in the correlation of shelf deposits (Jeletzky in Muller and Jeletzky, 1970; Matsumoto and Obata, 1963; Ward, 1978), both benthic and planktonic foraminifera are used for the correlation of deeper water facies (Almgren, 1973; Sliter, 1968, 1973). The rarity of sections that include chronologically useful molluscan and microfossil species together precludes a coherent integration of these zonal schemes. As a result, no single zonal scheme is used for the biostratigraphic subdivision of the Pacific Coast Upper Cretaceous.

Another complication is the lack of continuous marine sections where more than two zones can be found in stratigraphic contact (Ward and Haggart, 1984). Sections of the Nanaimo Group in British Columbia and the Great Valley sequence of California are a mix of marine and non-marine sediments (Muller and Jeletzky, 1970; Ward, 1978b; Ingersoll, 1979), while some parts of the Great Valley Sequence and other sections from the coastal areas of Oregon and California are composed of largely unfossiliferous sequences of turbidites and associated sedimentary facies (e.g. Bourgeois and Dott, 1985; Nilsen and Abbott, 1981; Ingersoll, 1978). Due to the tectonic complexity of the Pacific region, many

of the sections cited above are also structurally complex or were deposited under dynamic tectonic conditions (Bourgeois and Dott, 1985; Brandon and others, 1988; Filmer and Kirschvink, 1989; Ingersoll, 1979).

Early attempts at the biostratigraphic subdivision of the Campanian/Maastrichtian strata of the North Pacific region were made by Matsumoto (1959) for Japanese sections, by Matsumoto (1960) for California, and Jeletzky (*in* Muller and Jeletzky, 1970) for the Nanaimo Group in British Columbia and Washington State. Though Matsumoto (1959b) did not initially use baculitid ammonites in his zonation of Japan, he eventually divided the Japanese Turonian through Maastrichtian strata based on fourteen species of baculitids (Matsumoto and Obata, 1963). Matsumoto (1960) recognized nine species of baculitids from California and used them to subdivide informally the Campanian and Maastrichtian rocks of that area. In contrast, Jeletzky (*in* Muller and Jeletzky, 1970) recognized only three species of *Baculites* from coeval rocks in British Columbia, relying primarily on species of *Inoceramus* and regularly coiled ammonites for his biozones. The Nanaimo Group of British Columbia and Washington State was restudied by Ward (1978), who revised the molluscan biozones for the region and subdivided Santonian through Maastrichtian sections based on baculitids. However, correlation in the Pacific Coast region is hampered by disagreements concerning the ranges reported for some baculitid species (see Fig. 1). Matsumoto (1960) considers *Baculites rex* to be Maastrichtian in age while *B. occidentalis* is restricted to part of the upper Campanian *B. inornatus* zone and found below *B. anceps pacificus*. On the other hand, Ward (1978) considers *B. rex* to be restricted to the upper Campanian, whereas *B. occidentalis* is shown ranging from Upper Campanian into the Maastrichtian and above both *B. anceps pacificus* and *B. rex* based on his study of baculitids from the Vancouver Island area.

International Stages	California Matsumoto, 1960	Vancouver Island Region Ward, 1978	
Maastrichtian	<i>B. rex</i>	<i>Eubaculites ootacodensis</i>	not present
		<i>B. columna</i>	
		<i>B. lomaensis</i>	
Campanian	<i>B. inornatus</i>	<i>B. anceps pacificus</i>	<i>B. occidentalis</i>
		<i>B. occidentalis</i>	<i>B. rex</i> <i>B. anceps pacificus</i>
	<i>B. chicoensis</i>	<i>B. inornatus</i>	<i>B. chicoensis</i>

Figure 1. Ranges of baculitids in California and the Nanaimo Group (in part, after Ward, 1978).

REGIONAL BACULITID SPECIES CONCEPTS

The use of baculitids as biostratigraphic indicators is not unique to the North Pacific region. These ammonites are also preserved in Turonian to Maastrichtian rocks of the Western Interior (Cobban, 1993), Gulf Coast and Mid-Atlantic sections of the United States (Cobban, 1974; Cobban and Kennedy, 1992a, 1993; Kennedy and Cobban, 1993a, 1993b, 1993c), sections in South Africa (Klinger and Kennedy, 1997), and in Tethyan sections of Europe (Kennedy, 1986; Ward, 1988, 1990). In particular, baculitids are used extensively for biostratigraphic zonation in U.S. Western Interior sections.

However, the contrast in the number and duration of baculitid zones used for the Western Interior region and the Pacific Coast region is striking. Species of baculitids described from Western Interior sections have short stratigraphic ranges and are the basis for eighteen of twenty-six biozones for Campanian and Lower Maastrichtian rocks (Kennedy and others, 1992)(see Fig. 2), whereas Pacific Coast baculitid zones for the same period of time are based on only five to seven species (Ward, 1978b)(see Fig. 1). This difference in zonal schemes for the two regions suggests several possible scenarios. These are: 1) the ranges of baculitid species as shown currently for each region are real; 2) baculitid species have short ranges implying that zonal schemes used for the Pacific Coast region overestimate the species ranges and contain large hiatuses in time; and, 3) that baculitid species in the Western Interior region are oversplit relative to those species described from the Pacific Coast region.

The chronostratigraphic problems of the Pacific Coast region described above can be resolved either by improving the concepts used to identify chronostratigraphically useful species or by testing existing zonal schemes using other chronostratigraphic methods.

<p>Maastrichtian (part)</p>	<p><i>Baculites clinolobatus</i> <i>Baculites grandis</i> <i>Baculites baculus</i> <i>Baculites eliasi</i></p>
<p>upper Campanian</p>	<p><i>Baculites jenseni</i> <i>Baculites reesidei</i> <i>Baculites cuneatus</i> <i>Baculites compressus</i> <i>Didymoceras cheyennense</i> <i>Exiteloceras jenneyi</i> <i>Didymoceras stevensoni</i> <i>Didymoceras nebrascense</i></p>
<p>middle Campanian</p>	<p><i>Baculites scotti</i> <i>Baculites reduncus</i> <i>Baculites gregoryensis</i> <i>Baculites perplexus</i> <i>Baculites</i> <i>Baculites asperiformis</i> <i>Baculites maclearni</i> <i>Baculites obtusus</i></p>
<p>lower Campanian</p>	<p><i>Baculites</i> sp. (weak flank ribs) <i>Baculites</i> sp. (smooth) <i>Scaphites hippocrepis</i> III <i>Scaphites hippocrepis</i> II <i>Scaphites hippocrepis</i> I <i>Scaphites leei</i> III</p>

Figure 2. Western Interior fossil zones (after Cobban and Kennedy, 1992).

ALTERNATIVES TO BIOSTRATIGRAPHY

Until recently, only a limited amount of data from methods other than biostratigraphic zonation has been produced for the Pacific Coast region. Ward and others (1983) identified magnetic anomaly 33-34 at the Santonian/Campanian boundary in sediments of the Great Valley sequence containing *Baculites chicaoensis* (see Figs. 1 and 3). Bannon and others (1991) identified anomaly 32R associated with rare macrofauna of the Campanian/Maastrichtian boundary in submarine fan sequences of the Point Loma Formation in the San Diego area. The macrofauna included specimens of *Baculites occidentalis*, *B. rex* and *B. lomaensis*. The presence of *B. rex* in the fauna associated with polarity zone 32r also supports the idea that the range of this species is upper Campanian in part. Most recently, Ward and others (1997) have found magnetic anomalies on Texada Island and Hornby Island. These localities are found on the eastern margin of the Nanaimo Basin, and appear to correlate with magnetochrons 33r through 32r based on the presence of *Baculites chicaoensis* on Texada Island and *B. occidentalis* on Hornby Island (Ward, 1978a).

Sr ISOTOPE STRATIGRAPHY

An alternative method to biostratigraphic and magnetostratigraphic correlation is the use of chemostratigraphy, particularly Sr isotopic data. The evolution of Late Cretaceous seawater $^{87}\text{Sr}/^{86}\text{Sr}$ has been investigated from many regions (Nelson and others, 1991; MacArthur and others, 1993, 1994; 1995; Barrera, 1994; Huber and others, 1995; Sugarman and others, 1995; Howarth and MacArthur, 1997; Vanhof and Smit, 1997). In general, the Sr isotope data systematically increase in $^{87}\text{Sr}/^{86}\text{Sr}$ values (0.70743 to 0.70785) through Campanian/Maastrichtian time (MacArthur and others, 1993; Huber and others, 1995; Vanhof and Smit, 1997). The rate of change in $^{87}\text{Sr}/^{86}\text{Sr}$ values is

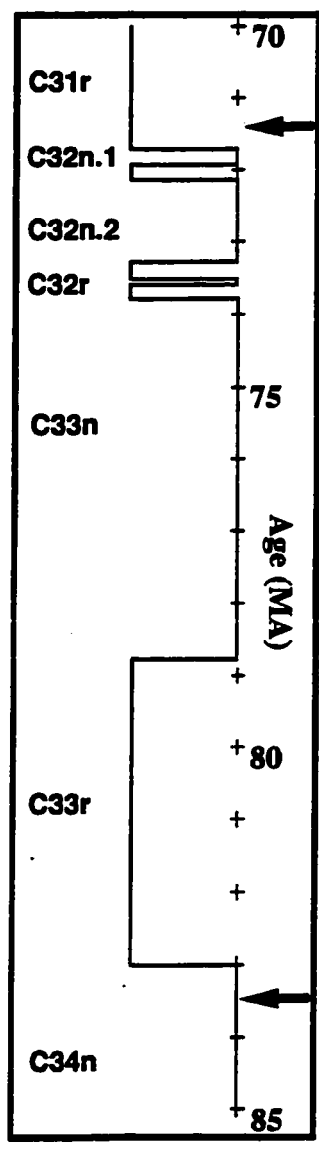


Figure 3. Geomagnetic polarity chrons for upper Santonian through lower Maastrichtian. Arrows mark Santonian/Campanian (lower) and Campanian/Maastrichtian (upper) boundaries (modified from Hicks and others, 1995). Stage boundaries from Obradovich (1993).

approximately 2.6×10^{-5} /my for the Campanian and 1.6×10^{-5} /my for the Maastrichtian (see Fig. 4).

Efforts more specific to the late Campanian and early Maastrichtian include the standard curve established by McArthur and others (1993) for European Boreal sections at Lagerdorf /Kronsmoor, Germany, which is calibrated against both macrofossil and microfossil biostratigraphy. A second curve at Norfolk, England, has also been produced but from data that are less precisely calibrated by biostratigraphy (McArthur and others, 1995). From the US Western Interior, MacArthur and others (1994) have produced a limited amount of Sr isotope data, which are calibrated against the well-established ammonite sequence of that region. Sugarman and others (1995) have described two different curves. The first was established for the New Jersey coastal plain using data primarily from a borehole in Clayton, NJ. This curve is calibrated against local macrofossil and microfossil biostratigraphy. The second curve is from borehole 525a in the southeast Atlantic, calibrated using nannofossil and microfossil biostratigraphy as well as magnetic polarity data from Chave (1984).

In addition, there have been attempts at calibrating $^{87}\text{Sr}/^{86}\text{Sr}$ values with numerical age. MacArthur and others (1993, 1994) have used $^{87}\text{Sr}/^{86}\text{Sr}$ values from the Western Interior to connect $^{39}\text{Ar}/^{40}\text{Ar}$ dates from bentonites associated with ammonite zones of the Western Interior to the well-defined Sr isotopic curve from Lagerdorf/Kroonsmor, Germany. A second attempt by Sugarman and others (1995) uses numerical age assignments from Cande and Kent (1992) for the chronozones of hole 525a. The age determinations for the chronozone boundaries are used as tie points to calibrate the Sr isotope curve of Sugarman and others (1995) from the Atlantic coastal plain of New Jersey. Most recently MacArthur and Howarth (1997) have compiled the data from all available curves and produced a table that can be used to assign a numerical age to single Sr isotopic measurements with varying degrees of confidence.

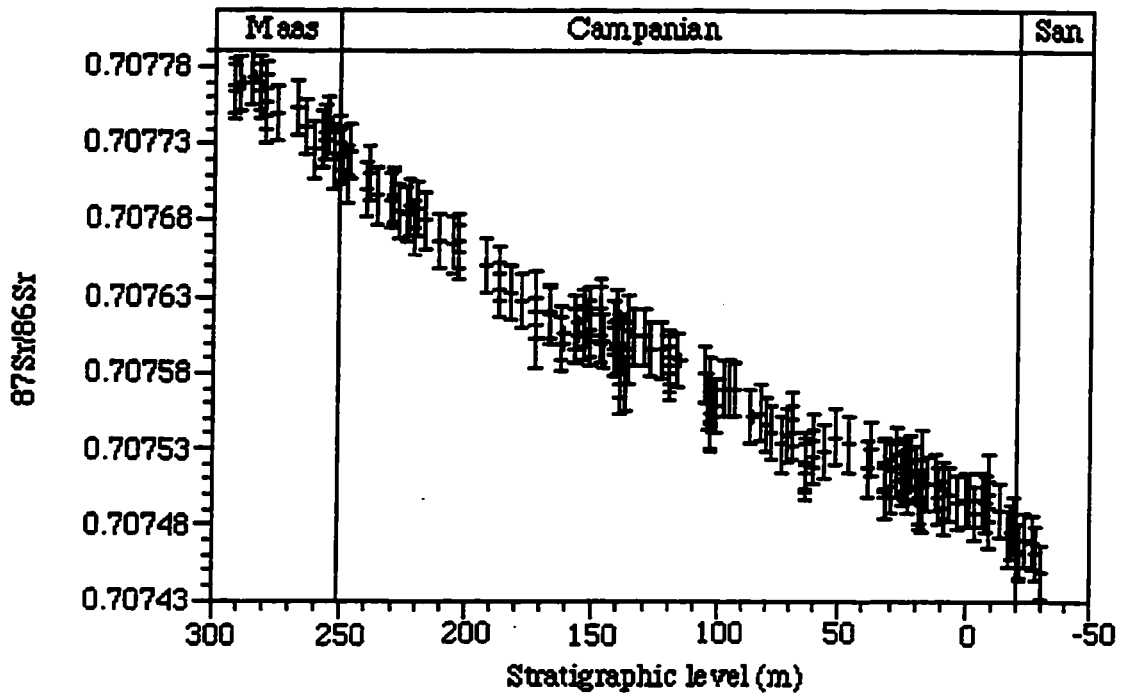


Figure 4. Sr isotopic curve for upper Santonian through lower Maastrichtian (after MacArthur and others, 1993)

The availability of this growing collection of Sr isotope data suggests the possibility of connecting sections from the Pacific Coast region into a worldwide Upper Cretaceous chronostratigraphic framework. However, there are currently no such data for west coast strata, due to the poor quality of shell material available from most west coast sections, and also to the relative newness of the technique. Recently rediscovered Upper Cretaceous sections from the Baja peninsula provide an opportunity to investigate some of the biostratigraphic and chronostratigraphic problems described above.

THE SECTION AT PUNTA SAN JOSE

The Rosario Group is a series of non-marine and marine facies exposed extensively along the Pacific Coast of Baja California and thought to represent most of the upper Campanian and perhaps all of the Maastrichtian (Gastil and others, 1975). In particular, the section at Punta San Jose (see Fig. 5) is highly fossiliferous, containing hundreds of well preserved ammonites, principally the genus *Baculites*.

The fossiliferous portion of the section at Punta San Jose is a well exposed 86m thick unit of greenish to dark-gray, concretionary, laminated to heavily bioturbated, sandy siltstones (see Fig. 6). Concretionary layers (10-40cm) are scattered throughout the sections. Individual (<1-10cm) thick beds of fine- to medium-grained sandstone are also relatively common as are armored mudballs and pebbles of crystalline rock. Scour-and-fill structures with rip-up clasts and shell debris are also relatively common. The section dips gently (generally <10°) to the west and unconformably overlies deformed volcanics and volcanoclastics of the mid-Cretaceous Alisitos Formation (Gastil and others, 1975). Locally, the Rosario Group is in turn unconformably overlain by Quaternary conglomerate. Local paleomagnetic data suggest that the Punta San Jose area has been transported ~1200km north and rotated about 30° clockwise since the Cretaceous (Filmer and Kirschvink, 1989).

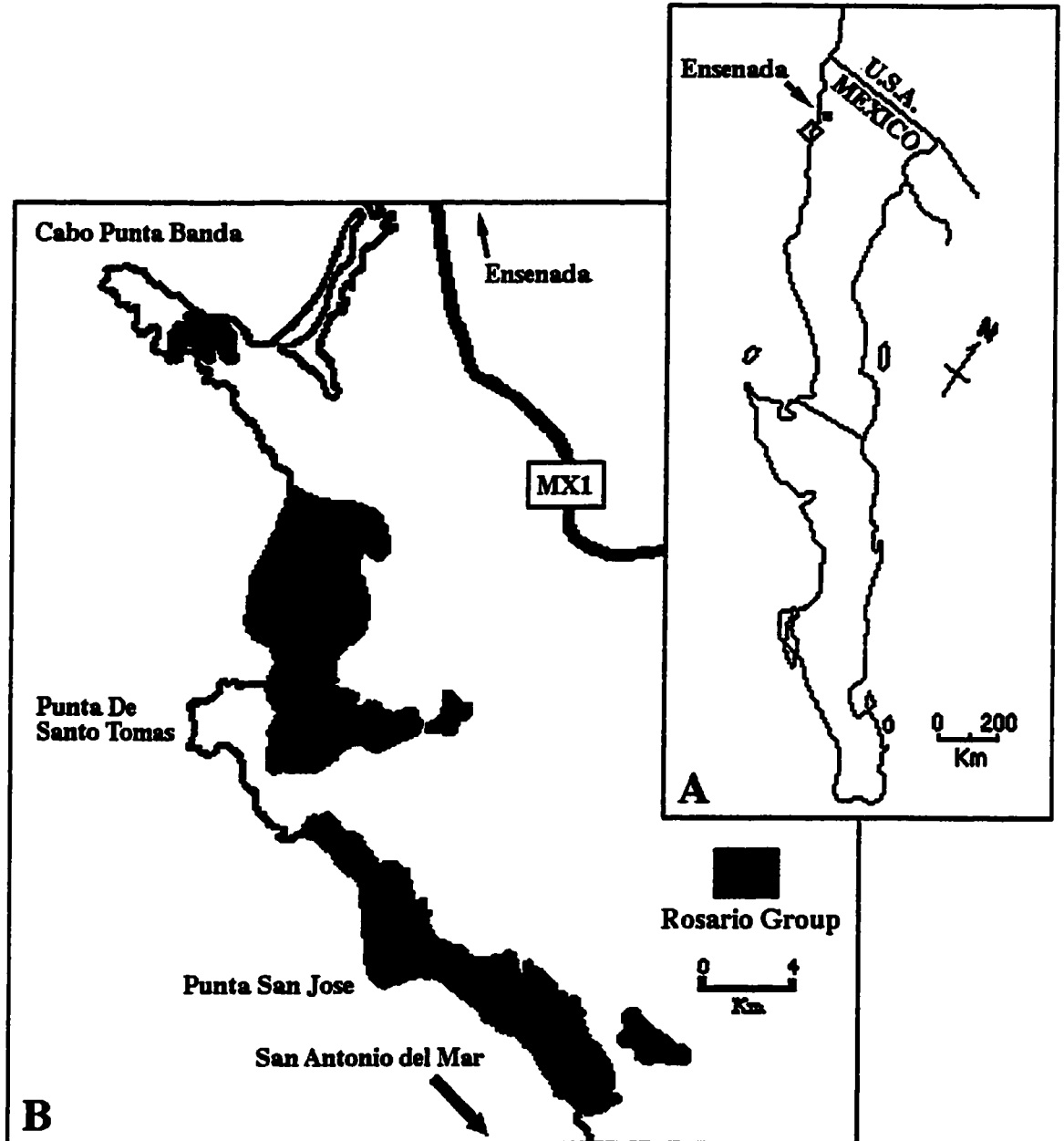


Figure 5a. Map of the Baja California Peninsula; **5b.** Blow-up of the area south of Ensenada showing the Rosario Group and the locality at Punta San Jose. (after Gastil and others, 1975)

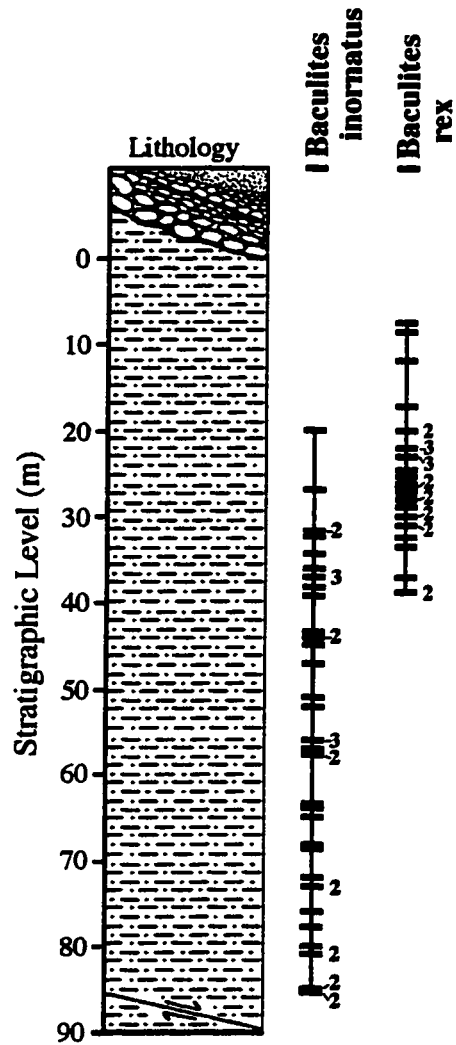


Figure 6. Diagram of the section at Punta San Jose with ranges of baculitid species.

Recent collections, now repositied at the University of Washington, of ammonites from the section at Punta San Jose currently include specimens that can be assigned to the species *Baculites inornatus* and *B. rex*. More than four hundred and fifty fragments of well preserved baculitids have been collected from Punta San Jose. In many of these specimens, the shell is composed of aragonite.

The possibility that Sr isotopic data of good quality could be obtained from material collected at Punta San Jose was suggested by previous work at this locality (Filmer and Kirschvink, 1989; Weiner and Lowenstam, 1980). Large specimens identified as *B. inornatus* and collected from this section were used by Weiner and Lowenstam (1980) in their study of diagenesis in the organic and inorganic fractions of fossil and recent molluscan shell material. They concluded that the inorganic fraction of the baculitid shell material collected from Punta San Jose was composed of original aragonite despite the partial degradation of the organic fraction.

This same site was also sampled by Filmer and Kirschvink (1989) for their paleomagnetic study of the Baja Peninsula terrain. They found no evidence for chemoremnant or thermoremnant magnetic overprints in the sediments at Punta San Jose. The unaltered nature of the sediments at Punta San Jose and the high quality of preservation for shell material suggest that a reliable strontium isotopic signal can be produced from this section

The potential high quality of aragonitic shell material at Punta San Jose as well as the presence at that locality of biostratigraphically interesting baculitid species (*Baculites inornatus* and *B. rex*) presents a rare opportunity to study some of the chronostratigraphic problems of the Pacific Coast region. Also, the extensive collections from Punta San Jose provide an opportunity to study a transition zone between baculitid species. This is the first time that a biostratigraphic study of this type has been possible in the Pacific Coast region.

In addition, the combination of biostratigraphic and chemostratigraphic information available at Punta San Jose is unknown from any other location where baculitids are found.

In particular, there is no other place where rocks containing *Baculites inornatus* and *B. rex* are found in stratigraphic contact. The stratigraphic relationship between these two species is based on their common occurrence in the Cedar District Formation of the Vancouver Island region (see Fig. 7). However, although the Cedar Formation is found on several islands in the Vancouver Island region (see Ward, 1978), in no location are both species found together.

PROBLEMS WITH SPECIES IDENTIFICATION

Sorting the collections from Punta San Jose into distinct species or forms using current descriptions for species of the Pacific Coast region is problematic. While there are individual specimens that conform closely to described forms, it is difficult to group most individuals systematically into discrete species or forms with high confidence using current species descriptions. For example UWB90036 is considered here to be a very large specimen of *Baculites inornatus* based on suture pattern and cross-section (see Fig. 8b; Plate 1a, b), whereas UWB78836 belongs to the species *Baculites rex* (see Fig. 8; Plate 1c, d). The type section for the species *Baculites inornatus* is located on Sucia Island, in the Vancouver Island region. A review of specimens collected from this locality and housed at the University of Washington Burke Museum also suggests that there is significant variation in the morphology for a single species.

MORPHOLOGICAL CHARACTERISTICS OF *BACULITES*

In order to identify the primary morphologic characters used to subdivide baculitids, a review of the described species from the Campanian/Maastrichtian of the Pacific Coast (Anderson, 1958; Matsumoto, 1960; Matsumoto and Obata, 1963; Meek,

International Standard	Formation	Baculitids
MAESTRICHTIAN	Spray Shale, turbidites 1000-1800'	<i>B. occidentalis</i>
	Geoffrey Conglomerate 400-1500'	
UPPER CAMPANIAN	Northumberland Turbidites 500-800'	
	De Courcy Sandstone conglomerate 1000-1500'	
	Cedar District Shale, turbidites 700-2000'	
MIDDLE CAMPANIAN	Protection Sandstone 300-1000'	
LOWER CAMPANIAN	Pender Siltstone, shale 300-700'	<i>B. chicoensis</i>
	Extension Conglomerate 100-1500'	
	Haslam Shale 200-1500'	<i>B. baileyi</i>
SANTONIAN	Comox Sandstone, conglomerate 150-2000'	

Figure 7. Nanaimo Group formations and ranges of baculitids (after Ward, 1978)



Figure 8A-D. Illustrations of sutures from Punta San Jose and Sucia Islands. 9A - Suture (2.5X) and cross-section (.75X) for *Baculites inornatus* from Meek (1876, Pl. IV). 9B - *B. inornatus* (UWB90036) from Punta San Jose (at 40mm). 9C - *B. inornatus* (UWB94628) from Sucia Island (at 22mm). 9D - *Baculites rex* (UWB78836) from Punta San Jose (at 19.5mm).

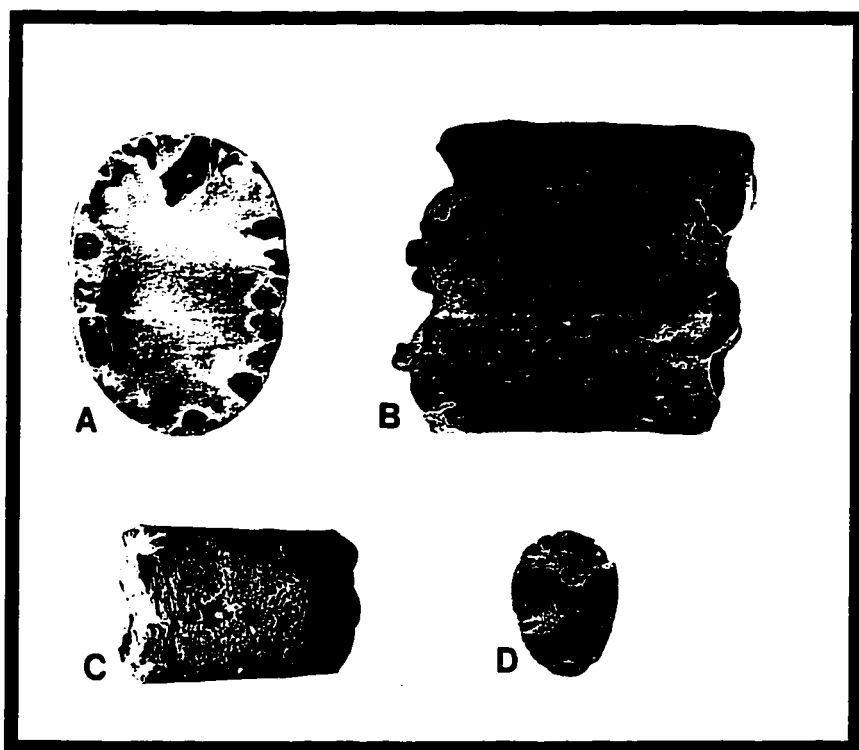


Plate 1: A, B, UWB90036; C, D, UWB78836.

1876; Ward, 1978) and the Western Interior (Cobban, 1951; Cobban, 1958; Cobban, 1962a ; Cobban, 1962b; Cobban, 1973; Cobban, 1976; Cobban, 1977; Cobban, 1993; Cobban and Kennedy, 1991; Cobban and Kennedy, 1992b; Elias, 1933; Reeside, 1927) was done. There are similarities and differences in the way baculitid species concepts are applied in the two regions. There also appear to be problems in the way baculitid species are defined in general.

In both regions, baculitid species are described using the shape of the cross-section, external ornament (ribs and lirae), and characteristics of the suture. Cross-section and external morphologic features are emphasized for the simple reason that it is far more likely to find and collect portions of the phragmocone that do not include the suture. For example, in a collection of over 450 specimens from Punta San Jose, Baja California, currently housed at the University of Washington, approximately one in six has a suture that can be viewed for study.

Matsumoto (1960, p. 154) seems to rely heavily on cross-section shape and ornament in his construction of circum-Pacific baculitid lineages. In an extreme example of this emphasis on external morphology, Matsumoto and Obata (1963) chose a specimen without a suture as the holotype for the subspecies, *Baculites subanceps pacificus* .

Regional differences in specimen size and collection size are also apparent. Species described from the Pacific Coast region and Japan tend to be based on small collections. For instance, there are several west coast species (*Baculites subanceps pacificus*, *B. lomaensis*, *B. regina*, and *B. tanakae*) that are described from very small individuals (<15mm in cross-section height) with very simple looking sutures (see Matsumoto, 1960; Matsumoto and Obata, 1963). In contrast, species from the Western Interior are typically described from large populations of specimens and in many cases the type specimens exceed 40mm in cross-section height and have very complex suture patterns (e.g. Cobban, 1962).

In general, species descriptions from both regions do not adequately illustrate the variation in cross-section morphology, external ornamentation or suture morphology for a given species. It is also not clear to what extent these characters change during the lifespan of an individual. Morphologically similar species can be confused if ontogenetic changes in morphology are poorly understood for individual species. For example, Matsumoto (1960) includes all Pacific Coast specimens with a keel in his synonymy of the species *B. occidentalis*. His illustrations of cross-sections are from the Coalinga area of California and from Hornby Island, British Columbia (see Fig. 9C, D). However, the sutures illustrated for the species are from California specimens while the types for the species are from Hornby Island. Comparison of the illustrated sutures from California and the original suture illustrated by Meek (1896) shows that very different types of sutures are associated with keeled phragmacones (compare Figs. 9 and Fig. 10A). The cross-sections illustrated by Matsumoto (1960) are also quite diverse despite the presence of a keel (see Fig. 10B, C). The difference in suture morphology for California specimens and Hornby Island specimens suggests that Matsumoto (1960) has grouped more than one form under the name *B. occidentalis*. This confusion is the cause for the confusion associated with the range of *B. occidentalis* in Pacific Coast sections (see Fig. 1). Ward's (1978b) extension of the stratigraphic range for *B. occidentalis* in the Vancouver Island region is based on the appearance of a keeled specimen at Sucia Island. However, characteristics of the suture suggest that this and similar specimens are more closely related to *B. inornatus*. These observations would suggest that it is not clear which characteristics of baculitid morphology are best suited for species identification.

External ornament is another morphological characteristic of baculitids that is highly variable. The spacing of ornament relative to the maximum diameter of the phragmacone and rib height are commonly used in describing species of baculitids. The variability of this morphological feature is evident in the following description of the

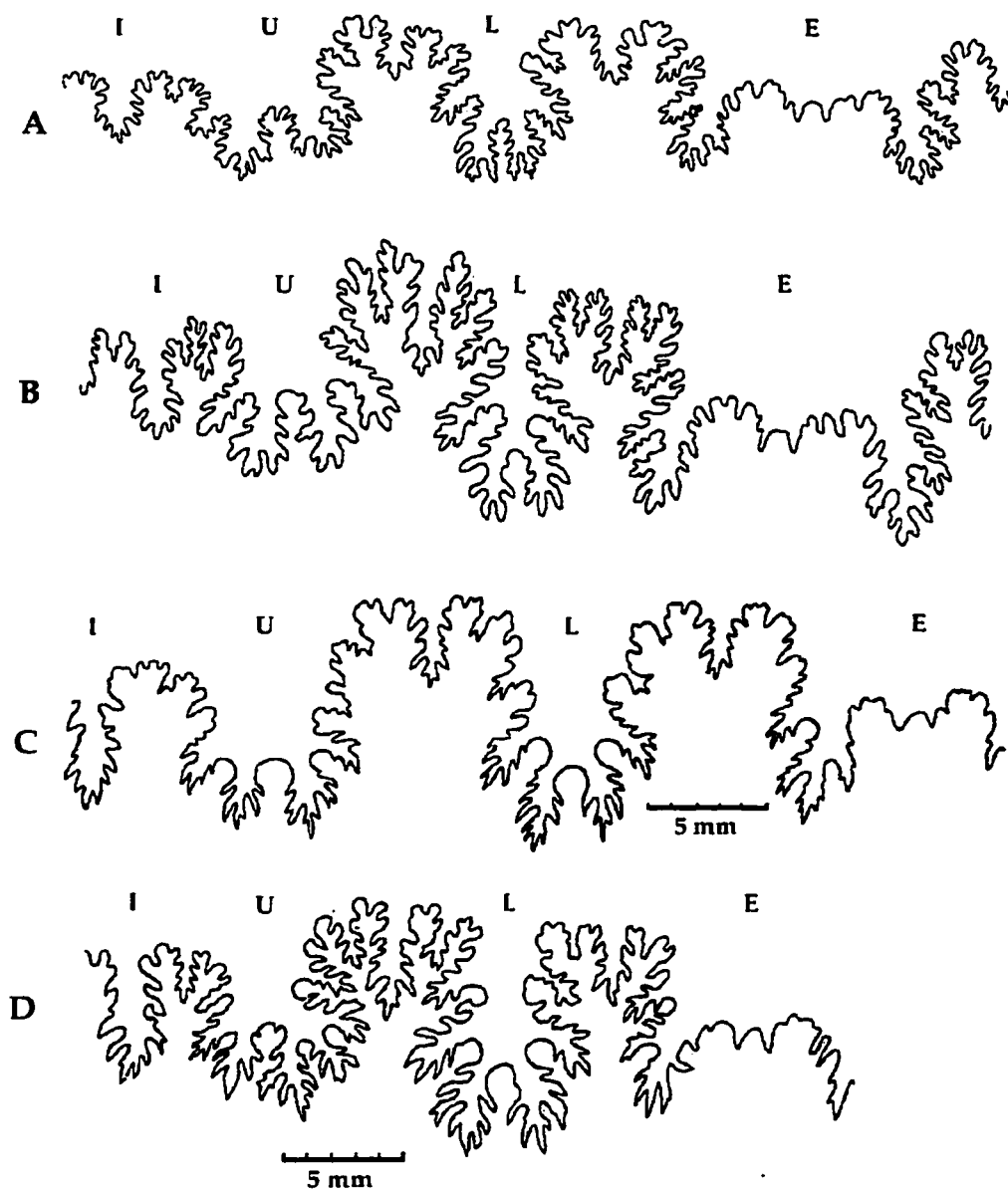


Figure 9A-D. Examples of baculitid sutures. 10A, B are from *B. ovatus* (after Cobban, 1974). 10C, D are from *B. occidentalis* (after Matsumoto, 1960). (I = internal lobe; U = umbilical lobe; L = lateral lobe; E = external lobe).

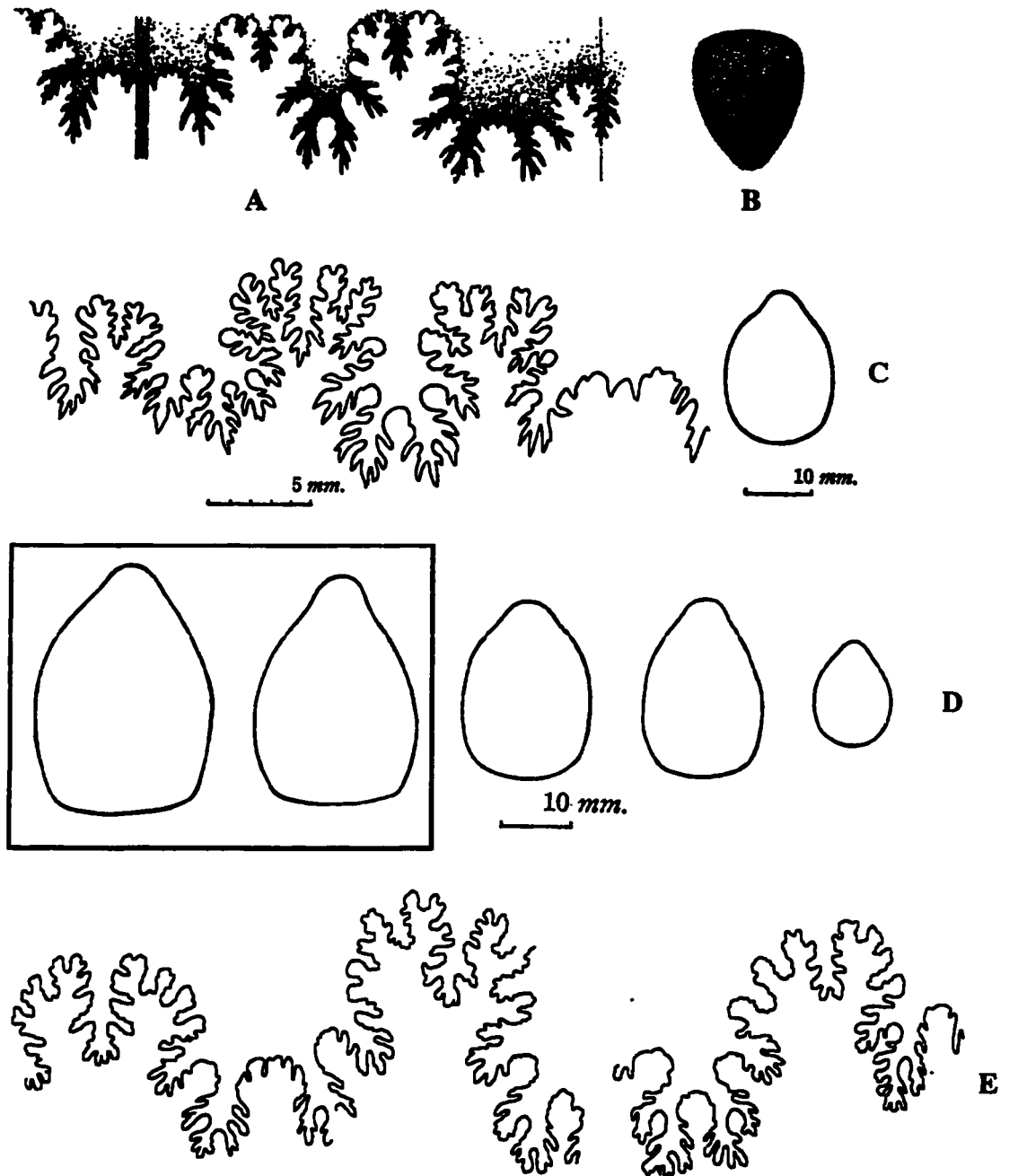


Figure 10A-E. Examples of Sutures and cross-sections attributed to *Baculites occidentalis*. 11A, B - Suture and cross-section from Meek (1876, Pl. IV). 11C - Suture and cross-section assigned to *B. occidentalis* by Matsumoto (1960, pg. 152). 11D - Cross-sections assigned to *B. occidentalis* by Matsumoto (1960, pg. 153). Cross-sections from Meek's type specimens are outlined by box. 11E - Suture (at 39mm) of *B. occidentalis* (UWB90053) from Hornby Island.

species, *Baculites ovatus*:

Lateral ribs may appear at diameters as small as 12-14mm (pl. 2, fig. 22-24) or at diameters as large as 38mm (pl. 2, fig. 13, 14). They are usually spaced about 1.5 for the shell diameter (pl. 1, figs. 9, 16, 23), but they may be as closely spaced as 3 per diameter or as widely spaced as 0.7 per diameter (pl. 1, fig. 31). The ribs are located on the dorsal half of the flank and range in shape from well-defined arcuate forms (pl. 1, figs. 9, 16) to poorly defined lateral swelling (pl. 1, fig. 31). (Cobban, 1974, p. 5).

A histogram showing the relationship of ribbing to the distribution of size frequency for the species *Baculites ovatus* in Cobban (1974) also suggests that the presence or absence of ribbing is not a species-level characteristic. In addition, the data suggest that ribbing is not restricted to any particular size range (see Fig. 11).

Proposed reasons for the presence of ribbing in ammonites include streamlining, and improving shell wall strength against predation (see Ward and Westermann [1985] for review). Streamlining is improved when the relief of the shell ornament is <1% of the shell radius (Chamberlain and Westermann, 1976; Jacobs and Chamberlain, 1996). Predation is difficult to link conclusively with the presence of ribbing.

Variation in external ornamentation can also be observed on individual specimens. For example UWB94629, a mostly crushed specimen of *B. inornatus* collected from the Cedar District Formation on Little Sucia Island, is ribbed at its short end (13.5 mm) while showing no ornament at its larger end (31mm)(see Plate 2, figs. C,D). This variation is not confined to small individuals. In another example (UWB78894), the specimen is smooth at its posterior end (30.6mm), then exhibits large, widely spaced crescentic ribs at its anterior end (33.0mm)(see Plate 2, fig. E). In this case there is visible evidence for damage to the shell corresponding to the appearance of ribbing. In contrast, specimens



Figure 11. Histogram showing frequency distribution of specimens collected from the Navasink Formation at Atlantic Highlands, NJ. Dark shaded area shows distribution of ribbed specimens (after Cobban, 1974).

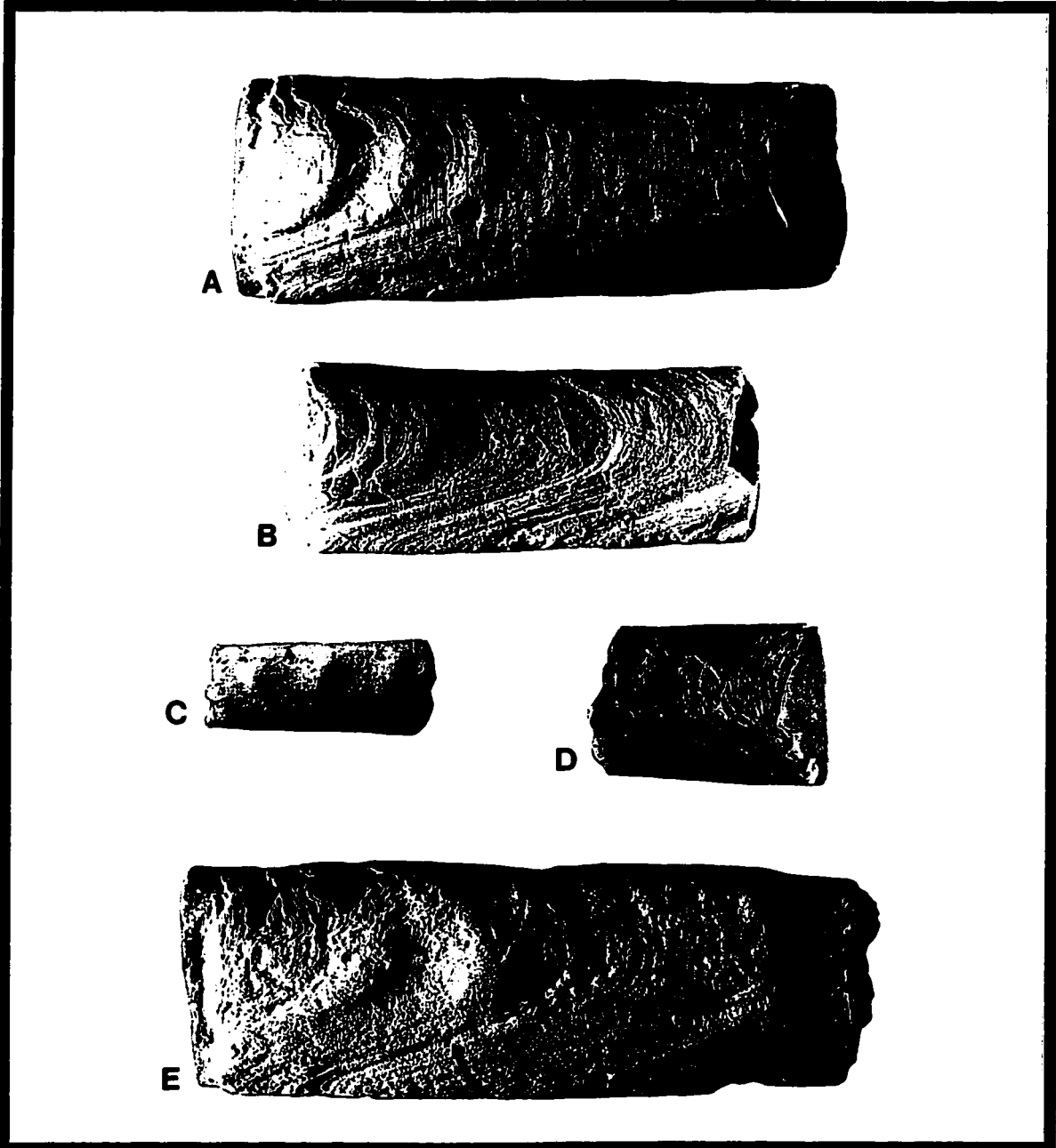


Plate 2A-E: A - UWB95130; B - UCB-A/8580-6; C, D - UWB94629; E - UWB78894

UWB95130 and UCB:A/8580-6 are examples that show no evidence for damage to the shell related to the appearance of ribbing (see Plate 2, figs. A, B). However, it is possible that damage to the animal occurred without coincidental damage to the shell. The evidence presented here linking damage to ribbing is anecdotal. However, the fact that ribbing can appear or disappear in a single specimen suggests that ribbing may not be a species-level characteristic but perhaps a feature that appears in response to some external stimulus.

At Punta San Jose, ribbed specimens are a small proportion of the population. Plotting the frequency of ribbed specimens as a function of stratigraphic level shows no trend (see Fig. 12). These data suggest that there is no gradual shift from a ribbed to a smooth species over time. If it is assumed that only two species are present at Punta San Jose, the data would also suggest that the presence and absence of ribs is not necessarily species specific.

EVOLUTIONARY PATTERN OF BACULITIDS

The identification of morphological features that can be used to define species is important not only for biostratigraphic utility but also for the study of evolutionary pattern. Species or populations of those species are the basic units used for both correlation and for defining evolutionary change in a lineage. Therefore, the recognition of species and the relationship of these species through time necessarily produces a pattern that can be interpreted in the context of evolutionary theory (Eldredge and Gould, 1977).

Two basic patterns of morphologic change are suggested by current evolutionary theory. The slow morphologic change of a lineage through time is termed phyletic gradualism. In this case, species are arbitrarily defined units. Hiatuses in the fossil record can artificially define species, and so the completeness of the fossil record is thought to be a strong though episodic control on the recognition of species. The other basic view of speciation and evolutionary change in a lineage is termed punctuated equilibrium. Species

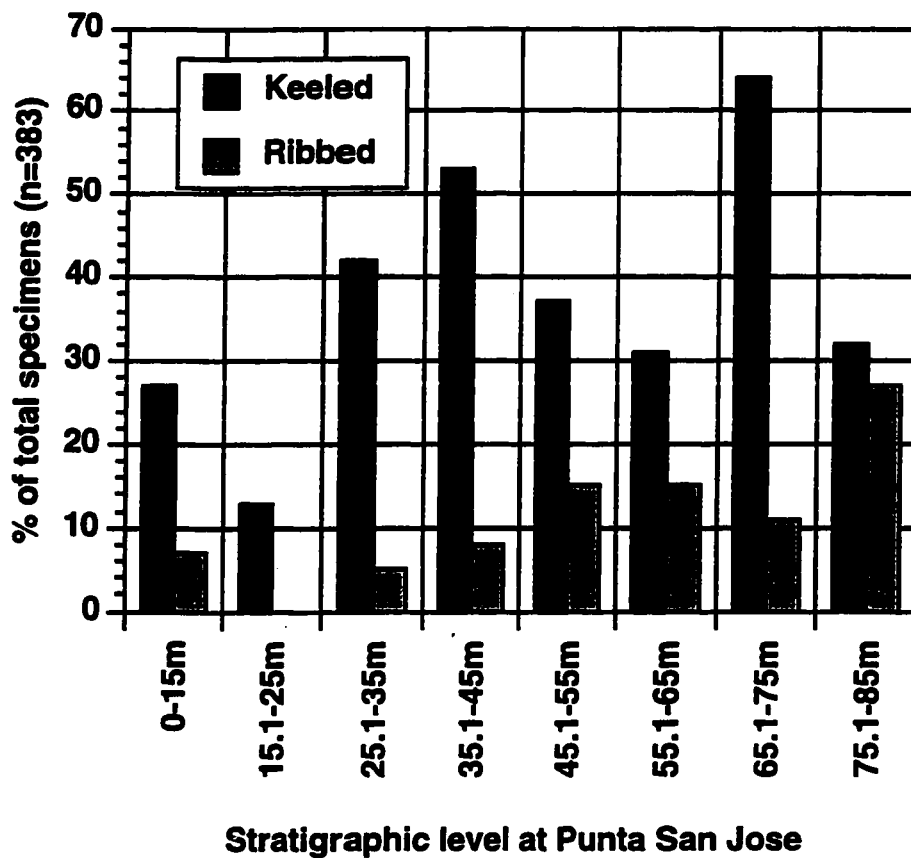


Figure 12. Histogram showing frequency distribution of keeled and ribbed specimens at Punta San Jose

are thought to remain unchanged morphologically throughout their range. Speciation occurs quickly and is recorded as the appearance of a new morphologically distinct form or forms.

A review of papers on Campanian/Maastrichtian baculitids of the Western Interior region gives the impression that baculitid evolution proceeded in a gradualistic way and unfolded as a series of dominant species that grade into one another with rare periods where perhaps as many as three species coexisted at a single time (Cobban, 1951; Cobban, 1958; Cobban, 1962a ; Cobban, 1962b; Cobban, 1973; Cobban, 1976; Cobban, 1977; Cobban, 1993; Cobban and Kennedy, 1991; Cobban and Kennedy, 1992b; Elias, 1933; Reeside, 1927). However, preservation or collection of baculitids in Western Interior sections often has large gaps, 100's of feet between samples. Numerical time constraints on deposition are provided by scattered radiometric dates, which are used (assuming constant sedimentation rates) with stratigraphic thickness data to assign dates to biozone boundaries and thus to determine zonal durations ($\approx 0.5-0.7$ my)(MacArthur and others, 1993; Obradovich, 1993).

The large variation in cross-section morphology and suture pattern of specimens from Punta San Jose would suggest a very different evolutionary pattern. Baculitids from Punta San Jose do not seem to evolve gradually or neatly from form to form through time. Instead they appear to act as group of morphologically plastic (=ecologically complex?) forms with no clear evolutionary pattern.

Part of the disparity in these two views of baculitid evolution may be related to the time scales (sampling interval and total stratigraphic thickness) associated with the data. At Punta San Jose all specimens have been collected over 86 meters of section. The environment of deposition for this section is in all probability an off-shore shelf environment. In Western Interior sections, specimens are commonly collected at sporadic intervals in (hundreds to thousands of feet) thick sections of the Late Cretaceous interior

seaway (e.g. Cobban, 1962). The collections at Punta San Jose may represent a detailed look at baculitid evolution over a short period of time, whereas Western Interior collections, for the most part, may represent sporadic glimpses of baculitid evolution over a much longer period of time.

HYPOTHESES TO BE TESTED

The highly fossiliferous nature of the section and the presence of a transition zone are attributes that make Punta San Jose an interesting locality to study the tempo and mode of evolution in baculitids. In particular, the fossiliferous portion of the section at Punta San Jose has no apparent unconformities in deposition. In addition, the chemostratigraphic data from this site provide an independent time component not commonly found in evolutionary studies. Therefore, the baculitid material collected from Punta San Jose provide an excellent opportunity to test several taxonomic, chemostratigraphic and evolutionary hypotheses.

As noted above, the inconsistent and wide variability in the characters used to describe baculitid species suggests that a re-evaluation of these morphologic characters and their effectiveness in species identification is necessary. In particular, the presence or absence of ribs and of a keel do not appear to be good primary characteristics for identifying baculitid species. However, cross-section shape and suture morphology are both complex characters that appear to be amenable to quantitative analysis.

The large number of specimens from Punta San Jose is the basis for a statistically robust study of baculitid cross-section shape and suture morphology. This data set can be used to test several hypotheses concerning the morphologic characters used to define baculitid species. These hypotheses are: 1) that baculitid species have unique cross-section shapes; 2) that keeling in baculitids is species specific; and 3) that variations in basic morphologic parameters of the suture can be used to distinguish baculitid species.

The resolution of biostratigraphic problems can be achieved potentially by improving species concepts through morphometric analysis. However, it is the integration of biostratigraphic information with other types of chronostratigraphic information that will provide the best pathway toward resolution of regional chronostratigraphic problems. In this instance, a chemostratigraphic study of the section at Punta San Jose using Sr isotopic data will provide chronostratigraphic information that will complement the morphologic study.

Analysis of the $^{87}\text{Sr}/^{86}\text{Sr}$ signal from Punta San Jose should permit the chronostratigraphic placement of the section and test the following hypotheses: 1) that the stratigraphic range of *Baculites rex* includes the Campanian and is not restricted to the Maastrichtian; 2) that the range of *B. inornatus* is Upper Campanian in part; and 3) that the section at Punta San Jose was deposited in a short period of time.

Constraints on the depositional rates at Punta San Jose will also provide estimates of the rates of evolutionary change for baculitids found in the section. Constraints on depositional rate in combination with biostratigraphic pattern will provide the opportunity to evaluate the tempo and mode of evolution in baculitids at Punta San Jose.

CHAPTER 2

STRONTIUM ISOTOPE STRATIGRAPHY

INTRODUCTION TO STRONTIUM ANALYSIS

As noted in the general introduction, Sr isotopic data can be used as an alternative to biostratigraphic data for the correlation of the section at Punta San Jose with other regions of the world. The presence of the species *Baculites rex* and *B. inornatus* at Punta San Jose also provides the opportunity to test hypotheses concerning the biozonal schemes of Matsumoto (1960) and Ward (1978) using a combination of chemostratigraphic and biostratigraphic data. The excellent preservation of shell material found at Punta San Jose suggests that it is possible to produce Sr isotopic data of high quality. However, in order to have confidence in the Sr isotopic data produced from Punta San Jose, the materials used for analysis must be screened for diagenetic alteration.

ANALYTICAL METHODS & RESULTS

A set of shell fragments from baculitids and calcitic bivalves were picked for visual and chemical analysis. Based on light microscope and S.E.M. study, samples of baculitid and bivalve shell material showing the best preservation were picked for chemical analysis (cf. MacArthur, 1993). Calcitic shell material was analyzed for the presence of dolomite using the JEOL 733 Superprobe at the University of Washington. In a clean lab, samples for chemical analysis were cleaned of any fine debris or deposits adhering to the shell surface using a regime that included a series of washings in ultrapure water, a rinse in 1.5N HCl for a few seconds, and 10 minutes of agitation in an ultrasonic bath (cf. MacArthur and others, 1994). The samples were then dissolved using 2.5N HCl. A separate (5-10 mg) of the resulting volume was then weighed out for Sr isotopic analysis while the rest of the sample was set aside for major element analysis. The separates used for major element

analysis were dried down, then redissolved using 1.5N nitric acid before analysis. Major element analysis was done using a Mat Finnegan Sola ICP-MS at the University of Washington (see Table 1).

Samples that passed the major element analysis screen were processed for Sr using standard ion-exchange chromatography. All procedural blanks were <0.7 ng of Sr for the extraction process. $^{87}\text{Sr}/^{86}\text{Sr}$ values were measured at the University of North Carolina using a VG Sector 54 Thermal-ionization mass spectrometer and using Ta filaments. The resulting $^{87}\text{Sr}/^{86}\text{Sr}$ values have been normalized based on a value of 0.1194 for $^{86}\text{Sr}/^{88}\text{Sr}$. The data were collected on October 4th and October 22nd, 1995, using three turrets. Each turret contained 3 or 4 samples of the standard NBS-987. The Fullagar Lab uses a value of 0.710240 for the standard NBS-987 and estimate their 2 sigma error as $\pm 15 \times 10^{-5}$ for measurements of NBS-987 during the period of analysis (Paul Fullagar, personal communication, 1/25/96). The data have been adjusted to the NBS-987 standard value in the following way: Measurement + (0.710240 - Turret Mean). In addition, a single sample of modern nautiloid was successfully run and yielded a value of .709162 $\pm 4 \times 10^{-6}$ (2 s.e.) after adjustment to the NBS-987 standard value. No corrections have been made for radiogenic Sr as Sr/Rb concentration ratios for all samples are $> 3.0 \times 10^7$.

Sr concentrations for samples analyzed fall within the values, reported by Morrison and Brand (1988), for unaltered baculitid shell material. Mg content for all samples is well below the maximum value of 400 ppm suggested by MacArthur and others (1994) for unaltered molluscan shell. Mn concentrations for all samples were well within the range of concentrations measured for unaltered molluscan shell material by Morrison and Brand (1988) and below the maximum value of 300 ppm suggested MacArthur and others (1994) for unaltered molluscan shell material. The $^{87}\text{Sr}/^{86}\text{Sr}$ ratios for the fifteen samples from

TABLE 1: Isotopic and chemical data for samples from Punta San Jose

Sample	Level (m)	* $^{87}\text{Sr}/^{86}\text{Sr}$	†Sr (ppm)	†Mg (ppm)	‡Mn (ppm)	Rb (ppm)
¥PSJ-9.9	9.9	0.707677	2852	117	10	$<3 \times 10^{-5}$
PSJ-15	15	0.707632	3219	190	28	$<9.5 \times 10^{-5}$
78939	33	0.707645	4514	141	28	$<5 \times 10^{-5}$
37	37	0.707656	4283	134	25	$<7 \times 10^{-5}$
95048	38.4	0.707653	4214	110	25	$<6.5 \times 10^{-5}$
78744B	41.5	0.707652	4882	94	22	$<2.5 \times 10^{-5}$
78872	45	0.707652	4932	90	24	$<3 \times 10^{-5}$
94749	55	0.707674	4470	103	24	$<5 \times 10^{-5}$
57.2	57.2	0.707642	1807	74	14	$<4 \times 10^{-5}$
61(II)	61	0.707654	4514	141	28	$<5 \times 10^{-5}$
95059	66.1	0.707664	3770	79	22	$<4.5 \times 10^{-5}$
67	67	0.707655	2498	100	24	$<5 \times 10^{-5}$
71.5	71.5	0.707654	4577	136	22	$<4 \times 10^{-5}$
76	76	0.707651	4094	101	24	$<4 \times 10^{-5}$
86(II)	85	0.707661	4156	125	13	$<5 \times 10^{-5}$
Nautilus #2	n/a	0.709162				

* Analytical error is ± 0.000006 † Analytical error is $\pm 3\%$ ‡ Analytical error is $\pm 25\%$

¥ calcite from bivalve

Punta San Jose range in value from 0.707632 to 0.707677 with an average value of 0.707655 (see Fig. 13).

DISCUSSION

Interpretation of the data and proper use of the data for correlation depend on the theoretical framework used to define the overall Sr isotopic curve. Two methods have been used to define Sr isotopic curves from a series of single point data. The first method assumes that short-term changes (100-400 kyr) in temporal $^{87}\text{Sr}/^{86}\text{Sr}$ are possible, and the curve is constructed by connecting the data point to point (e.g. Clemens and others, 1993). The second method assumes that changes in temporal $^{87}\text{Sr}/^{86}\text{Sr}$ seawater values act in a linear fashion over long periods of time ($>1 \times 10^6$ yrs) and can be described as a series of linear segments tied together by short-term periods of rapid evolution (e.g. Hodell and others, 1991).

The disparity reflected in these two approaches reflects the general poor understanding of factors that control the input and preservation of Sr in the geologic record. One group has proposed a link between the $^{87}\text{Sr}/^{86}\text{Sr}$ curve over the past 400 kyr and continental erosion rates driven by glacio-eustatic changes (Dia and others, 1992; Clemens and others, 1993). However, using simple models for the response of the oceanic Sr signal to periodic forcing, Richter and Turekian (1993) suggested that the shortest period resolvable, given the current levels of analytical precision, is around 1 myr. This suggestion is supported by the recent high precision work by Henderson and others (1994) on cores representing the last 400 kyr. They believe that data previously interpreted as short-term cycles were instead produced by analytical artifact. They also suggest that their data can best be modeled as a linear increase in the $^{87}\text{Sr}/^{86}\text{Sr}$ ratio over time (Henderson and others, 1994).

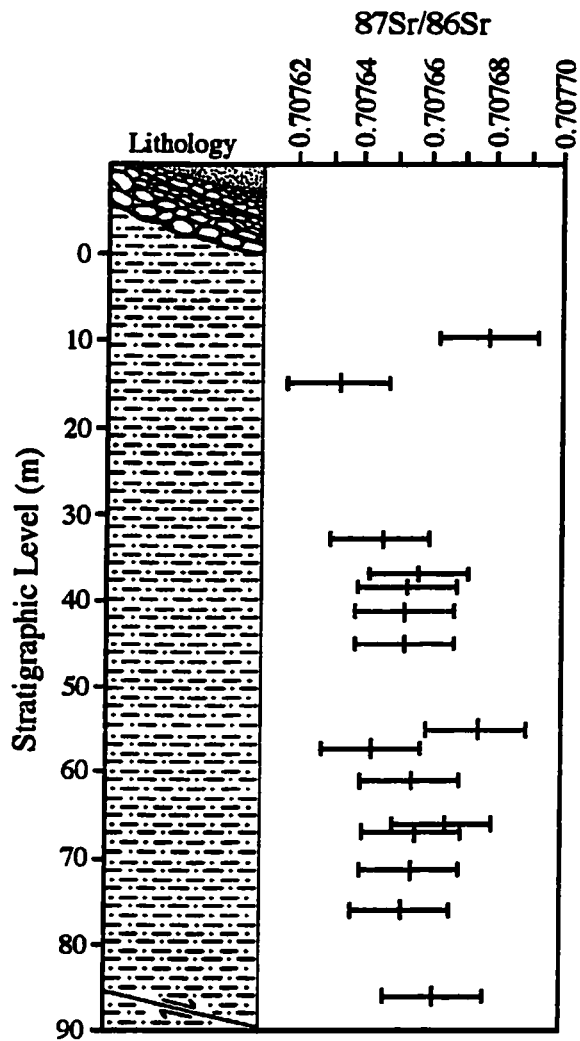


Figure 13. Sr isotopic data for Punta San Jose, Baja, California. Error bars are ± 0.000015 . Data is standardized to a value of 0.710240 for NBS-987.

The linear method of constructing the Sr curve has also been used on large data sets covering long periods of time. In some cases, data representing 6-8 myr have been modeled as linear (Hodell, and others, 1991; MacArthur and others, 1993). As noted before, the models of Richter and Turekian (1993) support the idea that the Sr isotopic signal acts in a linear fashion over short periods of time relative to the residence time of Sr in the world's oceans ($\sim 2-4 \times 10^6$ yrs). New evidence from Lower Cretaceous carbonates suggests that the residence time of Sr was considerably shorter than modern estimates, perhaps as short as 0.5×10^6 yrs (Stoll and Schrag, 1996). A lower residence time would shorten the theoretical response time of the evolving Sr seawater signal to significant changes in the Sr input. This shortened response would in turn limit the period of time over which a linear model can appropriately be used. Therefore, the validity of modeling the Cretaceous Sr curve as linear over longer periods of time ($>.5-1.0$ myr) is debatable.

The method used to model the Sr curve has significant effects on the precision of correlation. Correlation between Punta San Jose (PSJ) and the European standard section at Lägerdorf/Kronsmoor, Germany (L/K) might be done either by using linear age models, such as proposed by MacArthur and others (1993) and Howarth and MacArthur (1997), or by direct comparison of the two data sets. However, the Sr isotopic data from PSJ show no significant trend with respect to stratigraphic level (see Fig. 13). Consequently, it is necessary to compare the two data sets directly.

Some of the problems or factors that must be considered when attempting to compare Sr isotopic data sets are: 1) the analytical precision of the $^{87}\text{Sr}/^{86}\text{Sr}$ measurements for all data being compared; 2) the rate of change in the $^{87}\text{Sr}/^{86}\text{Sr}$ ratio over time; 3) the scale at which the Sr isotopic signal is sampled; and 4) other variations in the signal due to depositional history and preservation of the section being sampled (diagenesis, bioturbation, compaction, etc.). Comparison of the PSJ data set with the curve produced for the chalk sequence at L/K by MacArthur and others (1993) illustrates the complexities

of correlation using Sr isotopic data and points out two primary complicating factors to be discussed below (see Fig. 14). These are 1) the total error used when comparing data sets, and 2) compression and expansion of the Sr isotopic signal as a function of sedimentation rate.

ASSESSING ERROR

There is an incomplete understanding of how bioturbation, diagenesis, compaction and other factors affect the quality of preservation at an outcrop. All of these factors affect the precision of correlation and mystify the process of modeling the Sr isotopic curve. A conservative approach to assessing the error associated with Sr isotopic curves would seem prudent. The curve from L/K shown in figure 14 is based on raw data (from MacArthur and others, 1993), not the means. There seems to be a relationship between the complexity of the signal and the number of replicate measurements at a given stratigraphic level. The larger the number of data, the more complex the signal recorded. There is no indication that outcrop quality or sample preservation is a reason for the variable fit for the regressions used to model their data. Therefore it seems likely that the whole length of the curve is similarly affected by the portion of the total error in correlation that is not related to the slope of the data. While each of the segments modeled by MacArthur and others (1993) is statistically valid for the data available, a good regression with tighter fit in one part of the curve does not guarantee that the same quality of data exists throughout the curve. This is particularly true if areas of the curve with poorer fit contain more replicate data and doubly so, if one takes into consideration that the sampling interval may not accurately reflect the finest structure of the curve. If a linear model is used to fit the data, it should be based on replicate measurements at every stratigraphic level possible in order to reflect the fit accurately (spread of the data around the regression). This point is very relevant in the case of the L/K data as the suggested precision (2-sigma) in correlation is much smaller

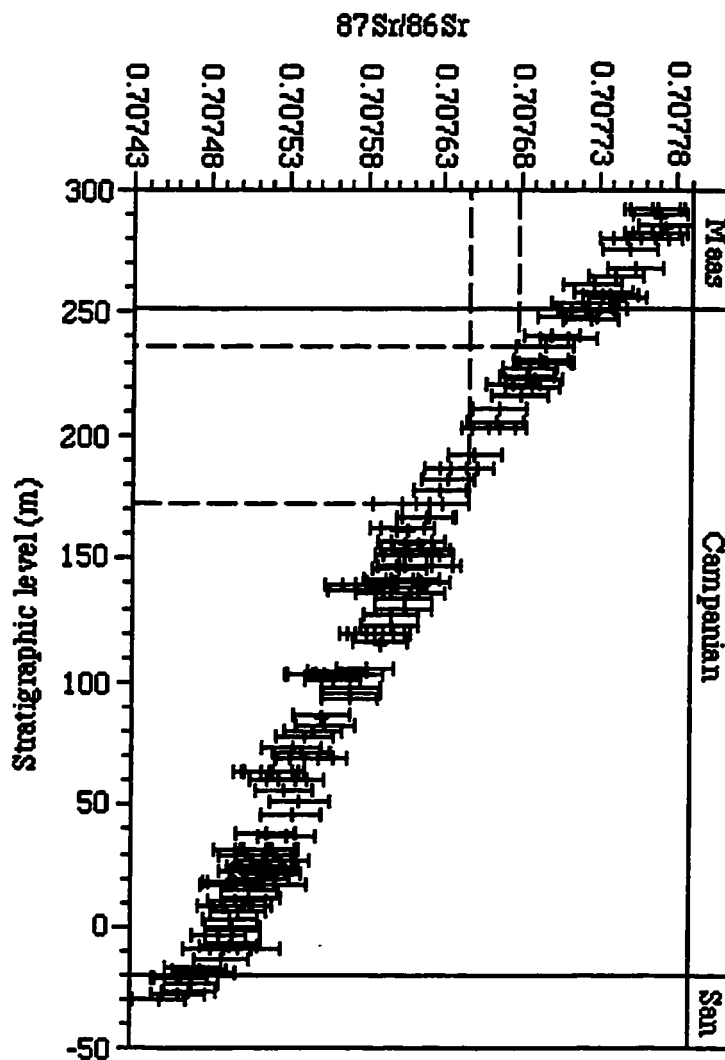


Figure 14. Sr isotopic data from Lagerdorf/ Kronsmoor, Germany. Data and stage boundaries from MacArthur and others (1993). Error bars are ± 0.000018 . Dashed areas show stratigraphic limits of correlation on x-axis based on Sr isotopic data from Punta San Jose shown on y-axis. PSJ data range is the mean value of data 0.707669 ± 0.000015 after being standardized to a value of 0.710248 for NBS-987 for the purposes of correlation.

than the analytical precision of the measurements used to construct each of the segments (e.g. $\pm 6.4 \times 10^{-6}$ vs. $\pm 18 \times 10^{-6}$) (MacArthur and others, 1993).

MacArthur and others (1993; p. 870) have suggested that a total error of $\pm 21 \times 10^{-6}$ is a useful approximation when correlating to **L/K** and assuming non-linearity. They based this calculation on the unexplained idea that the error for each point on their curve is constrained in some fashion by the error of its neighbors. It seems more realistic to use the (2-sigma) standard errors of both data sets when directly comparing Sr isotopic data sets until many of the untested assumptions that underlie this method of correlation are substantiated. All correlation reported in this paper uses a total error of $\pm 15 \times 10^{-6}$ for the data from **PSJ** and for the total error reported for each data set used in correlation.

COMPLICATIONS DUE TO LOCAL DEPOSITIONAL HISTORY

When comparing the Sr isotopic signals from **PSJ** and **L/K**, the data set from **PSJ** can be compressed or expanded in order to achieve the best possible fit with the Sr signal from **L/K**, and in the process we make inferences concerning the relative sedimentation rates of these two localities. The structure of the data from **PSJ** helps to limit the possibilities. If we assume somewhat comparable sedimentation rates for both localities, the only portion of the curve from **L/K** that is similar in structure to the data from **PSJ** is around the $^{87}\text{Sr}/^{86}\text{Sr}$ value of 0.707610. This scenario would suggest that ~ 90m of section at **PSJ** is equivalent to ~ 45m of section at **L/K**. However, this part of the **L/K** curve is on the extreme edge of the combined error envelope for the two data sets. A more likely possibility is that the sedimentation rate at **PSJ** was considerably higher than at **L/K** and that the **PSJ** data record a finer structure in the Sr isotopic curve relative to the data from **L/K**. If ~90m of section at **PSJ** are equivalent to ~ 20m of section at **L/K**, there are several areas within the envelope of error bracketing the $^{87}\text{Sr}/^{86}\text{Sr}$ value of 0.707663 that

could accommodate the data from **PSJ**. A most pessimistic correlation can be done by using only the full range of values from **PSJ** and ignoring the structure of the data. In this case, the section at **PSJ** would correlate to the stratigraphic interval (138.7m - 248.4m) at **L/K**. However, given the overall linear structure of the data it seems reasonable to use the average value as a basis for correlation. In this scenario, the section at **PSJ** would correlate to near the base of the *Belemnitella langei* macrofossil zone, or the 202m level at **L/K**. The shape of the curve and the combined error of both data sets suggest a 95% confidence interval across the range (172.3m - 235.9m) which includes the upper third of the *Galerites vulgaris* zone, the *Bostryoceras polyplacum* zone, the *Belemnitella langei* zone, and the lower third of the *Micraster grimmensis* / *Cardiaster granulatus* zone at **L/K** (see Fig. 15). This entire range is also contained in approximately the upper half of Nannofossil zone CC/B22 of Burnett (1990) or the upper third of the Campanian Stage as defined in MacArthur and others (1993).

The overall linear structure of the data from **PSJ** and the comparison with the structure of the curve from **L/K** also imply that the section at **PSJ** was deposited in a relatively short period of time. Using the preferred age model of MacArthur and others (1994) suggests a maximum time for deposition at **PSJ** on the order of 1.5my. For the purposes of this calculation, the Sr curve from **PSJ** is treated as a single datum with an error of ± 0.7 my. The error value is an estimate from the model of MacArthur and others (1994) that assumes non-linearity of the overall Sr curve. The compilation of depositional rates provided by Sadler (1981) can be used as a guide for a minimum time of deposition for the section at **PSJ**. Sadler's compilation suggests that a depositional rate of one meter per thousand years would not be unusual for a siliclastic shelf sequence. This depositional rate would suggest the section at **PSJ** could have been deposited in as short a time as 70-100 thousand years.

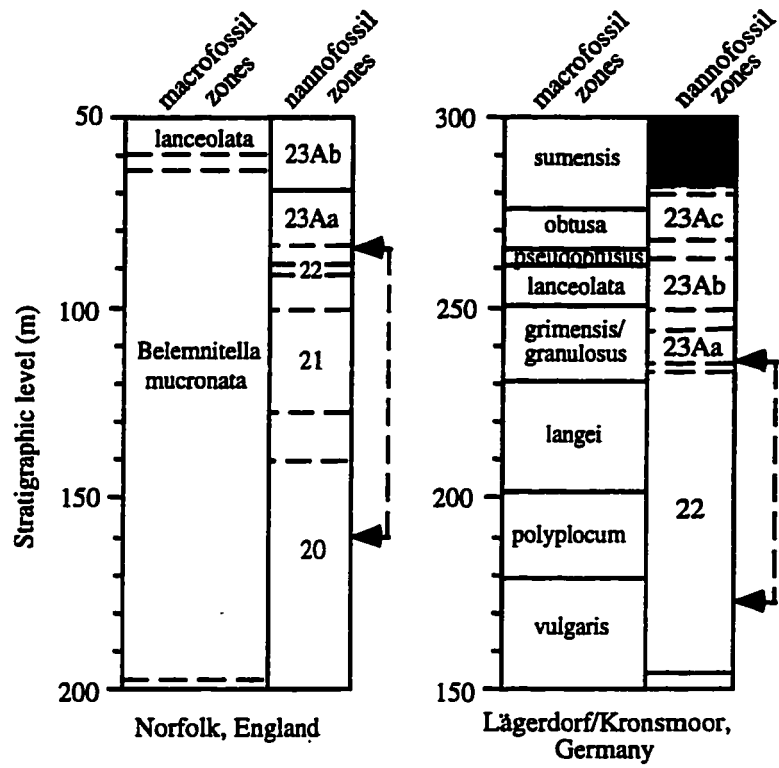


Figure 15. Comparison of macrofossil and nanno-fossil zones at Norfolk, England (after MacArthur and others, 1992) and Lägerdorf/-Kronsmoor, Germany (after MacArthur and others, 1993). Arrows mark range of correlation for Punta San Jose based on Sr isotopic data (see Figs. 21 and 23).

CORRELATION WITH OTHER SECTIONS

Correlation of the section at **PSJ** with the chalks at Trunch Borehole, Norfolk, England is complicated by the uneven sample interval used for that section. The section at **PSJ** correlates to the range (85m -175m) at the Trunch Borehole (see Fig. 16). This falls within the *Belemnitella mucronata* zone which spans the entire Upper Campanian as defined by MacArthur and others (1992) at that locality. However, assuming that nannofossil zone stratigraphy has been applied equally well at both the Trunch Borehole and the **L/K** section, the section at **PSJ** can be correlated to nannofossil zone **CC/B22**, further narrowing the range of correlation to 85m-100m at the Trunch Borehole (see Fig. 15). In this case, the nannofossil zones are more useful for correlation than the Sr isotopic signal, as nannofossil zone 22 at the Trunch Borehole (≤ 15 m thick; see Fig. 2, MacArthur and others, 1995) is condensed relative to the section at **L/K** (~80m thick; see Fig. 1, MacArthur and others, 1993).

The section at **PSJ** can be roughly correlated to the lowest 2 meters of section recovered from the Clayton Borehole located in the Coastal Plain of New Jersey, USA (see Fig. 17). This section of the Marshaltown Formation falls within nannofossil zone **CC20/21** and is considered to be Campanian in age (Sugarman and others, 1995). In this case, the nannofossil zones are based on the work of Perch-Nielsen (1985) and probably reflect different criteria when compared to the European zones discussed above. The zone **CC21/CC22** boundary was not identified at the Clayton borehole (Sugarman and others, 1995).

Correlation of **PSJ** with U.S. Western Interior sections is not possible because of the way Western Interior data were assembled. Samples used by MacArthur and others (1994) were taken from museum specimens unrelated to measured sections. The result is a collection of data from a series of fossil zones (see Fig. 18). In most instances, the samples representing a particular fossil zone were collected from different localities

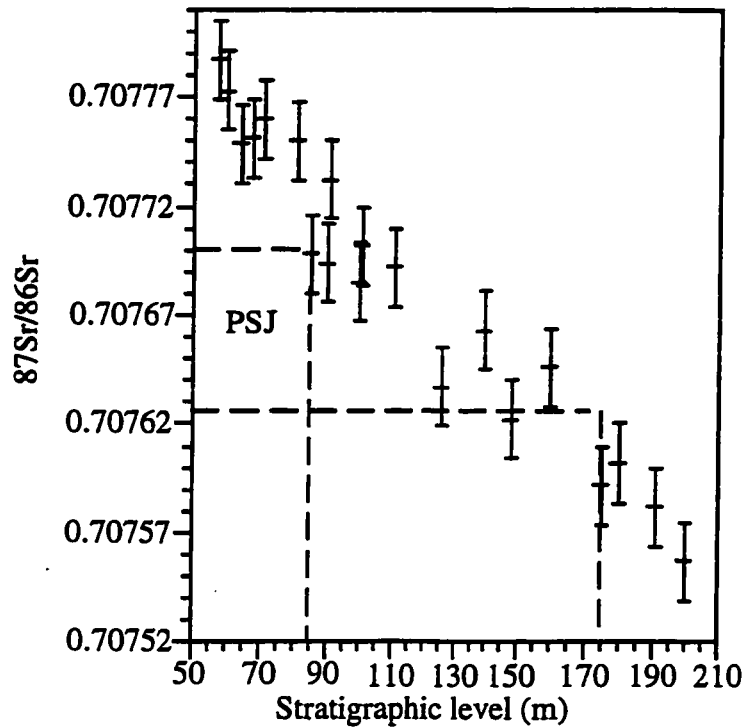


Figure 16. Sr isotopic data (part) from Norfolk, England. Data from Table 2 of MacArthur and others (1994). Error bars are ± 0.000018 . Dashed area shows stratigraphic limits of correlation on x-axis based on Sr data from Punta San Jose shown on y-axis. PSJ data range is (0.707640 to 0.707684) ± 0.000015 . All data are standardized to a value of 0.710248 for NBS-987.

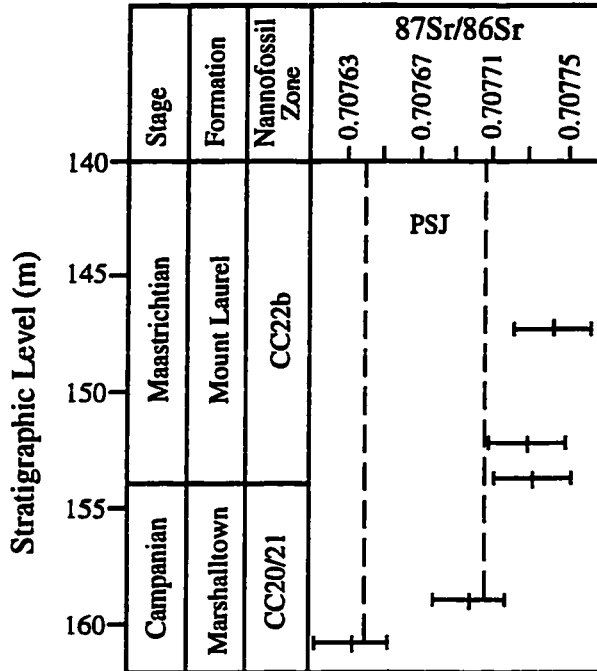


Figure 17. Sr isotopic data (in part) from the borehole at Clayton, NJ. Sr data from Table 3 of Sugarman and others (1995). Stage, zone and formation boundaries from Sugarman and others (1995). Error bars are +/- 0.00002. Area between dashed lines and labeled PSJ encloses data range from Punta San Jose. All data have been standardized to a value of 0.710253 for the purposes of correlation.

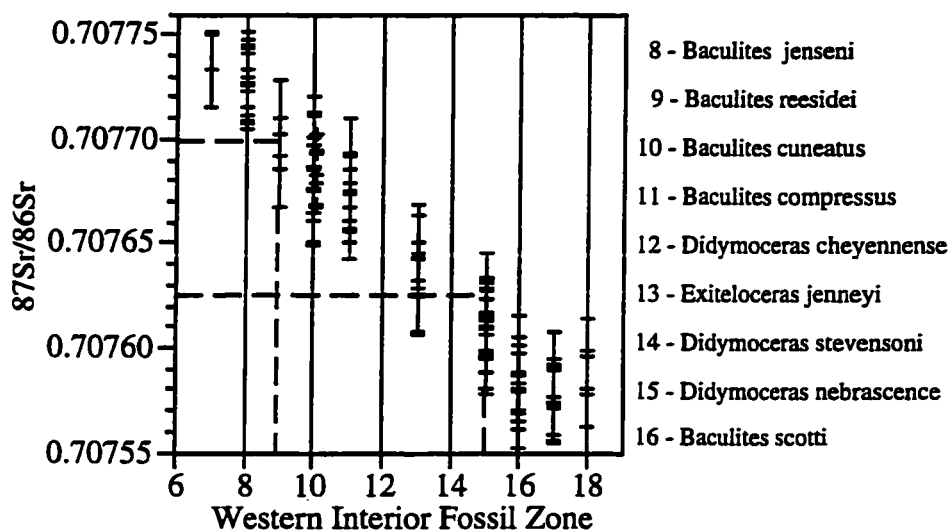


Figure 18. Sr isotopic data for some Western Interior fossil zones. Data and zones from Table 3 of MacArthur and others (1994). Error bars are ± 0.000018 . Dashed lines show correlation of section at Punta San Jose to Western Interior fossil zones using Sr isotopic data. PSJ data range is $(0.707640 \text{ to } 0.707684) \pm 0.000015$. All Data have been standardized to a value of 0.710248 for NBS-987.

(MacArthur and others, 1995; Table 1). There is considerable overlap in the range of $^{87}\text{Sr}/^{86}\text{Sr}$ values reported for adjacent ammonite zones. If we consider the 2-sigma error for both data sets, this overlap prevents the correlation of the section at Punta San Jose to anywhere more precise than within the *Didymoceras nebrascense* zone through the *Baculites reesidei* zone or almost all of the upper Campanian of the Western Interior as defined by Kennedy and others (1992).

DEPOSITIONAL RATES AND SAMPLING INTERVALS

The level of detail in the Sr curve that can be recorded at an outcrop depends on the rate at which carbonate grains accumulated over time. The level of detail for the Sr curve that can be extracted from an outcrop also depends on the sampling interval. Outcrops sampled at ten meter intervals will not record changes in the signal that occur over one meter intervals. If two outcrops are sampled at the same interval but one locality had a high rate of deposition and the other a very low rate of deposition, the resulting curves will also be very different in detail. In contrast, the accuracy of biostratigraphic zone boundaries depends on the presence and absence of diagnostic fossils as well as the interval at which those fossils can be found.

Comparison of the stratigraphic thicknesses for the nannofossil zones found at the L/K and Trunch borehole chalk sequences also illustrates the problem of assuming constant sedimentation rate for any stratigraphic section when modeling geochemical signals. While the macrofossil fauna are very different at these two localities, the nannofossil zones do provide a useful standard for comparison of depositional rates. The lower part of the section at Norfolk, England (below zone 23Aa) appears to be compressed relative to the German section (see Fig. 15). The Sr signal at Norfolk, England is also compressed below the lower boundary of nannofossil zone 23Aa (compare Figs. 14 and 16). Because the sampling interval at Norfolk does not compensate for the compression of

the Sr signal, the finer structure of the Sr signal is lost, and correlation is less accurate. In this case, correlation between Norfolk, England, and L/K can be done more precisely using biostratigraphy. Better resolution of the Sr curve at Norfolk could be achieved theoretically by using a smaller sampling interval to compensate for the compression of the Sr signal. This assumes that other factors such as bioturbation would not limit the scale of the sample interval.

CONCLUSIONS

The section at Punta San Jose can be assigned with high confidence to the upper Campanian. The presence of *Baculites rex* at Punta San Jose supports the zonal scheme of Ward (1978) with modification, as *B. occidentalis* is not found with *B. rex* at this locality. Both the base of the *B. rex* zone and the top of the *B. inornatus* zone are found to be within the upper Campanian. If a comparison is made of the Sr isotopic signal from Punta San Jose and the signal from European boreal sections, the base of the Pacific Coast *B. rex* zone can be roughly correlated to the base of the *Belemnitella langei* zone, and with less confidence to within the upper half of the nannofossil zone CC/22.

The structure of the Sr isotopic signal from Punta San Jose suggests that this section was deposited over a short period of time. However, the resolution of the overall Sr curve is not precise enough to allow for a proper estimation of the depositional rate at Punta San Jose. Therefore, the calculated period of 1.5my for the deposition of the section at Punta San Jose is likely to be a gross overestimate because of the large error associated with the Sr data used in the calculation. Average depositional rates (1m/1ky) for comparable siliciclastic sequences and the lack of any hiatus in deposition at Punta San Jose support a shorter (on the order of 0.1my) period of time for deposition.

The variation in the Sr isotopic data from Punta San Jose also suggests that there may be a finer structure to the Upper Campanian Sr isotopic curve than shown by the data

of MacArthur and others (1993) from Lägerdorf/Kronsmoor, Germany (compare Figs. 13 and 14). The structure of the data from Punta San Jose also supports the idea that the total error associated with models of the Sr curve which assume linearity over long periods of time is underestimated significantly.

In addition, comparison of $^{87}\text{Sr}/^{86}\text{Sr}$ data from different regions of the world suggests that the completeness of the Sr isotopic signal at any locality is influenced by depositional rates and sampling interval. As described above, a comparison of both the Sr signals and fossil zones at Norfolk, England, and at Lägerdorf/Kronsmoor, Germany, illustrates that depositional rate affects the precision of correlation using the Sr isotopic signal.

In general, when sections or subdivisions of sections have a compressed signal due to periods of low sedimentation rate (e.g. Trunch Borehole, England), correlation using Sr isotopic data may be less effective than biostratigraphic methods if the sampling interval is not shortened. In sections where the $^{87}\text{Sr}/^{86}\text{Sr}$ is expanded due to high depositional rates (e.g. Punta San Jose), there is the potential for Sr isotopic stratigraphy to exceed the precision of biostratigraphy in correlation.

CHAPTER 3

BACULITID MORPHOMETRICS

INTRODUCTION TO MORPHOMETRICS

As noted in the main introduction, the morphological characters currently used to describe baculitid species appear to be highly variable and in need of quantitative study. The study of morphological characters is necessary in order to identify the characters most useful for the delineation of species. Species that are described using ecophenotypic morphologies have no utility as biostratigraphic indicators. Therefore, the biostratigraphic utility of any species depends on an understanding of morphologic characters used to describe the species. Baculitid and other ammonite species are by necessity based on the observation of available morphological characters. Ultimately, it is essential to determine whether these morphological characters allow the discernment of true variation between species, or whether they simply reflect ecophenotypic variation within a species.

PREVIOUS MORPHOMETRIC STUDIES

For the most part previous studies have focused on measuring simple morphologic features of the ammonoid shell. For example, the classic study of the Middle Jurassic ammonite genus *Kosmoceras* by Brinkman (1929a, b) was based exclusively on external morphological features such as specimen diameter, height/width ratio of the whorl, rib density, and rib 'bundling' indexes. The measurements of these characteristics were then treated as univariant characters and used to identify forms. A similar approach was used by Howarth (1973a, b) in the study of the Lower Jurassic genus *Dactyloceras*. Once again, external morphological features including basic proportions of the whorl cross-section, rib density and other characteristics of rib morphology were used to define species.

The theoretical studies of Raup (1967) have led to the use of basic shape parameters to describe variation in the shape of coiled shells. These Raupian parameters are incorporated into more recent studies of ammonoid morphology along with information on ornament and sutural complexity (e.g. Ward, 1980; Saunders and Work, 1997). In addition, more recent studies take a multivariant approach to their data using principle components analysis to help in the discrimination of morphologically distinct groups (Checa and others, 1996; Saunders and Work, 1996, 1997). However, most of these recent studies are focused on genus or higher-level orders of variation in morphology. The studies that do analyze morphologic variation below the genus level have focused primarily on intraspecific (Dagys and Weitchat, 1993; Jacobs and others, 1994) and in one case interspecific (Hohenegger and Tatzreiter, 1992) variation. In all of these cases, only simple measurements of the shell and details of shell ornamentation are studied. There has never been a multivariant analysis of cross-section shape for any ammonoid species. In addition, quantitative information from sutures has never been used in the discrimination of ammonoid species. In those cases where quantitative studies have been done on suture morphology, the focus has been on family level or higher orders of variation (Boyajian and Lutz, 1992; Lutz and Boyajian, 1995; Saunders, 1995; Ward, 1980; Westermann, 1971). However, Saunders and Work (1997) do suggest that ammonoids can be systematically organized at all levels using characteristics of the suture.

Morphological data that are typically, but not always reported for Pacific Coast and Western Interior baculitid species include height/width ratios of the cross-section, rib frequency, taper, and suture morphology. Of these characteristics cross-section shape and suture morphology are two characters that are complex and can be quantified easily.

CROSS-SECTION

Cross-section height/width ratios are a commonly reported measurement in species descriptions for Pacific Coast species of baculitids. However, the small data sets and large overlap in the data suggest that this type of data is difficult to use in discriminating species. The problem with height/width and similar ratio data is that the position of maximum width or other features of the cross-section are not properly located on the perimeter of the cross-section. The following analyses illustrate this point.

I used a sample of 154 cross-sections that represents all forms found at Punta San Jose. The height/width (H/W) ratio, the ratio of heights to maximum width and midpoint width (Max/Mid), and the ratio of dorsal width to ventral width (DW/VW) were measured from enlarged printouts of the video snapshots used to record cross-sections (see Fig. 19). Regressions for the values of these ratios with respect to stratigraphic level are shown in figures 20, 21, and 22, respectively. In each case, the resulting values for R^2 suggest that none of these variables changes significantly with respect to time (stratigraphic level). Plotting the number of keeled forms at Punta San Jose as a percentage of the population also shows no systematic change with time (see Fig. 12). This analysis also suggests that this feature of cross-section shape may not be a primary diagnostic characteristic for baculitid species. In fact, there are different grades of keeling that can be found in the set of specimens collected from Punta San Jose. There are cases in which specimens are half-keeled or show the partial beginnings of a keel (see Fig. 23 and Plate 3D). In addition, it does not appear that keeled specimens share other characteristics of shape that would segregate them easily from other specimens.

A review of collections from Punta San Jose, Baja California, reveals a potential cause for some of the variation in baculitid cross-section morphology. Morphological change in cross-section shape is apparent in specimens that have been damaged by what may be failed predation attacks. In some cases damage to the shell is so extensive that it is

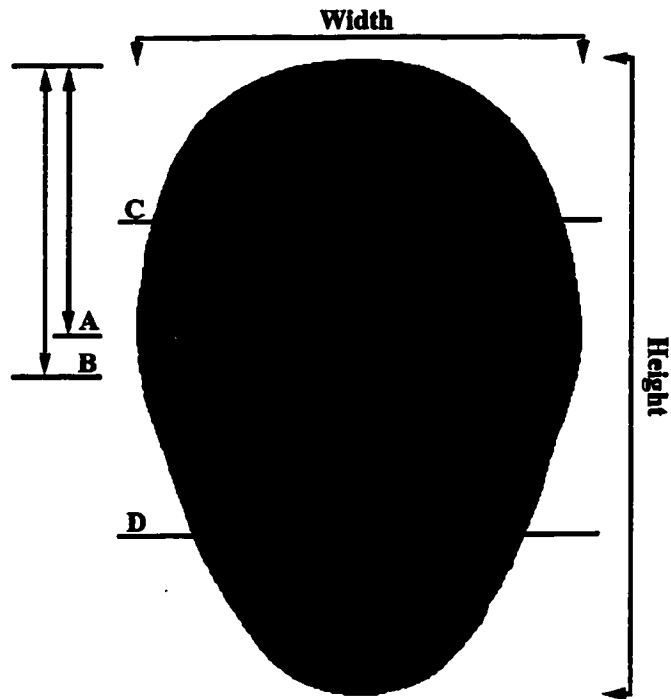


Figure 19. Explanatory Diagram for data measured from digitized cross-section images. The ratio $(H/W) = \text{Height/Width}$. The ratio $(\text{Max/Mid}) = \text{Length A/Length B}$. The ratio $(DW/VW) = \text{Width at level C/Width at Level D}$.

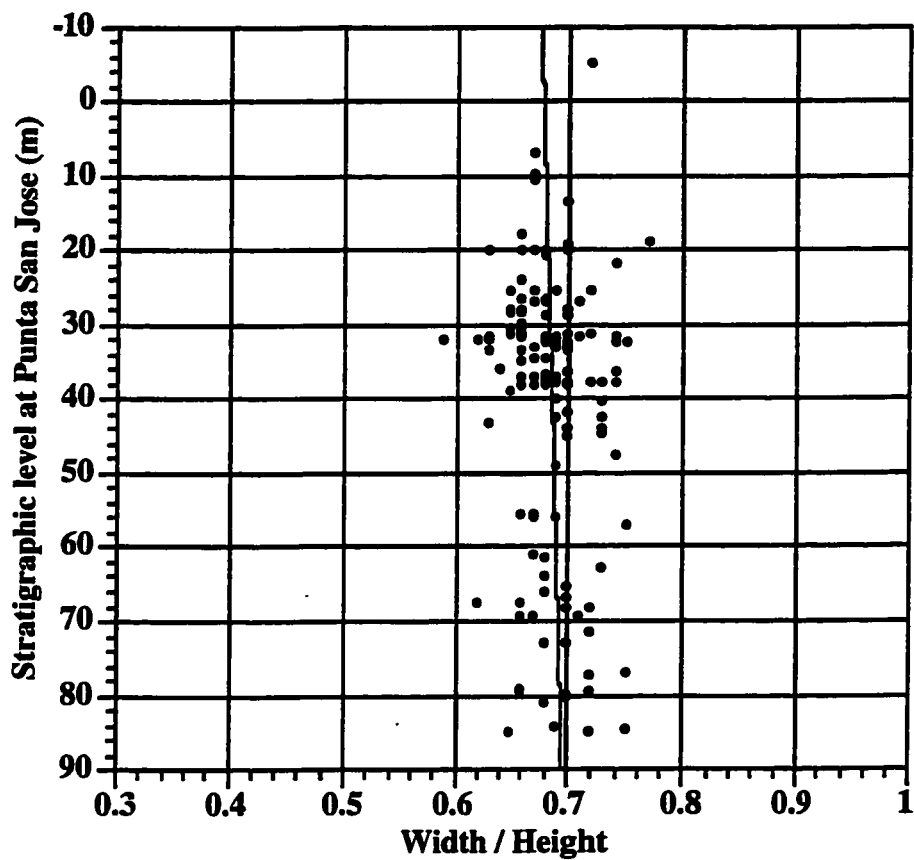


Figure 20. Regression of Width/Height ratio against stratigraphic level at Punta San Jose ($r^2 = 1.8 \times 10^{-2}$).

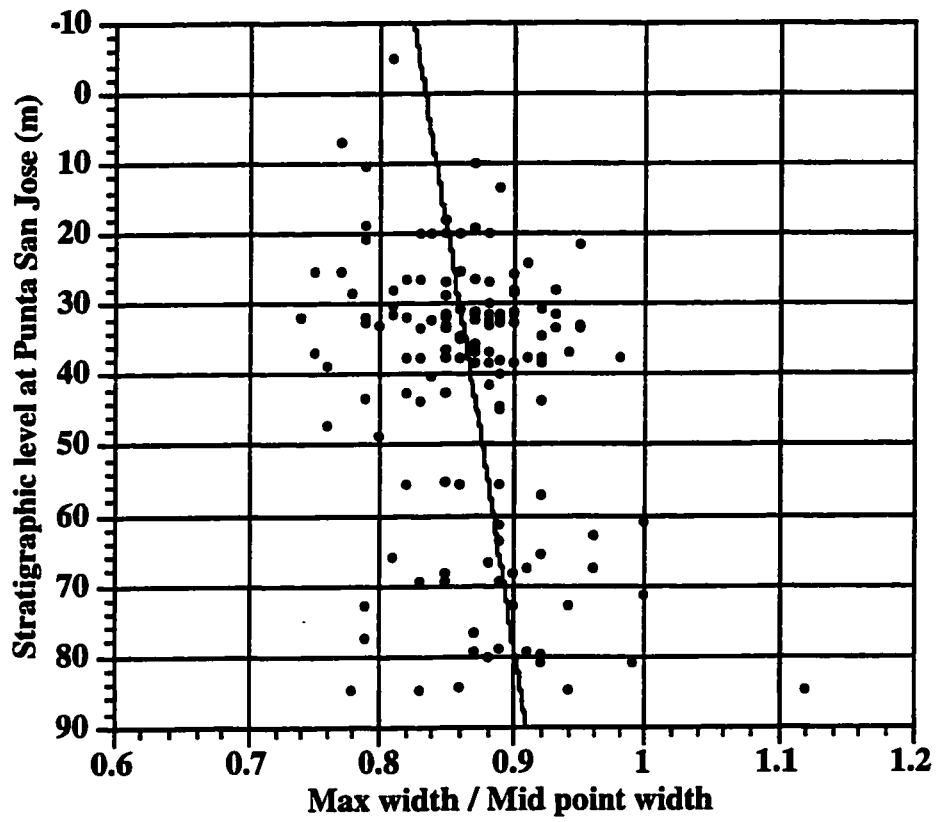


Figure 21. Regression of Max/Mid ratio data against stratigraphic level at Punta San Jose ($r^2 = 8.8 \times 10^{-2}$).

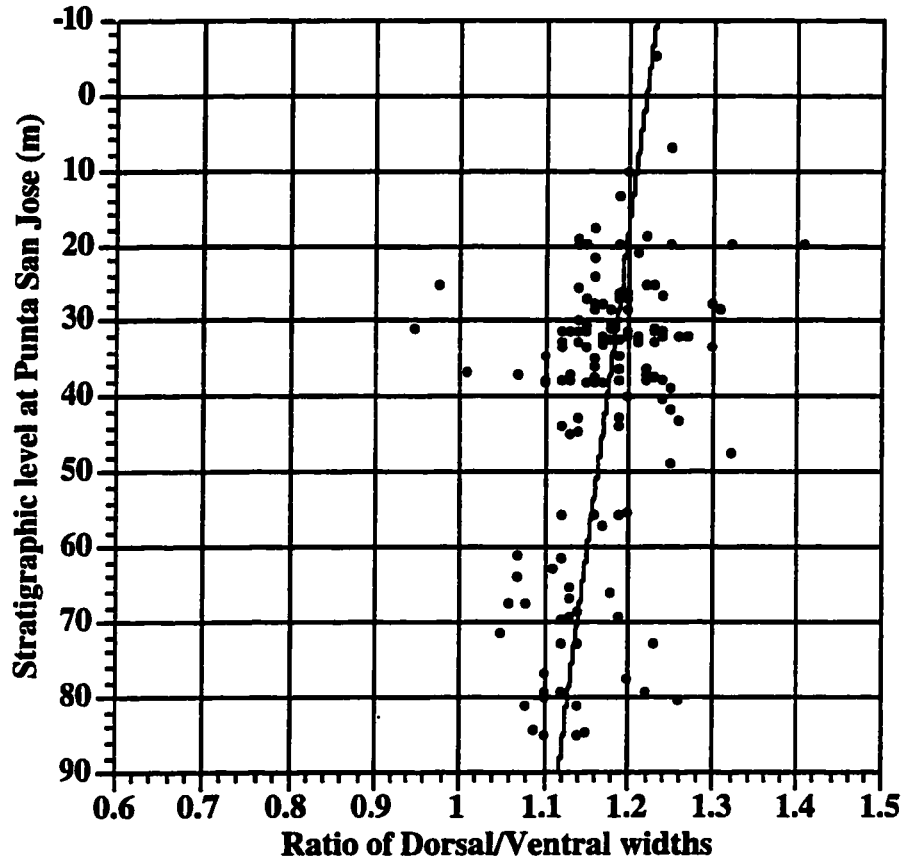


Figure 22. Regression of DW/VW ratio against stratigraphic level at Punta San Jose ($r^2 = 1.2 \times 10^{-2}$).

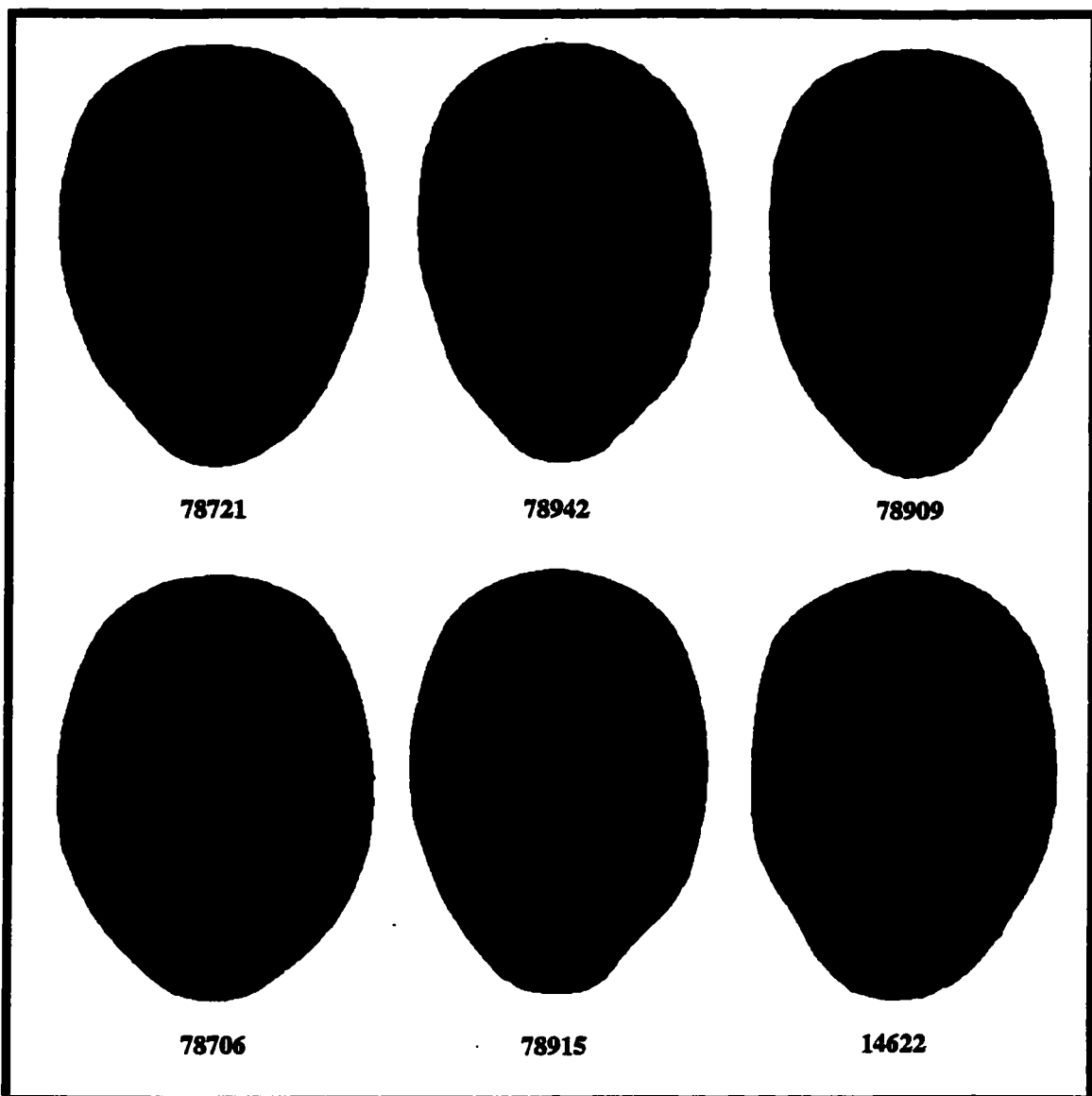


Figure 23. Cross-sections of six specimens from Punta San Jose showing the range of variation in the shape of the venter.

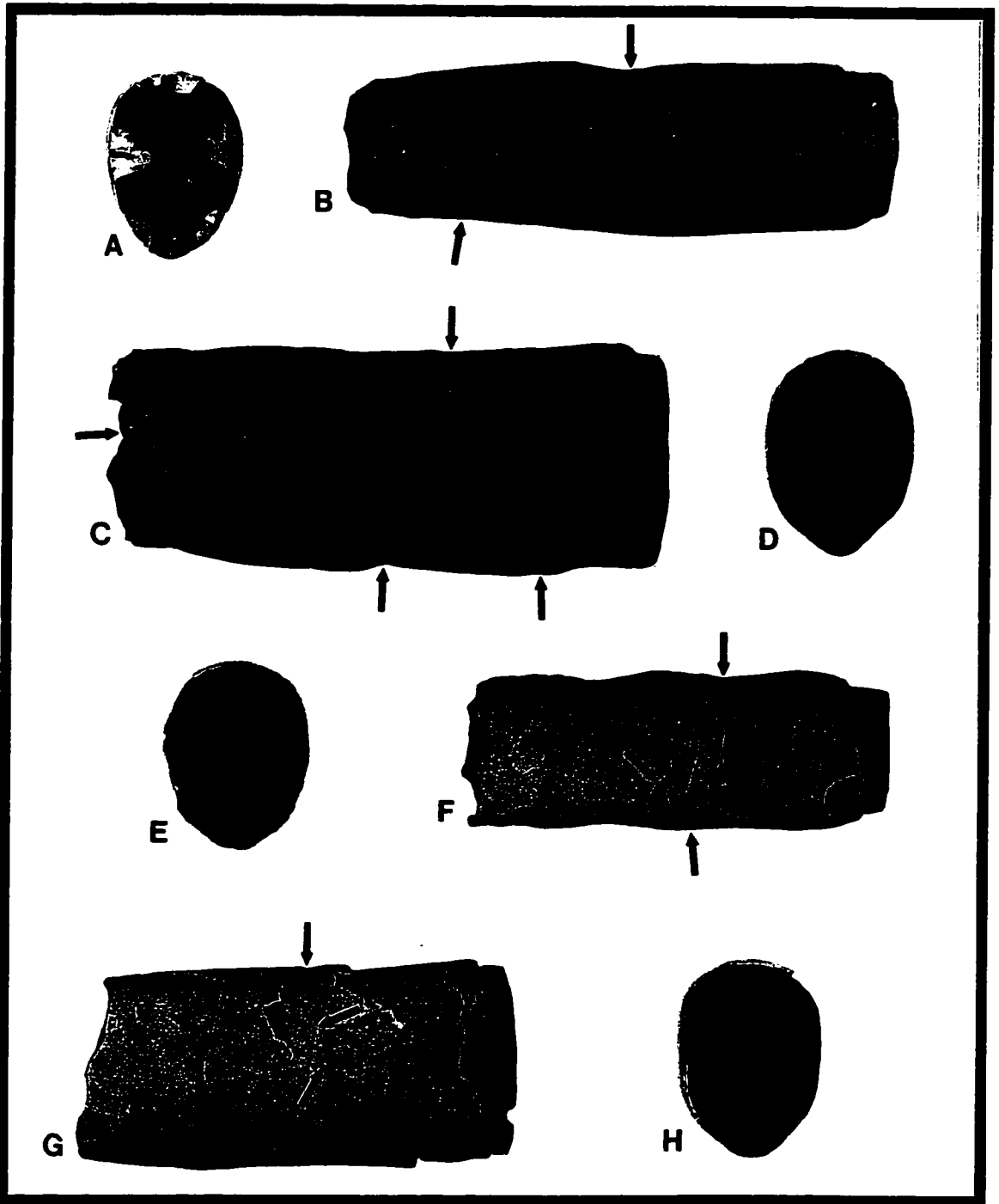


Plate 3A-H: A-D, UWB78718; E-H, UWB78719. Arrows point to edge where the shell has been broken and repaired.

astonishing that the individual survived to repair the wound (Plate 3B, C; Plate 4F, G).

Several types of modification can be seen in injured individuals. In some cases (e.g. UWB95044), the dorsum becomes enlarged relative to the venter. In addition, this individual becomes humpbacked after sustaining damage to the dorsal region of the shell (see Plate 5A-D). The height/width ratio before and after the damage is 1.49 and 1.39, respectively. In a similar example (UWB78927), a large portion of the dorsal region of the shell is broken away resulting in a fattening of the dorsal shoulders (see Plate 4E-H). The change in height/width ratio is from 1.48 to 1.31 in this instance. An additional example is specimen UWB78722, whose cross-section height/width ratio changes from 1.52 to 1.41 after having damage to the dorsal region (see Plate 5E-G).

In some instances, the individual acquires a keel or becomes more keeled after sustaining damage to the more ventral areas of the shell. In the case of specimen UWB78718, the cross-section becomes more squared and becomes keeled after sustaining substantial damage to the ventral area of the shell (see Plate 3A-D). However, the decrease in height/width ratio is not as dramatic (1.47 to 1.41) because the main modification to the shell is the fattening of the previously narrow venter. In a related example (UWB78719), the cross-section becomes straight-sided and the dorsum moderately squared after sustaining damage to the dorsal half of the shell, which is reflected in a change in the height/width ratio (1.60 to 1.10). In this case, the squaring of the side accentuates the projection of this individual's existing keel (see Plate 3E-H).

There are examples where changes in cross-section form are not accompanied by obvious damage, although there is clearly a point where there is a deviation in the growth pattern of the shell. An example of this case is UWB95064 whose cross-section becomes more square sided (see Plate 5H-J). There is obvious modification to the shell, as if the mantle that secreted the shell wall was damaged in some way. However, there is no obvious external damage. This suggests that the mantle used to secrete the shell may be

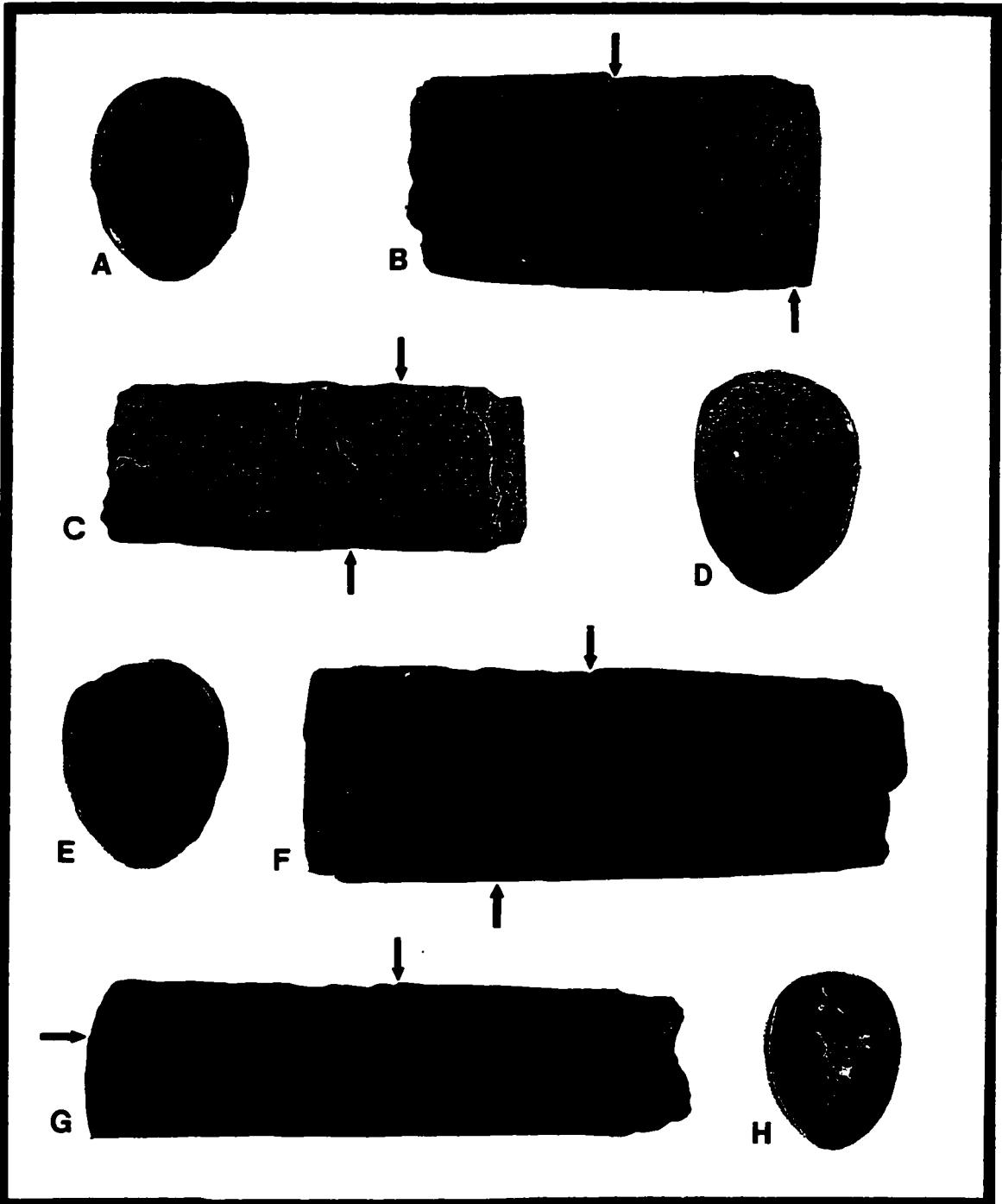


Plate 4: A-D, UWB95044; E-H, UWB78927. Arrows point to edge where the shell has been broken and repaired.

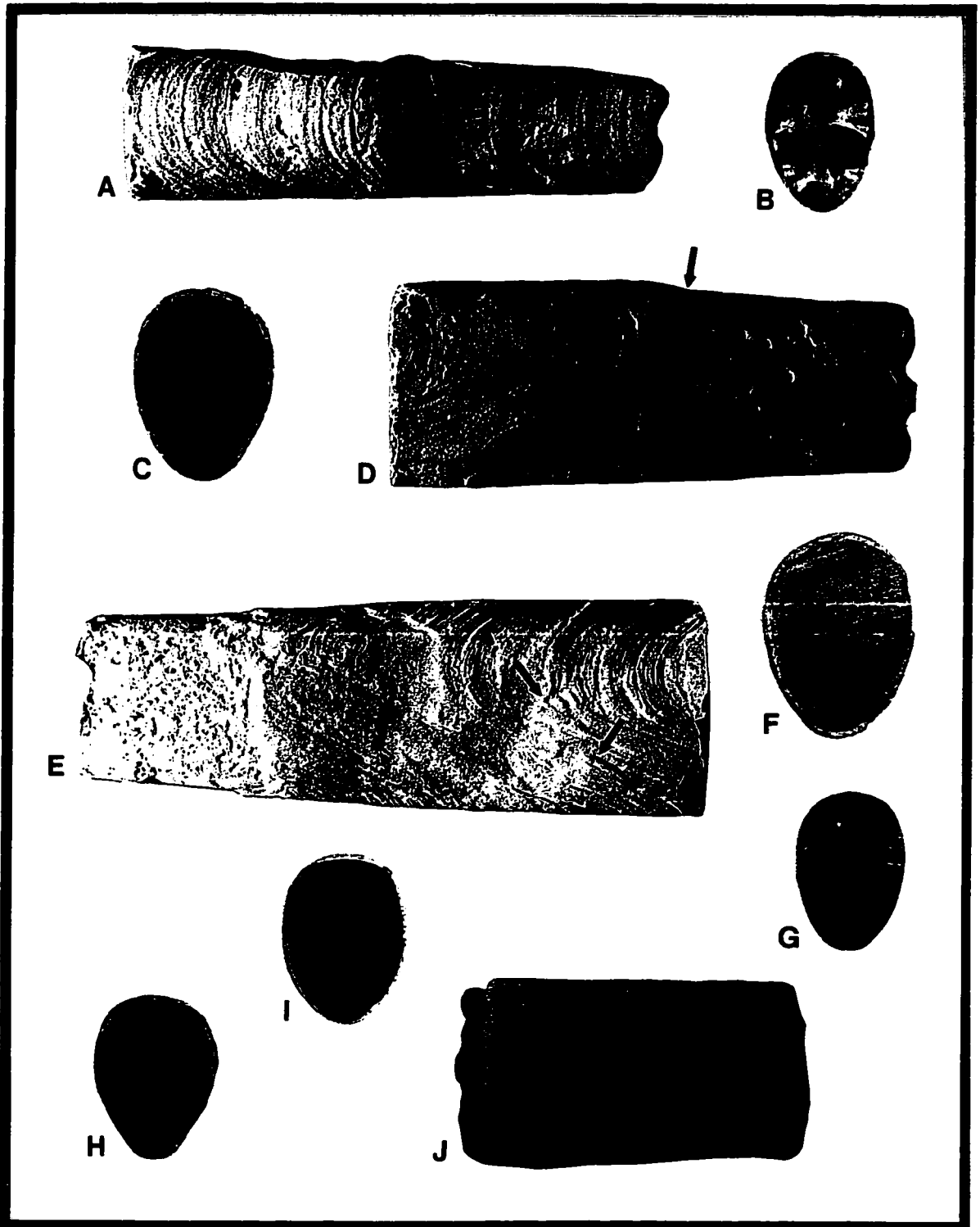


Plate 5: A-D, UWB90044; E-G, UWB78722; H-J, UWB95064. Arrows point to edge where the shell has been broken and/or repaired.

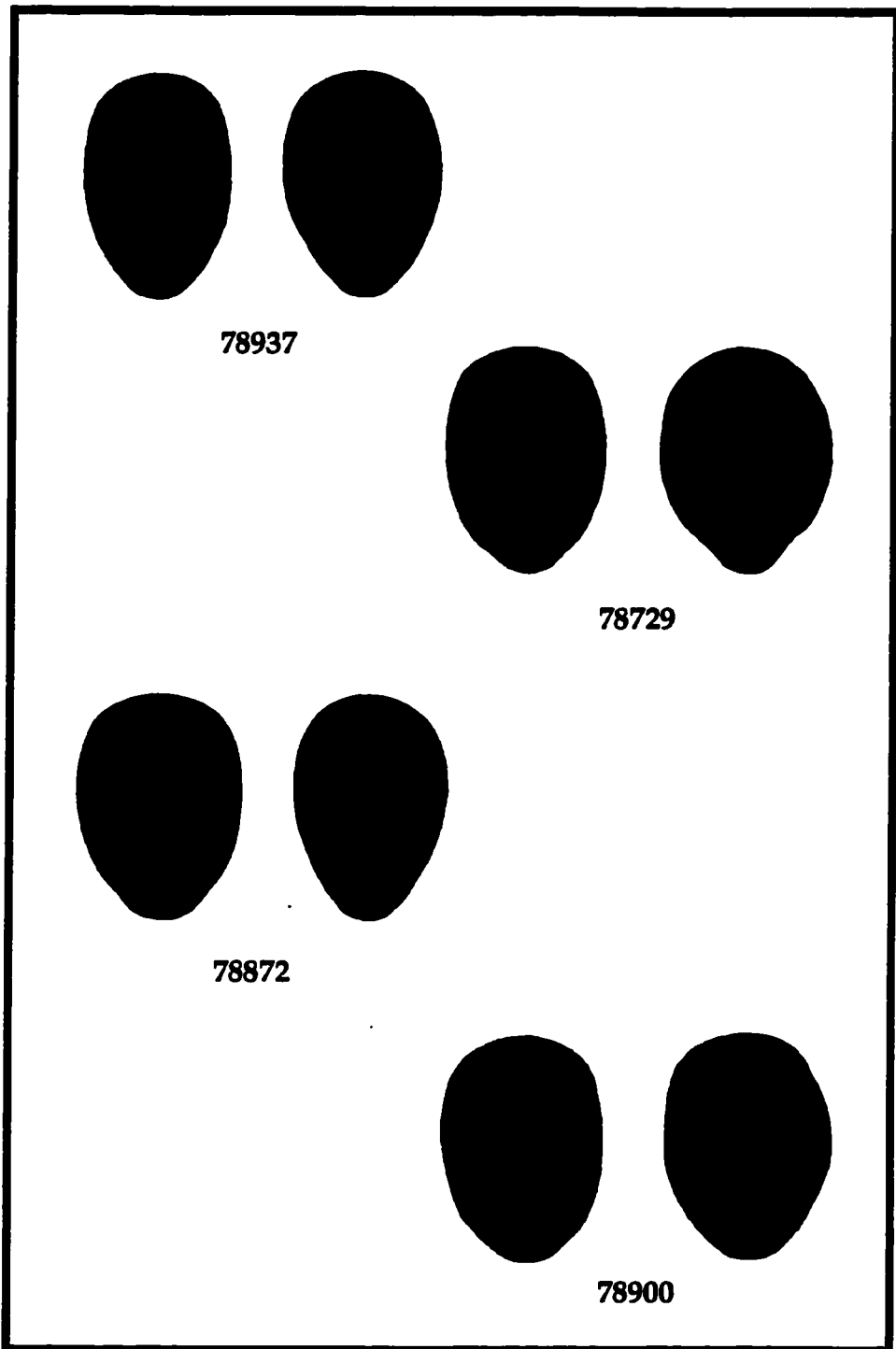


Figure 24. Baculitid cross-sections of four specimens from Punta San Jose that have been sampled twice in order to show some of the range in shape variation possible.

modified without obvious external evidence as to the cause.

Cross-sections of several specimens that were sampled in order to look at the range of cross-section shape found in a single individual are shown in figure 24. The range of shape found among these pairs is substantial. The modification in these examples, or the damaged individuals described above, does not appear to be confined to any particular pattern of response. Modification to the cross-section would theoretically depend on where the phragmacone and animal are injured and be as random or as patterned as the cause of the damage.

In general, damage to the dorsal area appears to produce stouter shoulders or dorsal flanks. In the case of damage to the venter or ventral flanks, the result is a squarer cross-section caused by an expansion of the ventral flank. In other cases, the production of keel-like elevations on the venter or keels, depending on the initial shape, occurs when injuries are received on more ventro-lateral portions of the animal. It may be that the presence of a keel or keel-like elevation of the venter is merely the byproduct of having been injured on the venter or ventral flank..

Damage of the kind described above is not confined to baculitids. Shell damage and repair to Paleozoic ammonoids is described by Bond and Saunders (1989), who suggest that damage of this type is due to failed predation attacks. Similar damage and repair studies have also been done on graphocerid ammonites of the Jurassic by Morton (1983) and Cretaceous scaphitids by Landmann and Waage (1986). An interesting insight of the study on scaphitids is the potential for damaged individuals to take on the morphological characteristics of another species.

Predation damage has not been identified in many studies of ammonoids. It is probable that in many cases poor preservation prevents the observation of damage and repair of cephalopod phragmocones. This would be particularly true in cases where baculitids and other ammonoids are preserved as internal molds. Any damage would be

smoothed over on the interior wall of the shell during repair of the phragmacone. As a result, fossils preserved as internal molds, if they lack any original shell and would not record any marks of the damage.

If predation attacks are the primary way in which cross-section form is modified, the larger (older) a specimen is, the more likely this type of modification has occurred. It can be hypothesized that the cross-section shape will be modified depending on a combination of factors. These are: 1) the region (dorsal, lateral or ventral) in which damage occurs, and 2) the severity of the damage sustained to the shell. Relatively minor damage to a limited region of the shell would result theoretically in a change of shape in that region only. In contrast, heavy damage to the phragmacone would result in significant changes to the cross-section in response to buoyancy and stability problems created by a significant loss of shell material.

The shape of the cross-section before a predation attack may also play a factor in the extent of cross-section shape modification after an attack. For example, a shell with a broad, rounded venter may be more likely to produce a keeled shape than a form that already has a narrow, v-shaped venter after sustaining damage to the ventral region.

It is not clear to what extent any modification of the cross-section becomes permanent during the subsequent growth of the animal. The degree of shape modification in an individual would depend theoretically on the number and severity of attacks sustained over its lifetime. It is possible that not sustaining damage over a long enough period of time would allow the animal to stabilize the cross-section to a specific shape that is diagnostic at the species level. Alternatively, the individual would continue to sustain the most recent shape change throughout its lifetime. These theoretical considerations and the observations made above suggest that a more complex, multivariate analysis of cross-section form needs to be used in order to assess the variation in this morphological character.

CROSS-SECTION SHAPE ANALYSIS

Baculitids as a group are unique among the ammonites because they grow a relatively straight phragmacone throughout most of their life. Because baculitids do not coil planispirally, the cross-section of baculitids is more easily studied than in some other ammonite groups where successive coils of the shell touch throughout ontogeny. With minor preparation, the perimeter of the living chamber of a baculitid can be traced. The perimeter tracing can then be used as the basis for multivariate shape analyses.

Cross-sections of baculitids from Punta San Jose (n=154) and the Sucia Islands (n=37) were processed for analysis. The sample set from Punta San Jose is from the full range of cross-section forms found at Punta San Jose. The sample set includes the full range of cross-sections forms, because it is hoped that a multivariate analysis will identify discrete species-level groups in the population of baculitids at Punta San Jose. The sample set from the Sucia Islands consists of specimens identified as the species *Baculites inornatus*.

Each specimen was cut across the larger oral end, perpendicular to the dorsal side, and avoiding any exterior ornamental projections. Shell material was then removed a few millimeters back from the trimmed edge to expose the internal cast of the shell. The cross-section face was blackened and the perimeter wrapped with white clay in order to enhance the edge of the cross-section. The perimeter of the cross-section was traced using a PC-based video digitizing system running the software JAVA (now Sigmascan). In each case the trace was initiated on the ventral side at the point of greatest diameter. The x,y coordinates of approximately 1000 points were recorded from around the perimeter of the specimen cross-section. The equivalent starting point is used in each case. The snapshots of the cross-sections were saved as video files.

The resulting outlines were then processed using the program "x,y-phi*" provided by Dr. Norm MacLeod. This program resamples the ~1000 points for a subset of 100

equally spaced points that are interpolated from the original data. The 100 points are also converted from their x,y coordinates into polar coordinates and used to generate the $f^*(l)$ function of Zahn and Roskies (1972). In this case, the $f^*(l)$ function consists of 100 measurements of angular deviation from a circle (Lohmann and Schweitzer, 1988). In other words, the values used to generate the $f^*(l)$ function are the net angle by which the n th point along the perimeter (l) of the sample deviates from the n th point along the perimeter of a circle. The perimeter length (l) is a function of specimen size. The larger the perimeter, the larger the spaces between the 100 equally spaced points that make up the function. The larger spacing between points results in a larger amplitude in the function. To look at form without regard to size, we need only standardize (l) and compare the 100 measurements that make up the f^* function for each specimen measured (Lohmann and Schweitzer, 1988).

In order to test the hypotheses 1) that baculitid species have unique cross-section shapes and 2) that keeling is a species-level characteristic, the outline data have been used in several ways. Conventional cluster analysis is used to see if species groups can be identified based on cross-section shape. Eigenshape analysis is used to identify the major components of form that account for the variation in the data sets studied. As stated before, the data set from Punta San Jose is thought to sample all baculitid forms from that locality. Therefore, it is expected that groups identified by both the cluster and eigenshape analyses will correspond to known species. In this case, the expected species are *Baculites inornatus* and *B. rex*.

CLUSTER ANALYSIS

Cluster analysis was performed on the specimens using similarities in the shape of the cross-section outlines. The 100 measurements for each sample were standardized to unit variance (down the column of measurements, not across samples for each

measurement). Using the program SYSTAT, the similarities in the shape functions were measured as correlations among specimens (Pearson Correlation Metric). Cluster analysis was then performed on the resulting correlation matrix using the JOIN option (Hierarchical Clustering Method), the Euclidean distance metric and the average linkage method of Sokal and Michner (1958). This produces a tree diagram which graphically illustrates the hierarchical relationship among all samples in the group analyzed.

Cluster analysis was performed on one data set consisting of specimens from Punta San Jose, one data set consisting of specimens from the Sucia Islands, and a combined set of specimens from both localities. The results of these analyses are found in Figures 25, 26, and 27, respectively.

DISCUSSION OF CLUSTER ANALYSES

Cluster analysis of the Punta San Jose data set alone grouped a significant portion of the data set in one central cluster with several smaller peripheral clusters (see Fig. 25). This is a surprising result. The expectation was that two large groups would be identified by the cluster analysis and that these groups could be assigned to either of two species, *Baculites inornatus* and *B. rex*. However, this analysis groups the data as one large, highly variable group and several smaller concentrations of individuals with extreme cross-section shapes.

Cluster analysis of the Sucia Islands data set groups the data in a similar way with a large central cluster surrounded by much smaller peripheral groups or scattered individuals (see Fig. 26). As the Sucia Islands area is the type area for the species *B. inornatus*, this is not surprising. However, the range of variation in the central group is considerable.

Analysis of the combined set clusters the data in an unexpected, yet interesting way. Once again, there is one large central cluster with much smaller peripheral clusters (see Fig. 27). However, specimens from both the central clusters of the Punta San Jose and Sucia

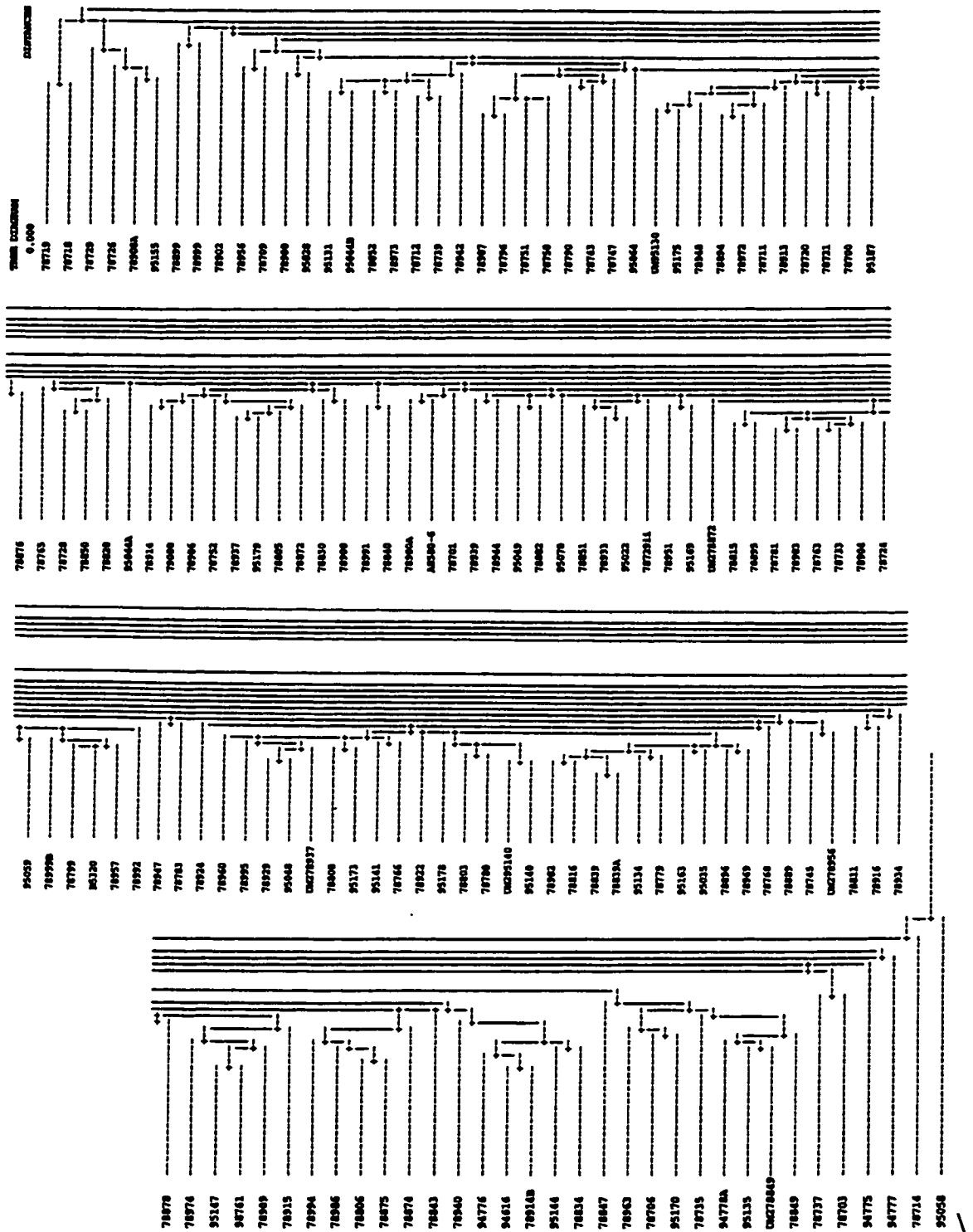


Figure 25. Graphic output from hierarchical cluster analysis of Punta San Jose data set (n=154). Analysis used euclidean distance metric and the average linkage method. Read left to right, top to bottom. Total distance of tree is 1.000 units.

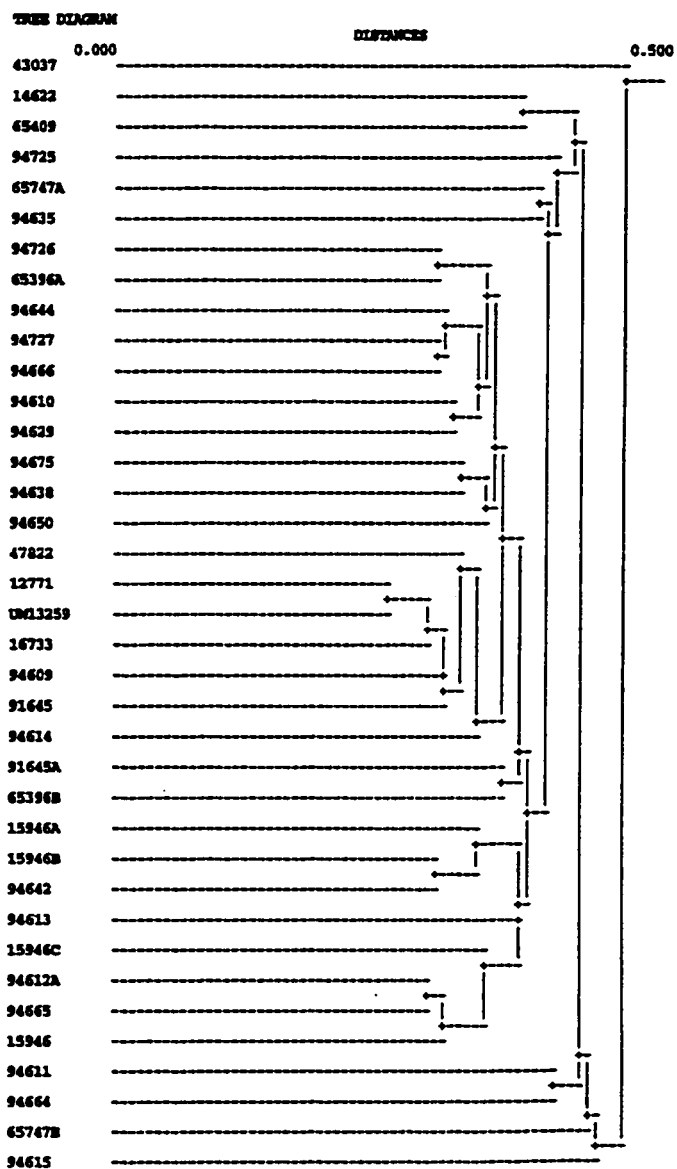


Figure 26. Graphic output from hierarchical cluster analysis of Sucia Islands data set (n=37). Analysis was done using a euclidean distance metric and the average linkage method. Total distance of tree is .500 units.

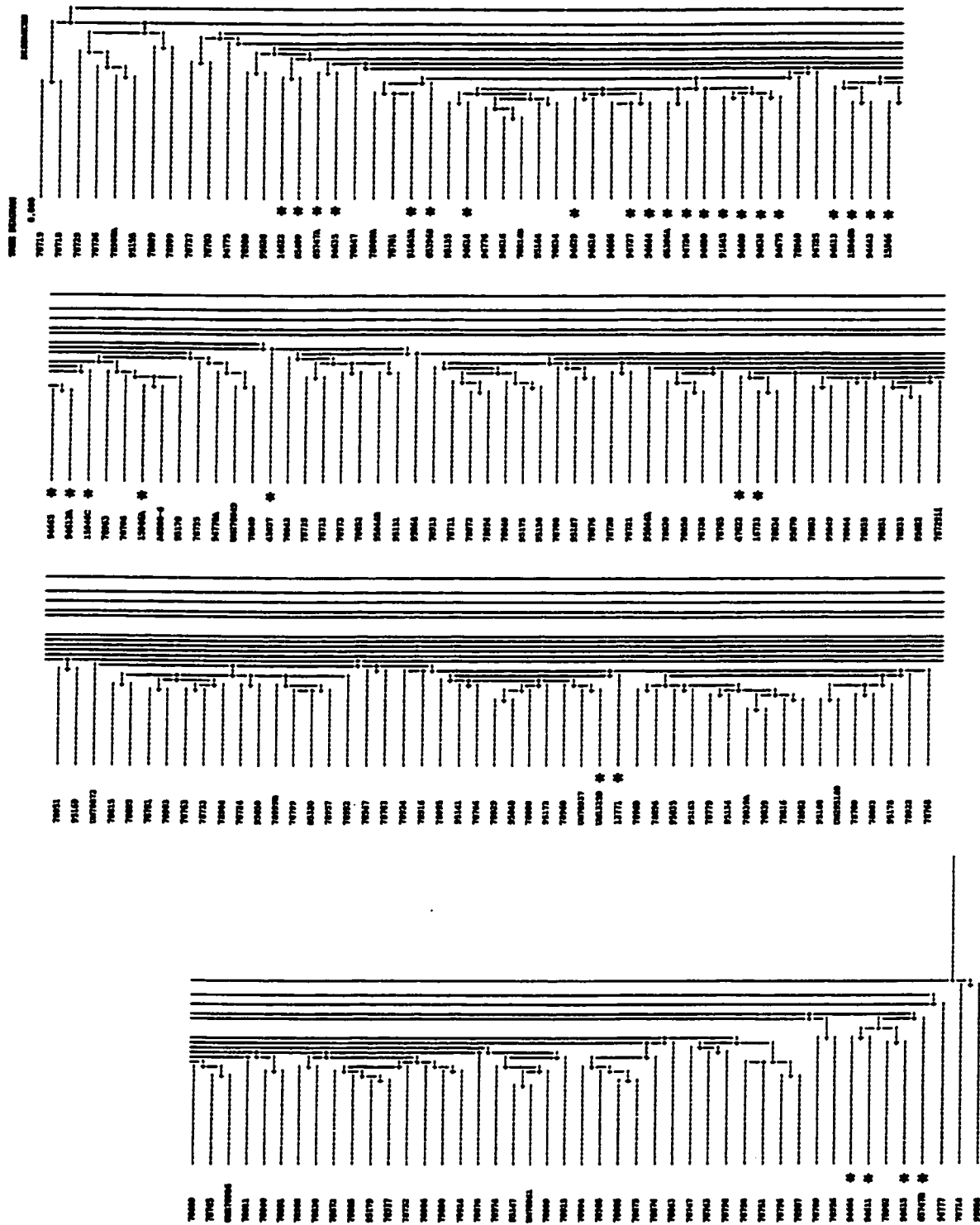


Figure 27. Graphic output of hierarchical cluster analysis of Combined data set (n=191). Read from left to right, top to bottom. Analysis used a Euclidean distance metric and the average linkage method. Total distance of tree is 1.000 units. (*) labels specimens from the Socia Islands.

Islands are found grouped together within the central cluster of the combined set, surrounded by the outlying members of the Punta San Jose data set.

While specimens from the Sucia Islands are generally grouped at one end of the central cluster, the separation between the Sucia Islands specimens and the Punta San Jose specimens is not a clean one. There is a some intermixing of specimens from these two localities.

Overall, the analysis of the combined set would suggest that the majority of specimens from the Sucia Islands and from Punta San Jose together form some sort of shape continuum that represents some part of a complex morphocline. Given that the Punta San Jose data set potentially includes specimens that could be assigned to at least three known forms (*Baculites inornatus*, *B. anceps pacificus* and *B. rex*) using only cross-section as the criteria, this analysis would imply that cross-section shape is very plastic and that species concepts that are based only on this morphological feature are suspect.

EIGENSHAPE ANALYSIS

In order to understand the shape variation found in the cross-section data sets used in the cluster analysis, the set of 154 baculitid cross-sections from Punta San Jose, Baja California, the set of 37 cross-sections from the Sucia Islands, WA, and the combined data set of 191 cross-sections were analyzed analysis using the program EIGENSHAPE written by Dr. Norm MacLeod. Analysis of the set from the Sucia Islands is used to describe the morphological variation for a known species so that there is some reference group to use as a guide during the interpretation of the data set from Punta San Jose, where *B. inornatus* is also found.

Eigenshape analysis can be viewed as a form of principal components analysis using the shape f^* functions of each shape as data. More simply, eigenshape analysis is a method of identifying the primary ways in which the cross-section shapes vary within the

group being analyzed. As in principal components analysis, eigenshape analysis can be based on either a matrix of covariances or correlations (standardized data set).

Any number of eigenshape vectors can be produced up to and equal to the number of samples analyzed. However, it is usual for the first five eigenshape vectors to account for a high percentage of the variance in the data. During analysis, a mean shape is produced for the data set, as well as a set of eigenshape functions that reflect the variation explained by the associated vectors. In addition, the loadings for individual specimens on each eigenvector are produced for the sample set. The loadings for each vector can then be plotted against each other and used as a visual aid in identifying patterns of variation in the data set.

One significant difference between eigenshape analysis and conventional principal components analysis is that the matrix of correlations is composed of data that are standardized, not across samples for each variable, but down column for each sample (Ray, 1988). This type of standardization, as noted above, is used in order to look at shape without regard to variation due to differences in size. In practice, using the correlation matrix as the basis for eigenshape analysis means that the first component of variation measures the similarity of each shape to the mean instead of describing the first component of variation about the mean. Because the first vector explains the highest percentage of variation in the data set, it is more informative to use the covariance matrix for analysis. However, using the covariance matrix means the analysis is based not only on form but also on the attributes of angularity and size (Lohmann and Sweitzer, 1988). Because ammonites grow continuously, it would be necessary to section and study a stepped series of cross-sections from each individual in order for the analysis to be meaningful. This type of study would be premature as there is not even the most basic understanding of variation in form for baculitids. Therefore, the analysis is limited to the study of form without regard to size.

It would be preferable to be able to analyze the shape data using the covariance matrix, as the first component accounts for greater than 90% of the variance in these particular data sets. This analysis can be accomplished by scaling each specimen to the same size (cross-section height) during the process of digitizing the outline and recording the outlines as pixel data. In this way, the outlines are effectively standardized before the shape analysis is done. As a check on this method of standardization, the same data sets were run using both covariances and correlations, and the first five eigenshapes from each analysis were compared (see Fig. 28). There are no significant differences in the shapes implying that this new method of standardization is a robust approximation of the standardization performed by the program EIGENSHAPE during an analysis based on correlations. All eigenshape analyses used for this study were standardized using the new method and processed using the covariances of each data set.

RESULTS OF EIGENSHAPE ANALYSIS

The first five components of the eigenshape analysis of the data set from Punta San Jose described 92.005%, 1.162 %, 0.821%, 0.596% and 0.567% of the variation, respectively. The list of the eigenvectors and the covariances of each specimen with the first 5 vectors can be found in Appendix A. The first five eigenshapes and a series of cross-sections illustrating the variation in shape represented by the associated vector are found in figure 29.

As in the analysis from Punta San Jose, the first 5 eigenvectors from the analysis of the data set from the Sucia Islands explained 95% of the variance. Individually, the 5 vectors accounted for 92.331%, 0.985%, 0.640%, 0.559%, and 0.503%, respectively. The list of covariances with the first five eigenvectors is found in Appendix A. Figure 30 shows the first five eigenshapes and a series of cross-sections from the data set that represent the range in shape variation for each relevant eigenvector.

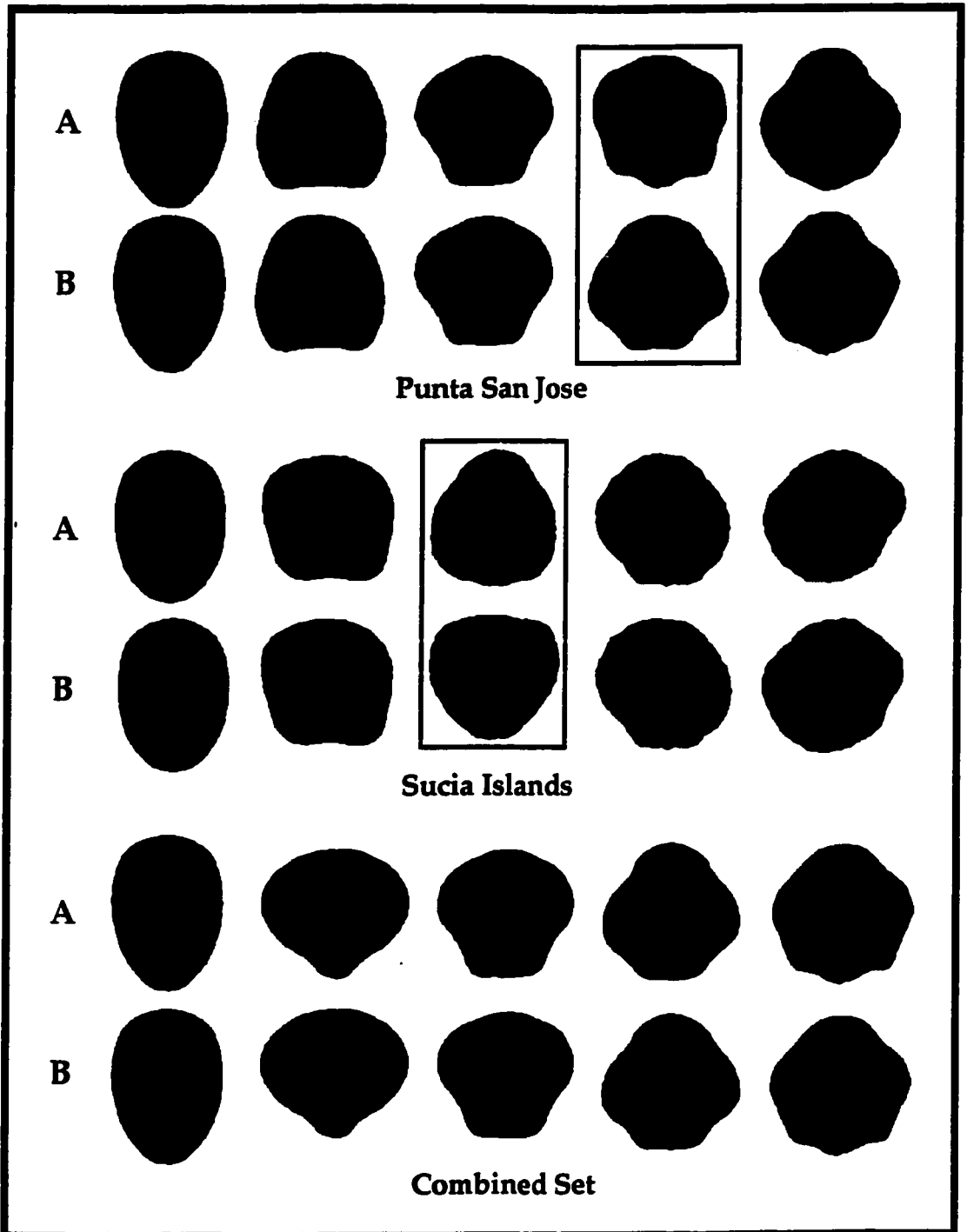


Figure 28. The first five eigenshapes generated by Eigenshape Analysis of the data sets from Punta San Jose ($n=154$), the Sucia Islands ($n=37$) and the Combined data set ($n=191$). The shapes in row A of each series were generated by analysis based on covariances. The shapes in row B were generated using correlations among the specimens. The shapes outlined by a box are from eigenvectors whose polarity was switched when the analysis was run using correlations instead of covariances.

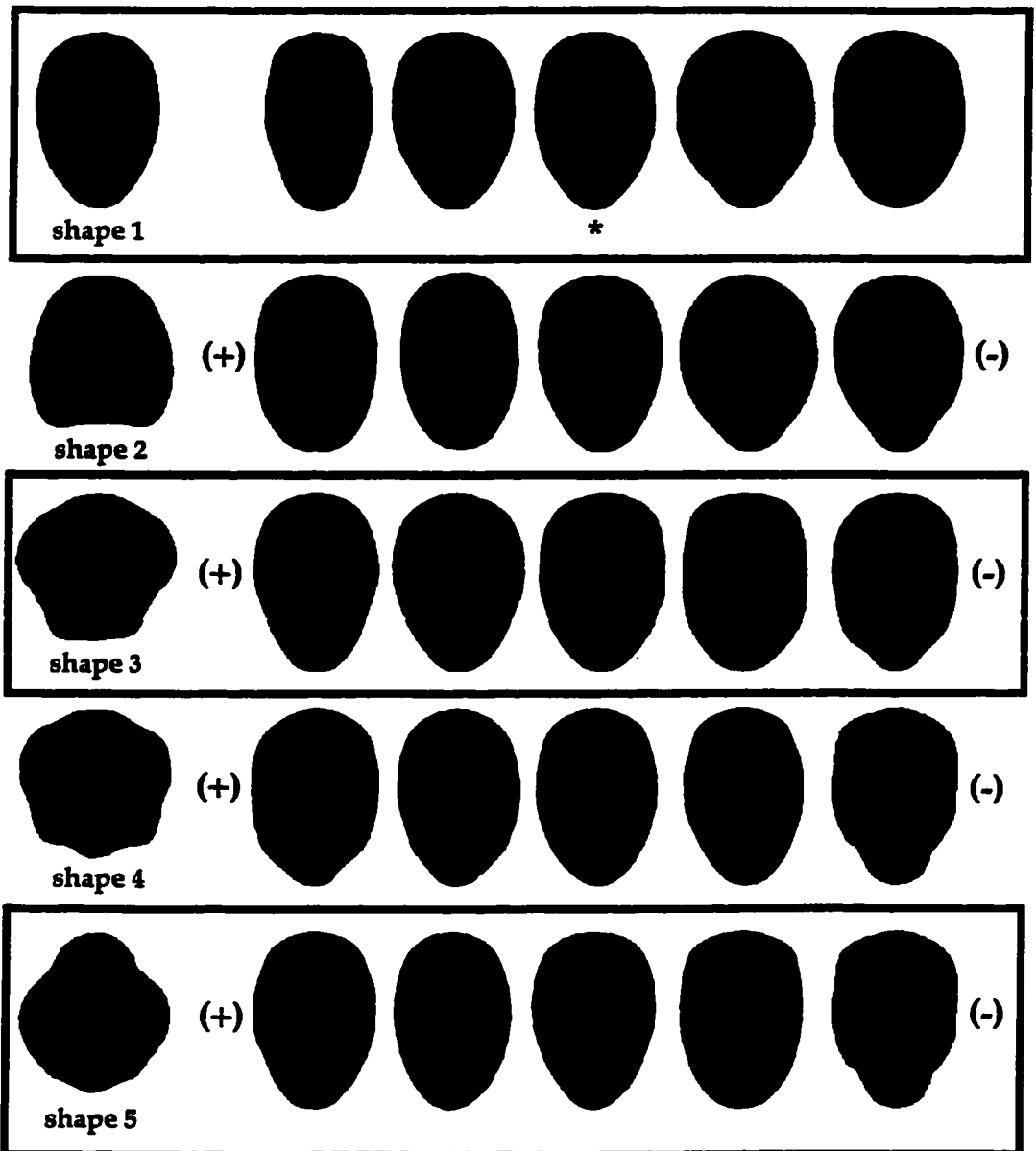


Figure 29. The first five eigenshapes for the dataset from Punta San Jose ($n=154$). In the case of shapes 2-5, the series of cross-sections associated with each shape illustrates the variation from the positive (+) to the negative (-) end of the vector. The first shape resembles the mean shape for the analysis and is most closely resembled by the shape in the middle of the first series labeled (*).

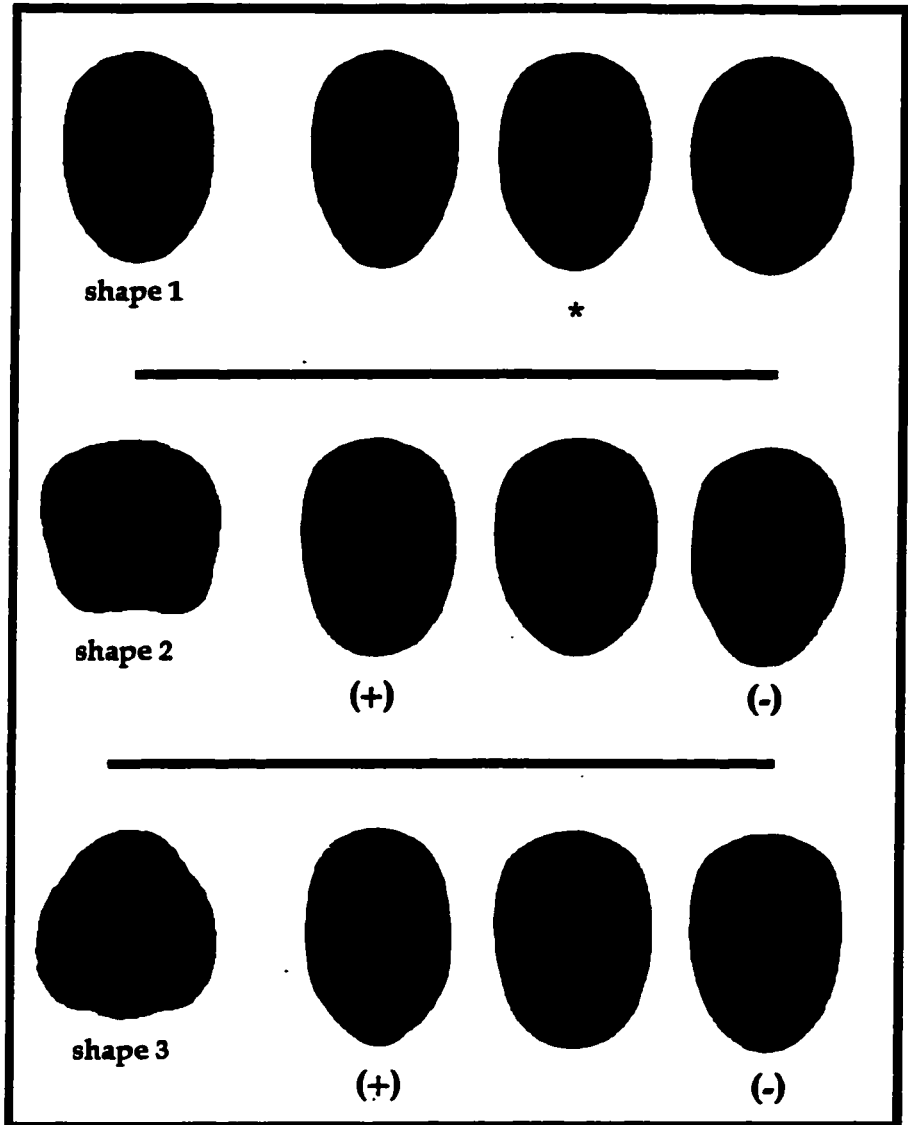


Figure 30. The first five eigenshapes for the dataset from the Sucia Islands ($n=37$). In the case of shapes 2 and 3, the series of cross-sections associated with each shape illustrates the variation from the positive (+) to the negative (-) end of the vector. The first shape resembles the mean shape for the analysis and is most closely resembled by the shape in the middle of the first series labeled (*).

Analysis of the combined data sets from Punta San Jose and the Sucia Islands produced 5 eigenvectors that account for 91.492%, 1.484%, 0.744%, 0.575% and 0.552%, respectively, for a total 94.85% of the total variance explained. The list of the eigenvectors and the covariances of each specimen with the first 5 vectors can be found in Appendix A. The first five eigenshapes and a series of cross-sections illustrating the variation in shape represented by the associated vector are found in figure 31.

INTERPRETATION OF EIGENSHAPE DATA - PUNTA SAN JOSE

The first eigenshape from the analysis of the Punta San Jose data set resembles the meanshape and looks most like a baculitid cross-section (see Figs. 28 and 29). This resemblance is because the first eigenshape vector accounts for most of the variation in the data set. Therefore, the first shape describes features that are common to the group. The rest of the shapes represent the variation that makes the objects look different. When looking at shapes 2-5 for any analysis, discriminating the shape characteristics associated with the positive end of the related eigenvector can be done by looking for how each eigenshape deviates from a circle.

As can be seen by the series of shapes representing the variation described by the first eigenvector, forms with low covariances are stoutly shaped with large width/height ratios. Forms with high covariances have slim shapes and low width/height ratios. The second eigenshape vector scores the data set based on the absence or presence of a keeled venter. Specimens with high scores are elliptical in shape with rounded venters, while cross-sections with low scores have keeled venters. Specimens with high covariances to the third eigenshape vector have cross-sections that flare out just above the lateral midline and broadly rounded venters. Specimens with low scores are relatively straight-sided with narrow venters. Specimen cross-sections that approach the 4th eigenshape in form have broadly rounded shoulders, narrow venters and a flaring of the cross-section perimeter just

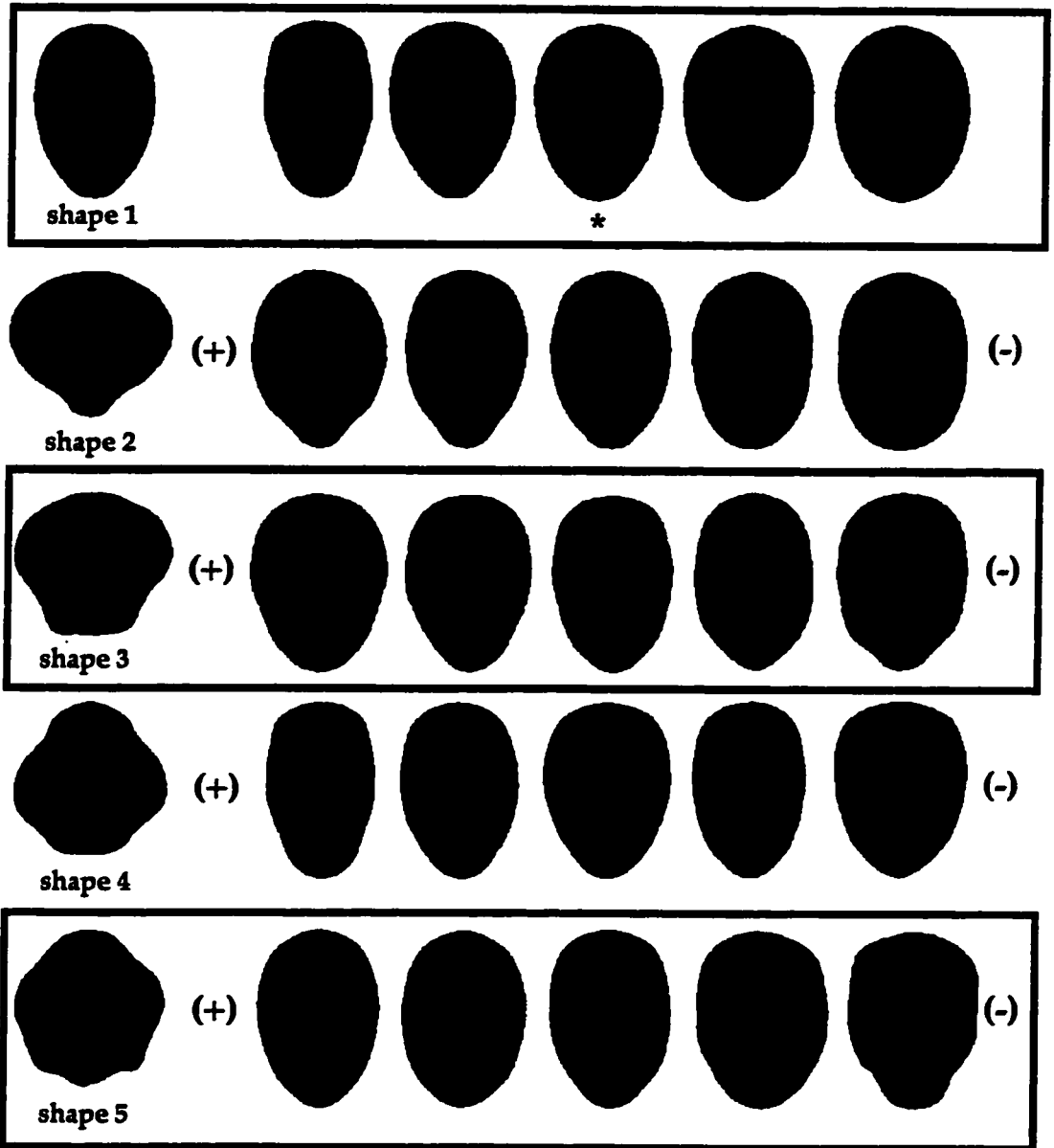


Figure 31. The first five shapes from the eigenshape analysis of the Combined Dataset ($n=191$). In the case of shapes 2-5, the series of cross-sections associated with each shape illustrates the variation from the positive (+) to the negative (-) end of the vector. The first shape resembles the mean shape for the analysis and is most closely resembled by the shape in the middle of the first series labeled (*).

above the venter that accentuates the narrowness of the venter. Specimens with low covariances have, in general, squared shoulders, and cleanly v-shaped, broadly rounded venters. The 5th eigenvector represents very subtle changes in the shape of the cross-section shoulders and the ventral flanks. Shapes with high covariances have obtusely squared shoulders, and the ventral flanks bend in towards the venter close to the venter. Specimens with low scores have more acutely squared shoulders while the bending of the ventral flanks towards the venter is initiated at a higher position along the flanks.

Plotting the individual specimen scores for various combinations of eigenvectors allows for a visual look at the data set in order to see if groups of any significance can be identified. Figures 32 and 33 show the plots for the Punta San Jose data set. In general, the plots of eigenvector 1 with the next four eigenvectors in figure 32 show a large central group surrounded by small peripheral groupings of no significance. The plots in figure 33 show less coherence to the central group, with very random distributions to the scores. The difference in the distributions for the two figures is due to the large amount of variance (>90%) associated with the first eigenvector for the data set.

The scores of the 5 eigenvectors were then plotted against size in order to see if any systematic trends could be identified. As can be seen in figure 34, there are no significant relationships between any of the eigenvector scores and specimen size. However, there is an expansion in the distribution of scores for eigenvector 1 with increased size. This expansion also originates around the mean score for the vector.

In addition, the scores for the five eigenvectors were plotted against stratigraphic height at Punta San Jose (see Fig. 35). There are no statistically significant trends to the data. However, there is a broad trend in the data for eigenvector 3 that suggests a general shift in shape variation over time. In this instance, there is an overall shift from positive values to negative values. This corresponds to a morphological change from more straight sided to more ovoid forms (see row 3 of figure 29). There are not enough data from the

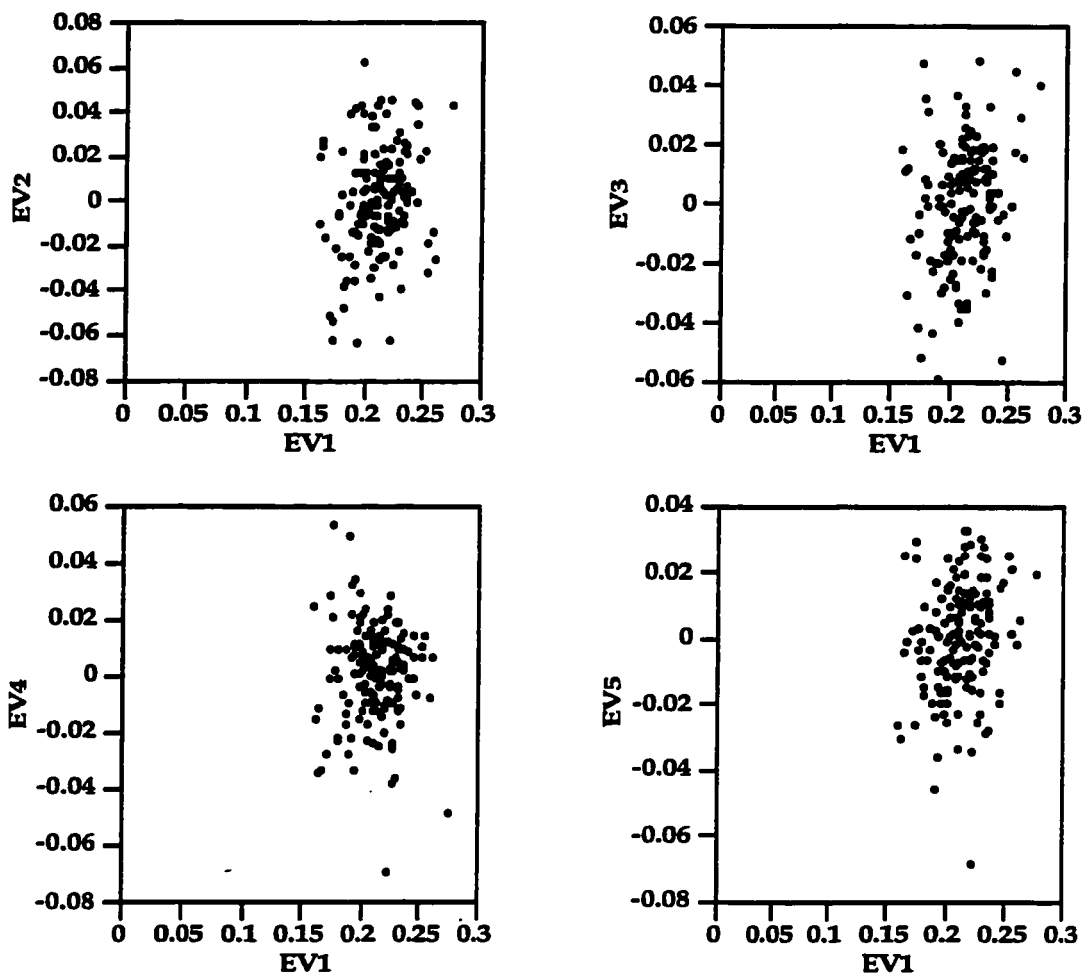


Figure 32. Plots of the individual specimen scores on the first eigenvector and next four eigenvectors for the Punta San Jose data set (n=154). Eigenshape analysis was based on covariances.

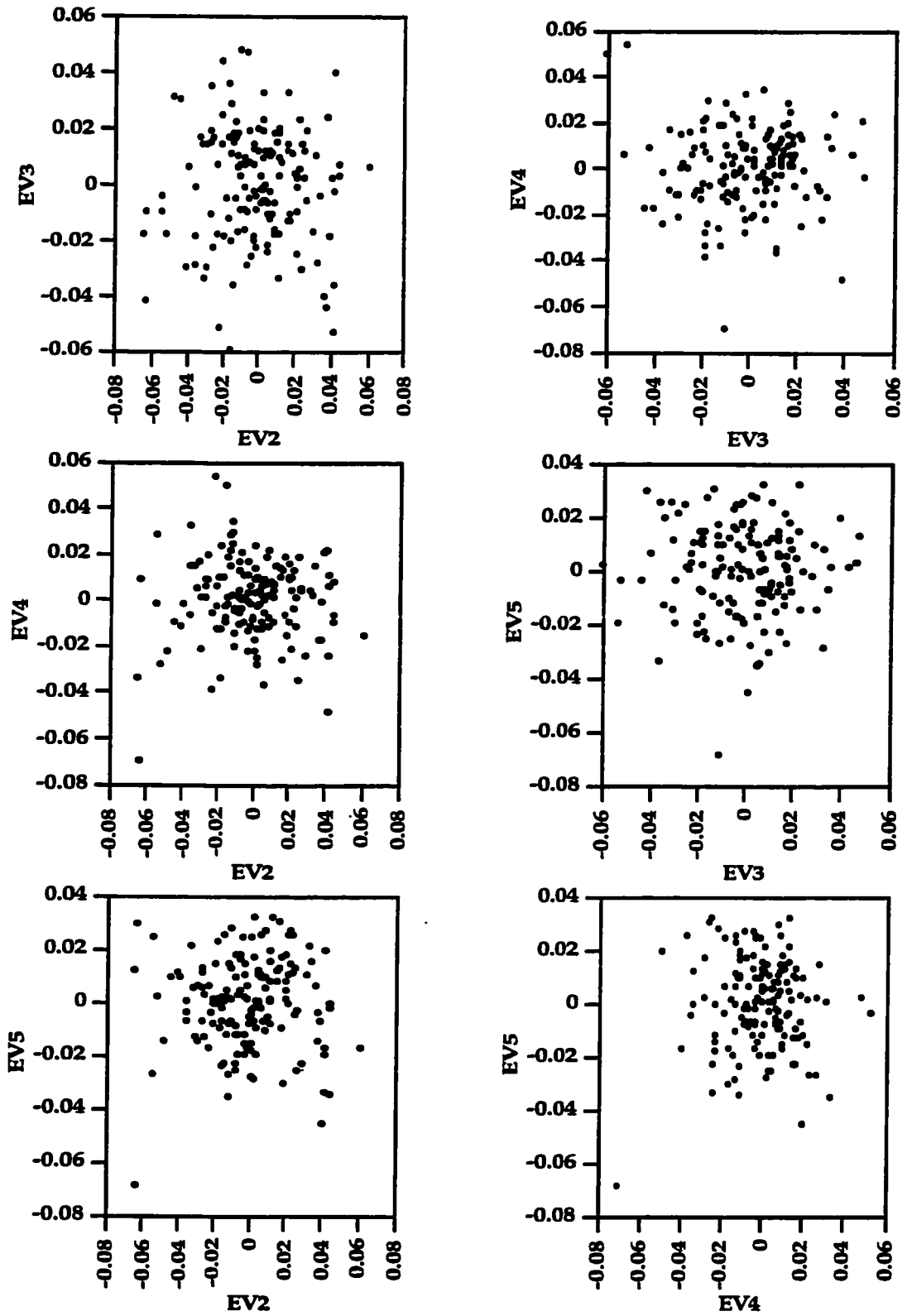


Figure 33. Plots of individual specimen scores on various combinations of eigenvectors from the eigenshape analysis of the Punta San Jose data set (n=154).

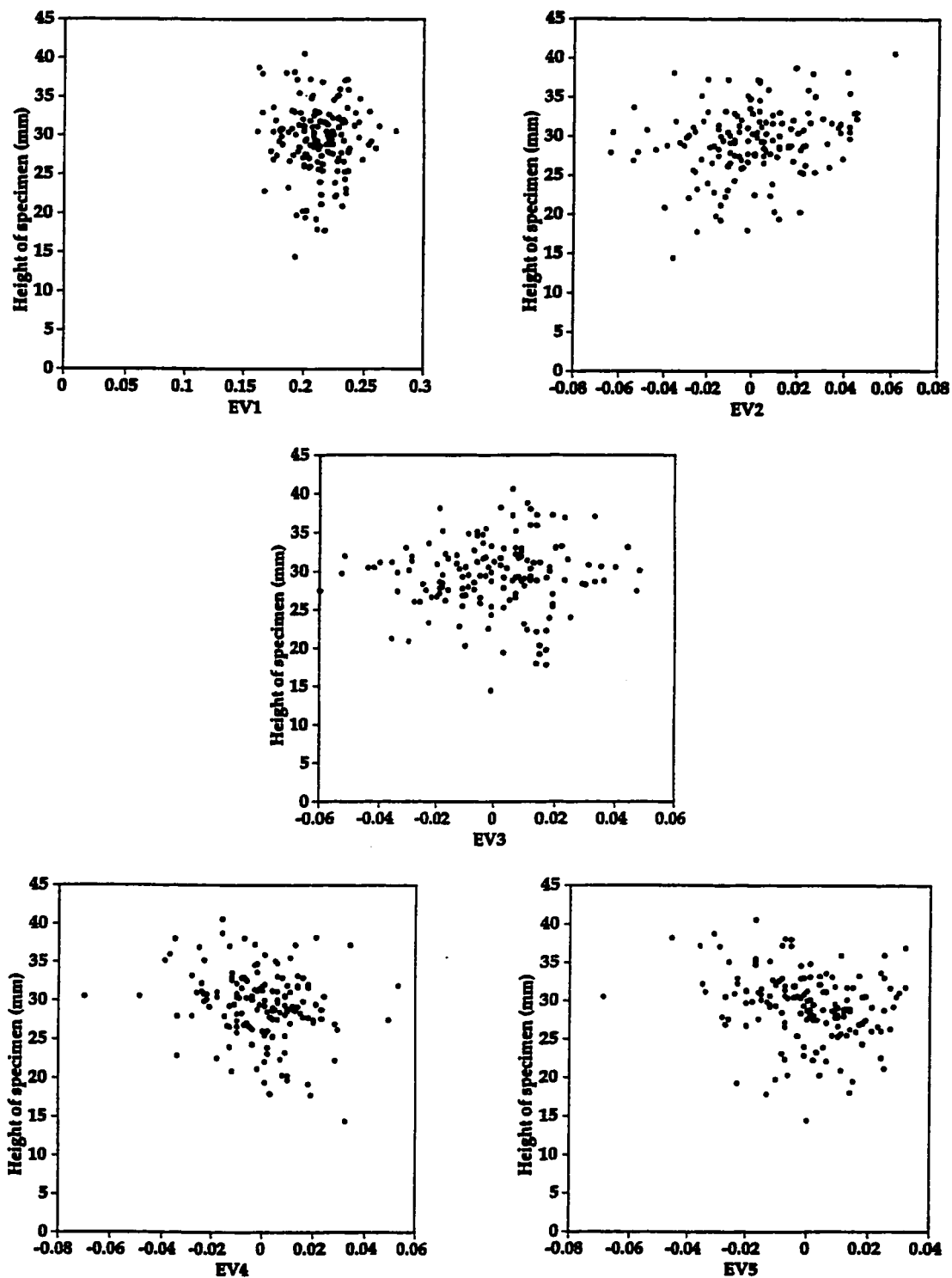


Figure 34. Plots of individual specimen scores on eigenvectors (1-5) vs. height of specimen (size) from the Punta San Jose data set (n=154).

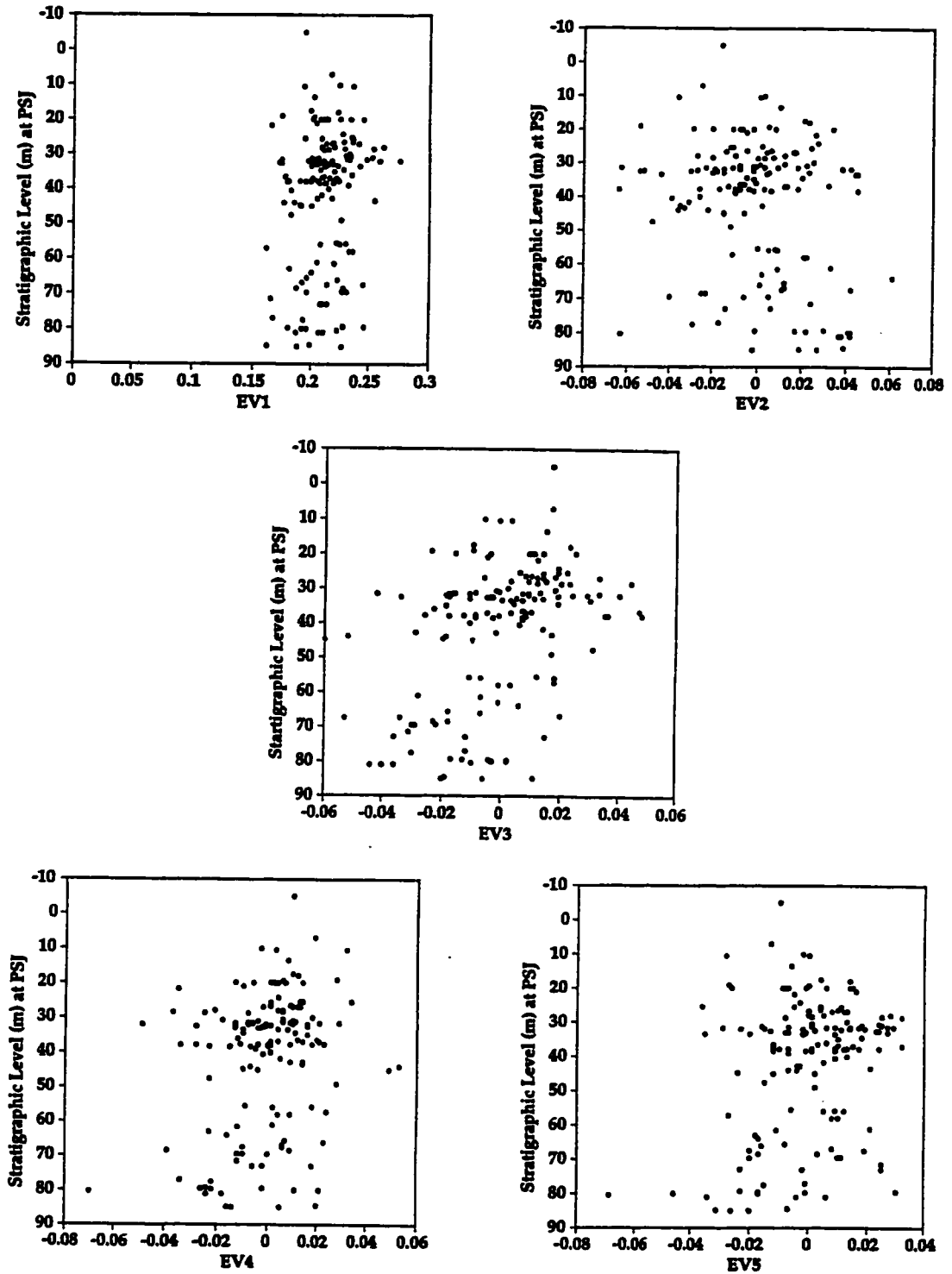


Figure 35. Plots of individual specimen scores from the Punta San Jose data set (n=154) for eigenvectors (1-5) vs. stratigraphic level at Punta San Jose.

upper 20-30 meters of the section to support this observation unequivocally. However, the trend in the data appears to be related to an expansion in the range of cross-section shapes associated with eigenvector 3 above 40m (see Fig. 35).

SUCIA ISLANDS

Plots of the various combinations of eigenvector scores for the Sucia Islands data set are shown in figures 36 and 37. It is worth noting the large amount of variation in shape found within this data set, given that this group of specimens can be assigned to one species, *Baculites inornatus*.

The first eigenvector for the Sucia Islands data set describes the same type of variation as the first vector for the PSJ data (see Fig. 30). Specimens with high covariances have slim cross-sections with low width/height ratios. Those specimens with low covariances are stouter and have high width/height ratios. Specimens with high covariances to the second eigenvector are more elliptical in shape, while those specimens with low scores tend to have narrowed venters or both dorsum and venter are more tapered. The third eigenshape from the Sucia Islands data set closely, though inexactly, resembles shape 5 from the PSJ sample. The principal feature of specimens with high scores of covariance with this vector is a narrowed dorsum. Specimens with low scores have narrower venters relative to their dorsums. Eigenshapes 4 and 5 are erratic in outline and lack any sort of bilateral symmetry. They represent variance in the outlines that is attributable to irregularities in individual outlines and therefore not useful for the discrimination of species-level form.

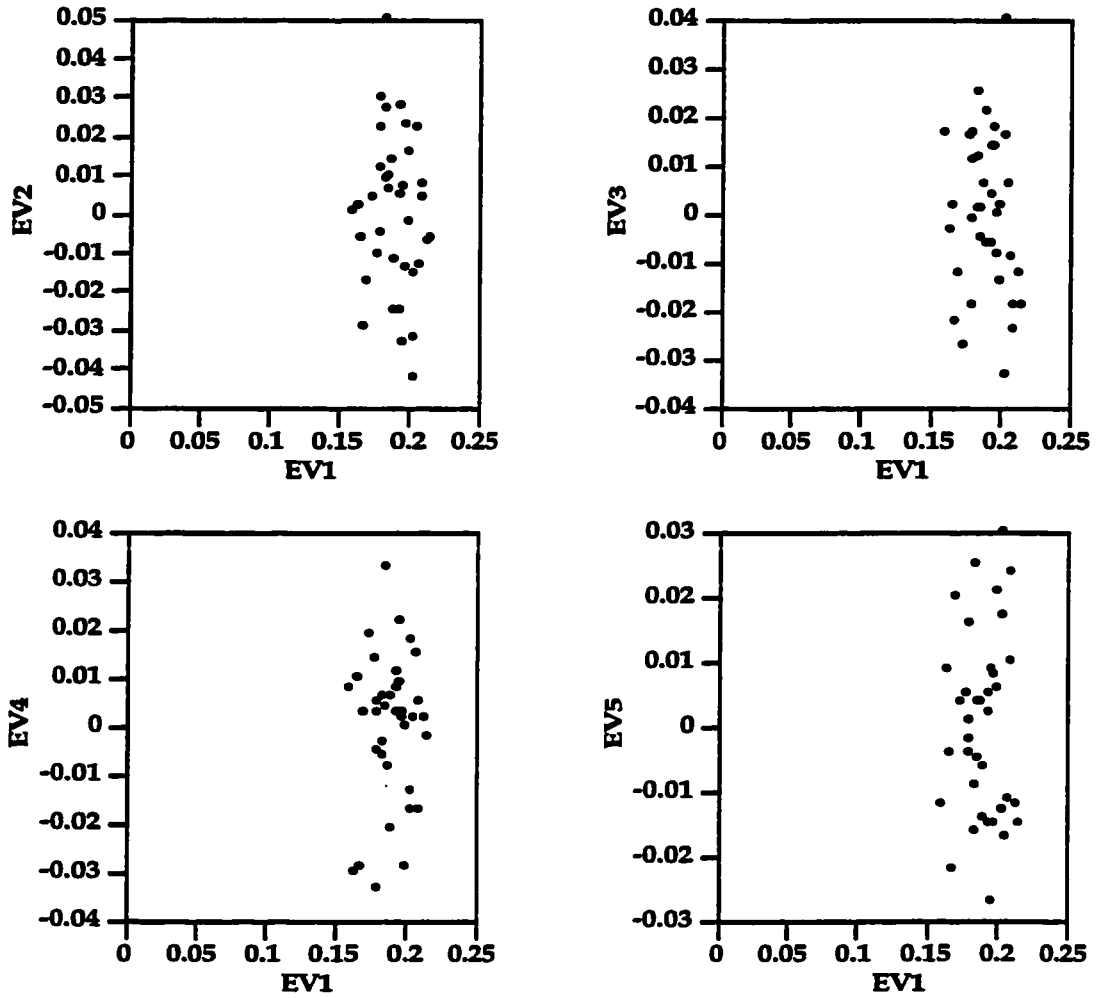


Figure 36. Plots of individual scores on the first eigenvector and next four eigenvectors for the Sucia Islands data set (n=37). Eigenshape analysis was based on covariances.

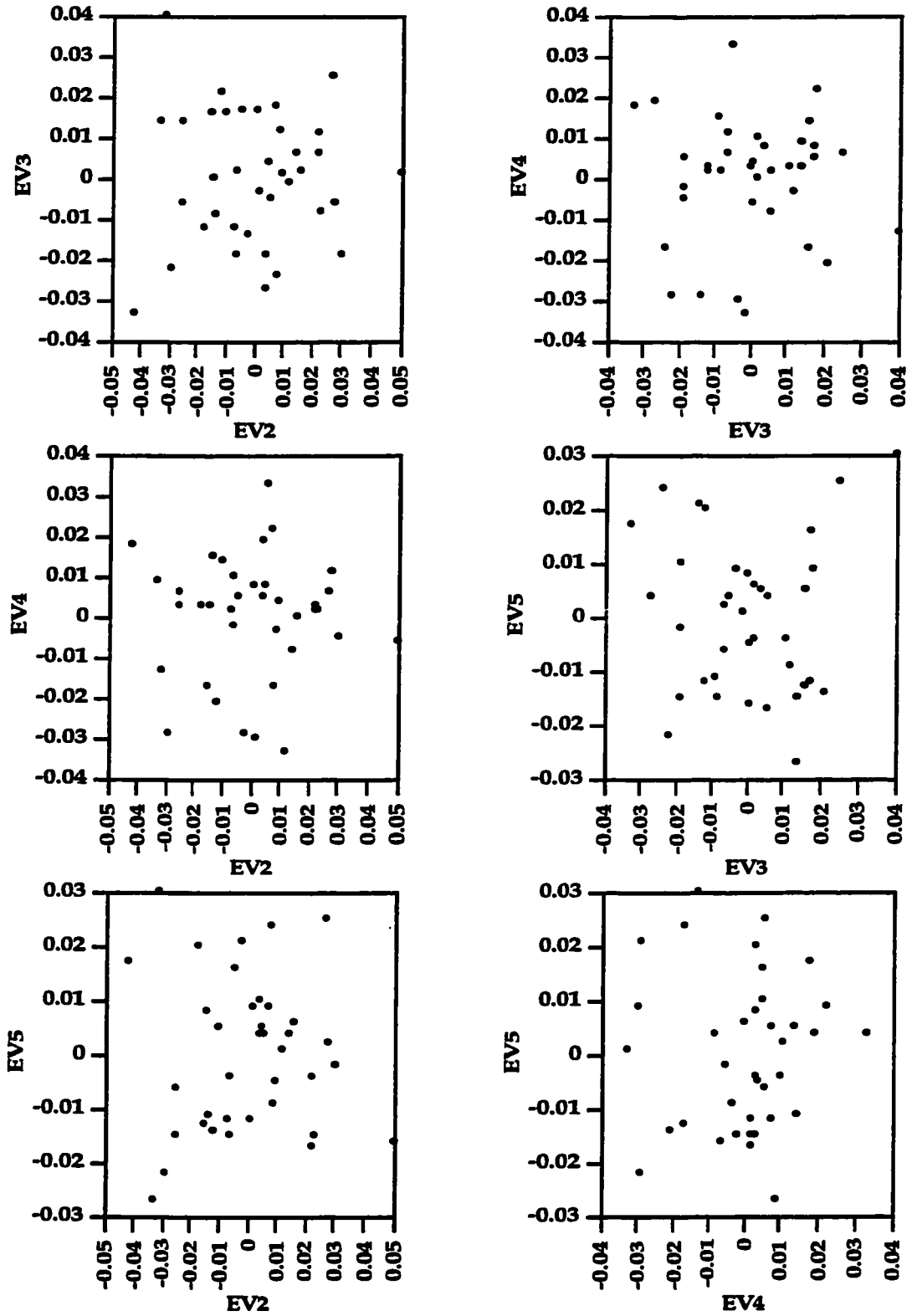


Figure 37. Plots of individual scores on various combinations of eigenvectors (2-5) from the eigenshape analysis of the Sucia Islands data set (n=37).

COMBINED DATA SET

Similar to both previous analyses, the first eigenvector of the combined analysis arranged the data set based on width/height ratios (see Fig. 31). High scores were given to slimly shaped cross-sections, with low scores assigned to more stout cross-sections.

Although the 2nd eigenshape for the combined analysis is very different in form relative to the 2nd eigenshape from the Punta San Jose analysis, the second eigenvector from both analyses organizes the specimens based on the presence or absence of a keel. The difference is that keeled specimens are given positive scores in the case of the combined data set as can be confirmed by looking at the listings of scores found in Appendix (A). In addition, most of the specimens from the Sucia Islands have low covariance scores and cluster at the negative end of the vector.

Eigenshape 3 of the combined set resembles eigenshape 3 of the Punta San Jose analysis almost exactly. As was the case in the Punta San Jose analysis, specimens with high covariances to the third eigenshape vector have cross-sections that flare out just above the lateral midline and have broadly rounded venters. Specimens with low scores are relatively straight-sided with narrow venters. Notably, the specimens from the Sucia Islands are interspersed with the Punta San Jose specimens and form no coherent grouping along this vector.

The combined set is scored on the 4th eigenvector in a manner similar to the scoring of the Punta San Jose data set on its 4th eigenvector. The primary difference in the 4th eigenshapes from the two data sets is due to a polarity switch of the vectors associated with each data set. During eigenshape analysis, the polarity of the eigenvectors is arbitrarily chosen. Eigenshapes 2-5 are associated with the positive end of their respective vectors.

As can be seen by comparing the 4th eigenshapes from the two data sets, there is also a greater emphasis on the narrowness of the dorsal shoulders at the positive end of the vector for the combined data set (compare Figs. 29 and 31). Specimens with high

covariances have, in general, narrow squared shoulders, and broadly rounded venters. Specimen cross-sections with low scores have broadly rounded dorsal shoulders, narrow venters.

The 5th eigenvector from the combined set and the 5th eigenvector from the Punta San Jose data set generally describe the same type of variance. Comparison of the 5th eigenshapes from both data sets shows that the analysis of the combined set gave greater weight to specimens with less narrow dorsal shoulders and a more narrowed and pinched venter.

Plots of various combinations of the eigenvectors for the combined data set are found in figures 38 and 39. Plots of eigenvectors 2-5 against the first eigenvector are similar to those for Punta San Jose as they show a relatively compact central group of data with much smaller peripheral groupings of no significance (compare Figs. 32 & 38). Plots among eigenvectors 2-5 show a much less concentrated central grouping of the data with a more random distribution to the data. There are linear spaces that run through the data in several of the plots (see Fig. 39). These spaces roughly divide the data based on the presence of a keel or a pinched keel-like venter. In an effort to enhance this feature visually in the data, the original data sets from Punta San Jose and Sucia Island were altered by removing individuals that were considered outliers based on the initial cluster analysis and the eigenshape analysis. The new sets of data were then rerun as a combined set (n=144).

The list of covariances with the first five eigenvectors is found in Appendix B. Figure 40 shows the first five eigenshapes and a series of cross-sections from the data set that represent the range in shape variation for each relevant eigenvector. The first and second eigenvectors from the rerun combined set are almost identical to the eigenvectors from the initial set (compare Figs. 31 & 40). While eigenshapes 3-4 are generally the same for both the initial and rerun combined data sets, there are some differences. In both analyses, the 3rd eigenvector scores triangularly shaped specimens at the positive end of

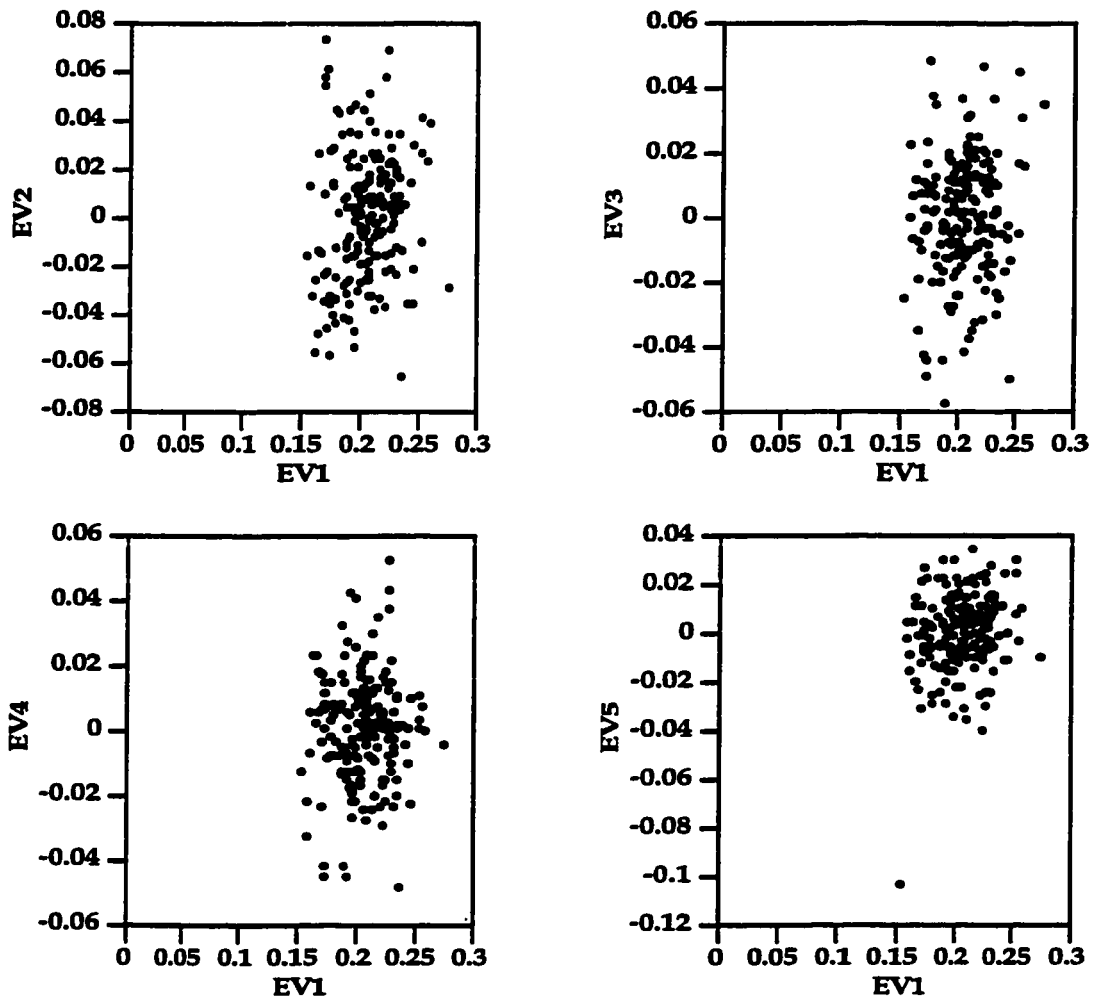


Figure 38. Plots of individual scores on the first eigenvector and next four eigenvectors for the Combined data set (n=191). Eigenshape analysis was based on covariances.

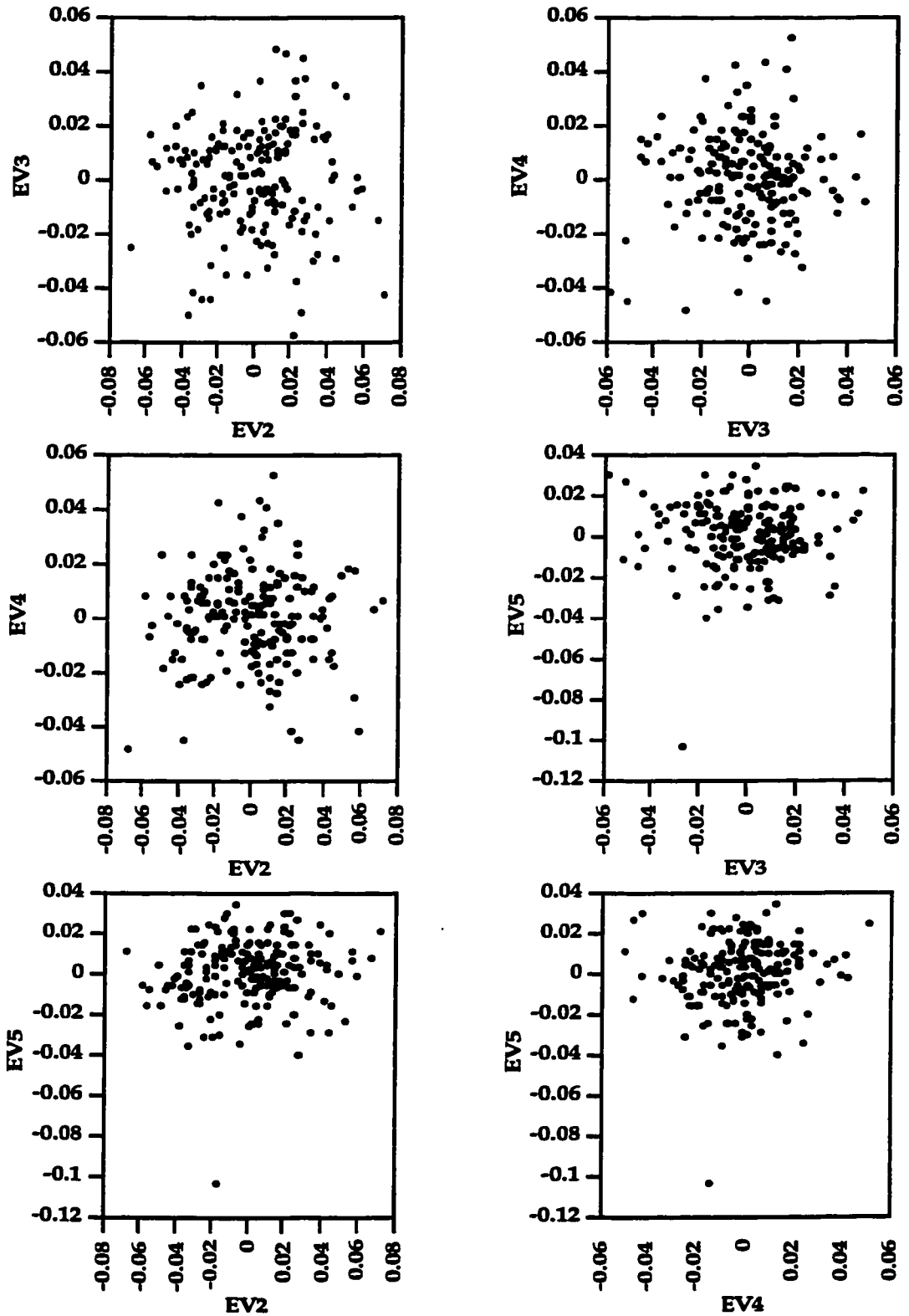


Figure 39. Plots of individual scores on various combinations of eigenvectors (2-5) xfrom the eigenshape analysis of the Combined data set (n=191).

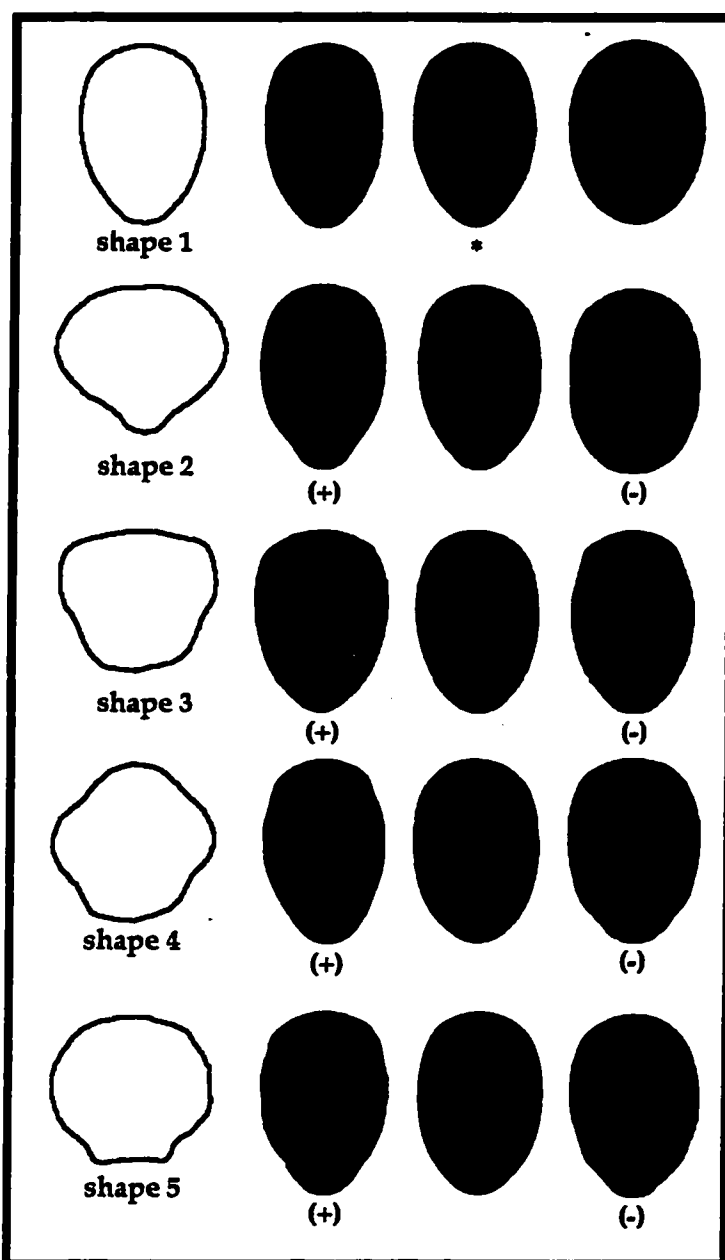


Figure 40. The first five shapes from the eigenshape analysis of the Combined Dataset ($n=144$). In the case of shapes 2-5, the series of cross-sections associated with each shape illustrates the variation from the positive (+) to the negative (-) end of the vector. The first shape resembles the mean shape for the analysis and is most closely resembled by the shape in the middle of the first series labeled (*).

the vector. However, the 3rd eigenvector from the rerun analysis emphasizes broader and more squared dorsal shoulders as well as specimens with more acute venters. The 4th eigenvector from the rerun analysis differs from the original analysis in that the positive end of the vector gives the highest scores to specimens whose maximum width is at the midline, not below the midline as was the case in the original analysis. In addition to a polarity switch, the 5th eigenvector of the rerun analysis places greater emphasis on changes in the shape of the ventral flanks and venter and not on the structure of the dorsal shoulders. Specimens with high scores in the rerun analysis have flanks that pinch in just below midflank, while specimens with low scores are pinched in just above the venter.

Plots of the individual scores on the various eigenvectors from the rerun analysis are found in figures 41 and 42. The overall structure of these plots is similar to that produced for the original combined data set (n=191) analysis. The separation of keeled or partially keeled specimens by a quasi-linear space is evident in several of the plots of the rerun analysis, but most notably in the plot of eigenvectors 4 and 5 (see Fig. 42). While keeling has been isolated to some extent in these plots, it is interesting that in the plot of eigenvectors 1 and 2 from this analysis, there is a gradation of keeling from the positive end of the vector and not a gap as might be expected if keeling were a species level characteristic in baculitids.

DISCUSSION OF EIGENSHAPE ANALYSIS

As might be expected from the results of the cluster analysis, the eigenshape analysis was not definitive. There were no cleanly identified groups, though clearly there are a number of small groups of outliers with extreme shapes. As noted before, the specimens from the Sucia Islands do group together at one end of eigenvector 2 in the combined analysis. However, there is a lot of overlap with forms from Punta San Jose

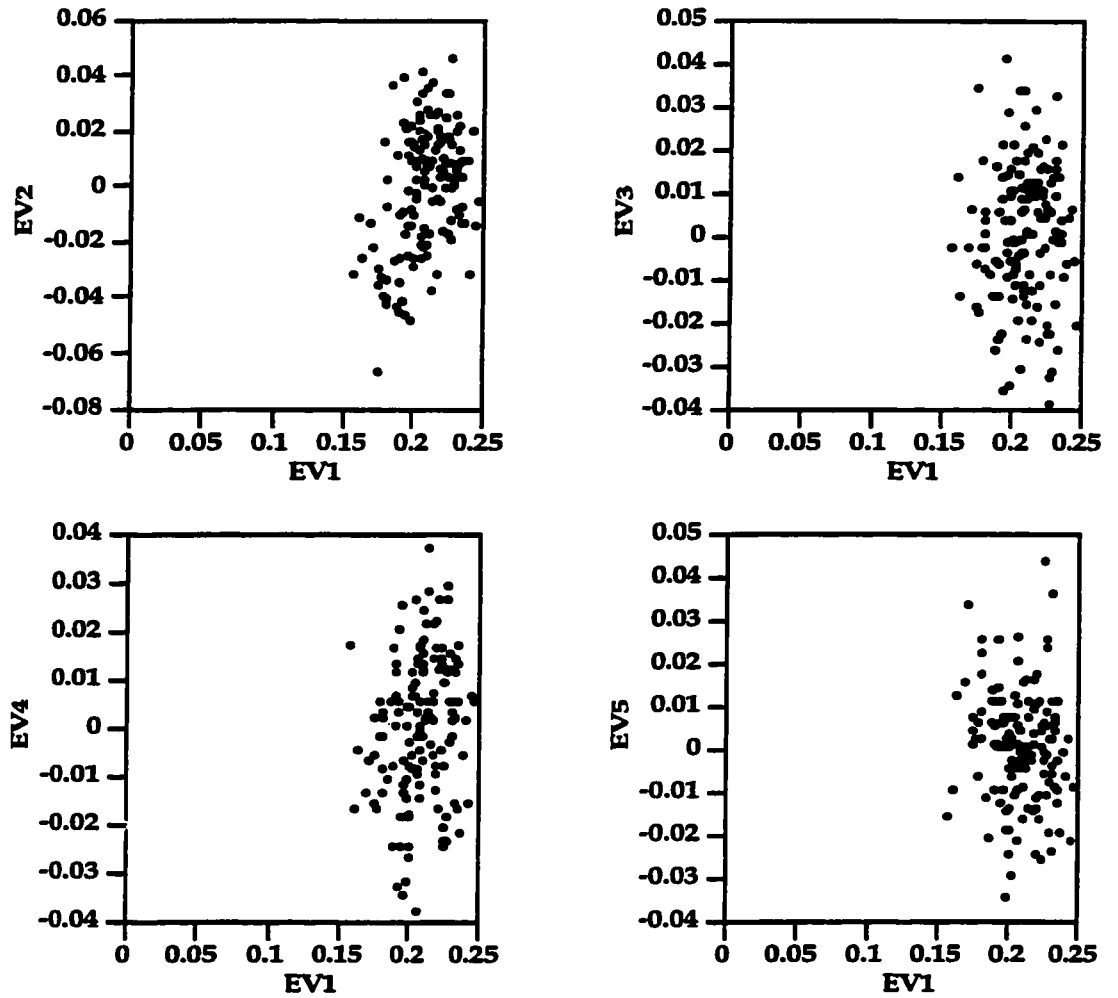


Figure 41. Plots of the specimen scores on the first eigenvector and the next four eigenvectors from the Combined subset (n=144). Eigenshape analysis based on covariances.

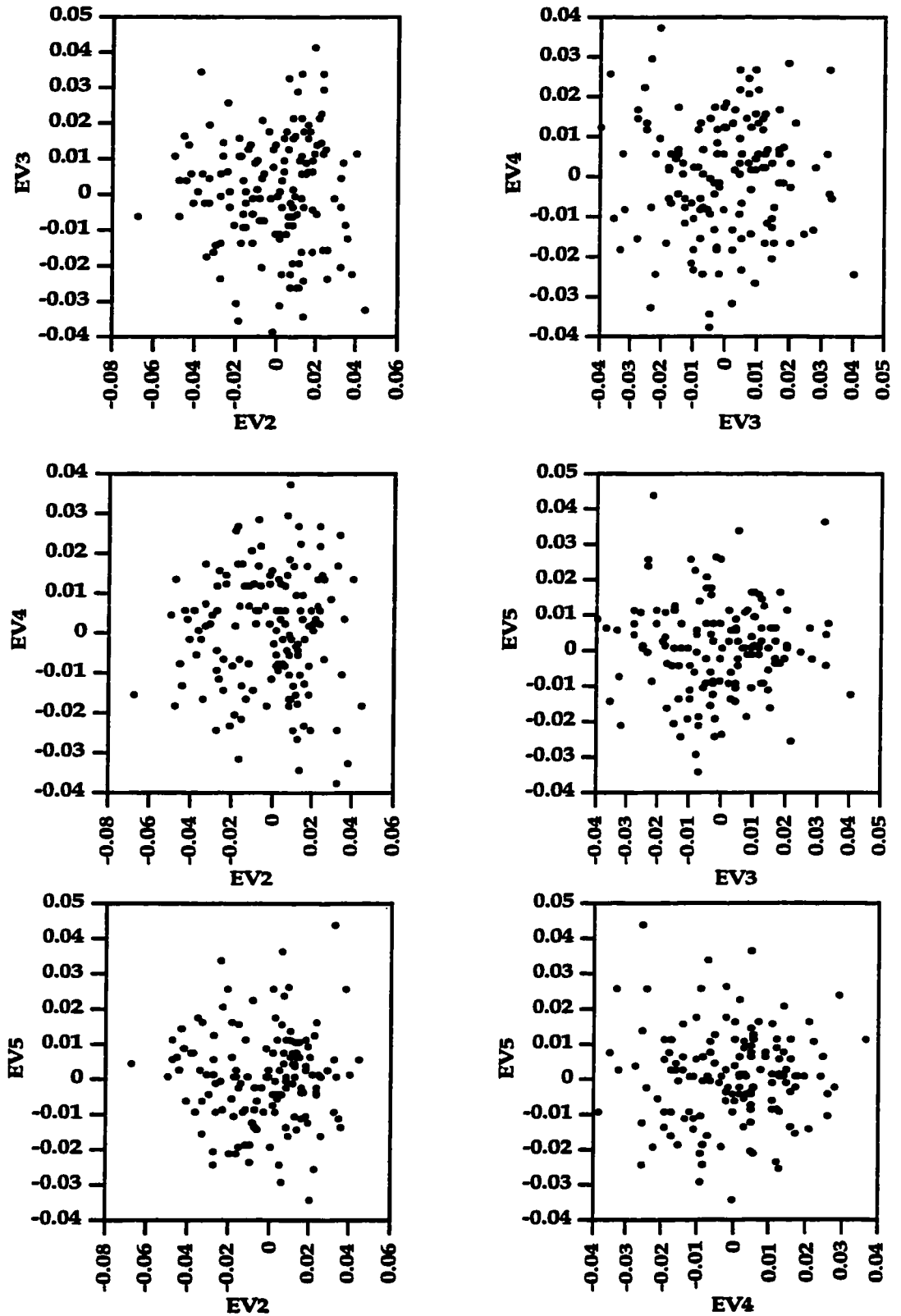


Figure 42. Plot of specimen scores for various eigenvectors from the Combined subset (n=144). Eigenshape analysis based on covariances.

along this shape vector. Clearly some specimens from the Sucia Islands share shape characteristics with forms from Punta San Jose. There are also forms found at the Sucia Islands that are not found at Punta San Jose. The overlap in forms at the two localities would suggest that they were time-equivalent to some degree. The majority of forms from Sucia Island are most similar to forms from the lowest 10-20 m of section at Punta San Jose.

Most notable in the analysis is the identification of various aspects of cross-section shape (height of maximum width; squared vs. rounded shoulders etc.) that seem to be randomly mixed to some degree. In particular, keeling or the pinching in of the ventral flank that gives a specimen the keeled look, is found associated with a variety of other shape characteristics.

The complexity of form described by the eigenshape analysis of cross-section would suggest that this morphological feature may be ecophenotypic in derivation and of limited use in the description of baculitid species. At the very least any theoretical "true form" of an individual may be lost or at least overprinted by modification to the phragmacone over the lifetime of the individual.

There are other possible explanations for modifications to the cross-section that are not considered by this study. There may be changes in the shape of the phragmacone that are ontogenetically related. For example, sexual maturation may raise the need for extra space to accommodate reproductive materials or functions. Taking into consideration the possibility that baculitids are nektonic or nekto-benthic dwellers, it is not inconceivable that cross-section morphology and other attributes of the shell (e.g. ribs) are controlled to some extent by hydrodynamic factors associated with swimming or maintaining stability in a variety of water conditions. Theoretically, the removal of shell material would change not only the shape, but also the buoyancy and stability of the shell during an attack. Morphologic responses to extensive enough damage may be driven to some extent by these

factors. It is also worth noting that repair of the phragmacone is often done so that bilateral symmetry is achieved over much of the cross-section.

If cross-sectional morphology is primarily an ecophenotypic characteristic of baculitids, this suggests that baculitids as a group may repeatedly utilize a restricted set of cross-section morphologies throughout their history as a group. It also suggests that cross-section shape may be limited in the extent that it can be used as an identifying characteristic of baculitid species.

It is not clear, however, that cross-section information is invalid in all circumstances. The analysis presented here suggests that great care is needed in assigning a particular shape to a species. Any such shape would be the form that a member of that species would theoretically have, if it came through life unscathed. As a precaution, it would seem wise to compare and describe species using specimens of moderately small individuals that have not experienced a great number of predation attacks. If very large individuals are able to return to their "true" form after growing large enough to avoid most predation attacks, it would also be possible to use these individuals in a similar manner.

There are other aspects to cross-section morphology that are not addressed by this study which would have bearing on the problem of defining North American baculitid species. In particular, this study doesn't look at how cross-section form changes over ontogeny for a group of individuals of the same species. As noted before, there are several species of baculitids from the Pacific Coast region described by Matsumoto (1963) from very small individuals. Matsumoto relies heavily on cross-section morphology when describing species. Given the immaturity of sutures described from species such as *B. tanakae* and the lack of understanding as to the ontogenetic change in sutures for a given species, it is not clear that Pacific coast species are properly defined.

It may be that some species defined from small groups of small individuals are in reality synonymous with species described from larger-sized individuals from the Pacific

coast or other regions of the world. Another idea to consider, which would have the same effect, is that juveniles and adults of the same species, but with different cross-section form, may live in different environments that have different potentials for preservation in the fossil record. These problems are very evident when comparing individuals from the Sucia Islands and Punta San Jose. Some specimens from the base of the section at Punta San Jose look similar to forms from the Sucia Islands. However, the specimens from Punta San Jose are much larger in size than specimens typically collected from the Sucia Islands. In addition, specimens with sutures from Sucia Island are from much smaller individuals than those from Punta San Jose. In this case, given the problems with interpreting cross-section morphology, any species designation must be made based on a best guess as to what modifications might occur to the suture of a species through ontogeny.

SUTURE MORPHOLOGY AND BACULITID SYSTEMATICS

Suture morphology is a characteristic of baculitids that is less emphasized in the description of baculitid species than other shape characteristics. Sutures are generally described using the shape of the major elements (trapezoidal to rectangular), relative size and symmetry of the major elements (lobes and saddles) and level of incision by the branches of the elements. Other less quantitative factors used to describe sutures are complexity (simple to complex), and the shape of the folliole terminations (smoothly rounded or notched). The three follioles are found at the top of the umbilical lobe (U)(see Fig. 10). As in the case of cross-section morphology, suture pattern appears to be highly variable and difficult to use as a species level characteristic. For example, in his description of *Baculites occidentalis*, Matsumoto (1960) illustrates two examples of sutures from that species, which are visually very different in complexity and form (see Fig. 10C, D). A less dramatic example can be found in Cobban's (1974) illustration of the sutures for the

species *B. ovatus* from the Navasink Formation of New Jersey (see Fig. 10A, B). These are examples where sutures from different individuals with similar morphologies are compared.

Ward (1978b) illustrates several sutures for individual species from the Vancouver Island region. In all but one case, the sutures are from different positions on the same specimen. The exception is a case where the illustrated sutures are from two specimens from the same locality. It is rare for species descriptions to illustrate sutures of specimens taken from several geographic regions.

When specimens of the same species but from different geographic regions of the US and Japan are compared, there is a much greater range in suture variation than would seem plausible for a single species (e.g. *B. occidentalis* sensu Matsumoto, 1960). Either baculitid species exhibit a wide range of variation in suture morphology or there are more forms of baculitids present than have been described from the Pacific Coast region. Choosing between these two possibilities depends on one's taxonomic approach to baculitid species. Either sutures are secondary characteristics, not useful for species identification, or they could be used more prominently for the identification of baculitid species or forms.

SUTURE ANALYSIS

As noted in the introduction, the septal suture pattern has been less prominently used as a means of identifying Pacific coast species than other shape characteristics of baculitids. However, given the plasticity of other morphological characters of baculitid phragmacones, the suture pattern may be useful as a primary way of identifying baculitid lineages.

Baculitids, as with other ammonites, have a chambered shell. Each septum or chamber wall blocks off a portion of the straight tube. As the animal grows and secretes a

larger tube, the most recent septal wall separates the living chamber from older portions of the shell. It is the intersection of the periphery of each septum with the outer shell wall that creates a suture with a characteristic pattern. The suture is exposed when the outer shell is removed or as a sinuous groove on the surface of preserved internal molds. The suture of *Baculites* consists of several lobes that project from the oral end of the shell towards the aboral end of the shell. They include the dorsal or internal lobe (I), and the ventral or external lobe (E). Running between the external (dorsal) and internal (ventral) lobes, the suture outlines two more lobes along each side of the shell. These are the umbilical lobe (U) and the lateral (L) lobe (see Fig. 10). Between the lobes and projecting towards the oral or open end of the shell are the saddles. Starting from the dorsal side and moving around the perimeter of the shell towards the venter, the saddles are identified by their relationship to the adjacent lobes. For example, the U/L saddle or second lateral saddle is positioned between the umbilical lobe and the lateral lobe. The major elements of the suture are branched and are, in the broadest sense, quadrate in shape with variation in element squareness and relative size. Sutures are also described using several other factors including suture complexity (simple to complex), incision of the lobe or saddle branches (shallow to deeply), and the shape of the folliole terminations (phylloid or non-phylloid). The three follioles are found at the top of the umbilical lobe (U).

The septal suture is presumed to be produced by a mantle in a manner analogous to that used by modern species of *Nautilus* to secrete their chamber walls (Ward, 1987). The mantle responsible for depositing the septum is likely to be located on the posterior of the animal. This position implies that the posterior mantle is afforded some protection by the walls of the phragmocone and therefore is less likely to be modified by predatory attacks. This suggests that characteristics of the suture may be less subject to modification and therefore more productive as the basis for the systematic identification of baculitid species or lineages.

Despite all the possible variations noted above, it is possible that the basic shapes and patterns of sutural elements can be used to trace lineages, and to group specimens in a coherent manner, for use in correlation. As a test of this idea, a portion of the suture was digitized and measured. The data set includes specimens from Punta San Jose (n=77) and the Sucia Islands (n=11).

Features that have been previously used to describe the suture pattern of a given species are the squareness of the elements, the depth of pattern incision, and the relative height of the lobes. These features can be reasonably described using simple linear measurements. However, it is difficult to record easily and accurately the entire suture pattern. The curve of the shell surface from which the suture must be traced is problematic and it is difficult to find enough complete sutures to work with. Therefore, only one element of the suture was used to investigate the variability in baculitid septal sutures. This is the saddle found along the dorsal flank of the shell between the umbilical lobe and the lateral lobe (see Fig. 10).

METHOD OF MEASURING SUTURE ELEMENT

Shell material is cleaned off of the exterior of the fossil using a compressed air hammer. This exposes the septal suture pattern exposed on the surface of the internal mold of the phragmacone. The suture pattern is then recorded as a black and white photographic image using a flat-bed scanner. Up to 5 images are used to scan the suture pattern from a single side of a baculitid fossil.

Images of the (U/L) saddle were imported into the program *NIH image* as a digitized image. Points of interest on the suture were then recorded as x,y coordinates in a pre-determined sequence (see Fig. 43). Using routines written in FORTRAN, the coordinates were subsequently rotated into the same orientation and then used as the basis for measuring the lengths of prominent features of the element from the base of the

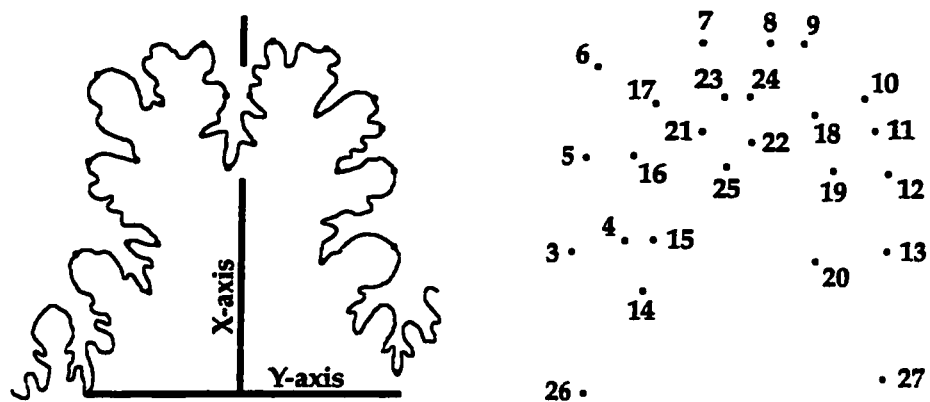


Figure 43. Example of U/L suture element and schematic showing the location of points used for measurements. Coordinate axes show relative position of the suture element after rotation. X-axis is oriented using the same point on successive septae.

element.

A set of ratios based on the original measurements were then calculated and used as the basis for several types of analysis (see Table 2). The basic univariant statistics for the ratios are found in Appendix B. The suture data are based on ratios and not on the original measurements, in order to eliminate size from consideration during the analysis. Baculitids are animals that grow their shell continuously, not incrementally, so there is no way to compare stages of growth between individuals. By using ratios, the measurements are standardized so that it is possible to look at variation within the group without regard to size.

The U/L saddle is the area between the umbilical and lateral lobe. The lateral branches of these lobes penetrate the saddle area and terminate at points 14-20 (see Fig. 43). This set of points measures the interior features of the saddle. The lobe branches that penetrate the saddle form complementary lateral branches of the saddle which terminate at points 3-6, 10, 12 and 13. These points are used to measure the exterior widths and lengths of the saddle. The base width of the saddle is measured using points 26 and 27. The height of the saddle is the measured distance between point 8 and point 16. The last important feature of the saddle is the central lobe that terminates at point 25.

In order to test the idea that these simple measurements of the U/L saddle element can be used to show changes in suture pattern over time, correlation of the ratios with stratigraphic level and size were computed for the specimens from Punta San Jose (see Appendix B). In order to test the idea that these measurements can also be used for the discrimination of baculitid species, the ratio data were also analyzed using cluster analysis. The cluster analysis was performed by the program SYSTAT using the JOIN option, the Euclidean distance metric and the Average linkage method. The data set used for the cluster analysis included specimens from both Punta San Jose and the Sucia Islands.

Table 2: List and description of ratios for U/L saddle

R1: 3-13y/26-27y	R28: 3-13y/3x
R2: 5-12y/26-27y	R29: 3-13y/13x
R3: 6-10y/26-27y	R30: 5-12y/5x
R4: 14-20y/26-27y	R31: 5-12y/12x
R5: 16-19y/26-27y	R32: 6-10y/6x
R6: 17-18y/26-27y	R33: 6-10y/10x
R7: 8-26x/26-27y	R34: 14-20y/14x
R8: 8-27x/26-27y	R35: 14-20y/20x
R9: 27-7x/26-27y	R36: 16-19y/16x
R10: 3-26x/8-26x	R37: 16-19y/19x
R11: 5-26x/8-26x	R38: 17-18y/17x
R12: 6x/8-26x	R39: 17-18y/18x
R13: 14x/8-26x	R40: 6x/8x
R14: 16x/8-26x	R42: 17-18y/16-19y
R15: 17x/8-26x	R43: 16-19y/14-20y
R16: 20x/8-26x	R44: 17-18y/6-10y
R17: 19x/8-26x	R45: 16-19y/5-12y
R18: 18x/8-26x	R46: 14-20y/3-13y
R19: 13x/8-26x	R47: 8-26x/8-27x
R20: 12x/8-26x	
R21: 10x/8-26x	
R22: 8-25x/8-26x	
R23: 16-25y/16-19y	
R24: 6-17xy/6-25xy	
R25: 19-25y/16-19y	
R26: 16y/16-19y	

RESULTS OF SUTURE ANALYSIS

Basic univariant statistics of the ratios measured for the U/L saddle provide information about the variance of ratios commonly used to distinguish or describe baculitid species. The squareness of the saddle element R7 (s.d.= 0.191) and R8 (s.d.= 0.160), the depth of the central lobule R22 (s.d.= 0.046), the relative depth of insertion for the two lobes adjacent to the U/L saddle R47 (s.d.= 0.095), and asymmetry in the size of the main branches of the saddle R26 (s.d.= 0.073) are some of these characteristics (see Table 2). All of these ratios have low to moderate standard deviations and show a univariant distribution of the data that suggests that these characters are not useful for the discrimination of groups in the data (see Appendix B).

The ratios that show the highest standard deviations are R34 (s.d.= 0.528) and R35 (s.d.= 0.539) which essentially describe the depth of incision for the lateral branches of the umbilical and lateral lobes that terminate within the U/L saddle element at points 14 and 20. Higher than average standard deviations are also found for ratios R28 (s.d.= 0.380) and R29 (s.d.= 0.435) which describe the position of the lateral branches of the U/L saddle that terminate at points 3 and 13. As described before, there are three lateral branches of the U/L saddle and three complementary lateral branches that penetrate the saddle from the adjacent lobes. The ratio pairs R32 (s.d.= 0.097) & R33 (s.d.= 0.103); R30 (s.d.= 0.169) & R31 (s.d.= 0.211); and R28 (s.d.= 380) & R29 (s.d.= 0.435) describe the termination positions of the lateral saddle branches, whereas, the ratio pairs R38 (s.d.= 0.065) & R39 (s.d.= 0.070); R36 (s.d.= 0.151) & R37 (s.d.= 0.162); and R34 (s.d.= .528) & R35 (s.d.= 0.539) describe the terminations of the lateral branches from the adjacent lobes (see Fig. 44 and Table 2). In both cases, the variance in the position of the branch terminations increases with respect to the height of the U/L saddle element. This suggests that the principal way in which the U/L saddle varies in form is the depth at which the saddle is incised by the topmost lateral branches of the adjacent lobes. It is also worth noting that the

limited amount of data from the Sucia Islands (n=11) does not group in any meaningful way in relation to the Punta San Jose data (n=77) for any of the variables discussed.

In an attempt to see if any of the ratio data from Punta San Jose change in any systematic way relative to size and stratigraphic level, the correlations among the ratios and these two variables were computed. There is no meaningful correlation between any of the variables and either size or stratigraphic level at Punta San Jose (see Appendix B).

Cluster analysis of the ratio data segregates the sample set into small groups of 2-4 individuals (see Fig. 44). Specimens from Punta San Jose are sometimes grouped stratigraphically. In these cases, it is common for the specimens to have been collected within 5-10m of each other. However, larger clusters do not hold together in the same manner. Individuals with similar dimensions, as recorded by the coordinate data and measurements, do not always have similar overall patterns when the full complexity of the U/L saddle is considered. Clearly, there are important components to the pattern that are not described by the measurements used here.

DISCUSSION OF SUTURE DATA

Figure 45a-f shows several examples of variation in the suture patterns which demonstrate the limitations of the ratio data and explain the cluster diagram. Figures 45a and 45b are two examples of the U/L saddle that look visually similar, but have both different height/width ratios for the element and different depths of incision at the base of the element. Figures 45c and 45d are examples of the species *B. inornatus* collected from Sucia Island. Again, these two suture elements are visually very similar except that the base of the saddle is much more incised in figure 45d. Figure 45e and 45f are a pair of examples from Punta San Jose. In this case, the element in figure 45e has a higher height/width ratio and is more deeply incised at the base of the saddle than its similar counterpart in figure 45f. The six examples illustrated in figure 45a-f are highlighted in the tree diagram

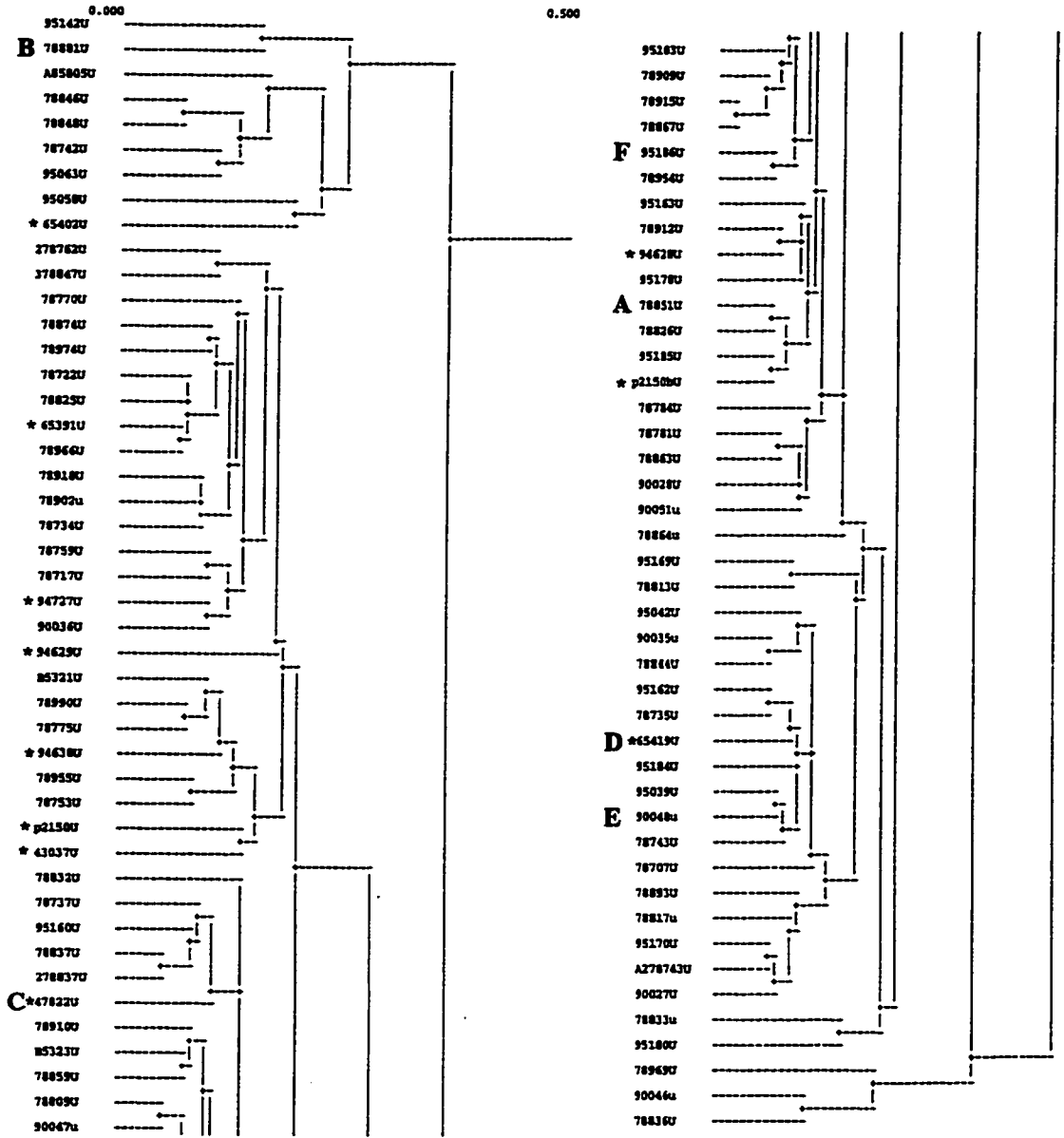


Figure 44. Graphic output for cluster analysis of U/L suture element data. Specimens from the Sucia Islands are labeled with an (*). Letters A-F are examples shown in Figure 46. Total distance of tree is 0.500 using the Euclidean Distance Metric and Average Linkage Method.

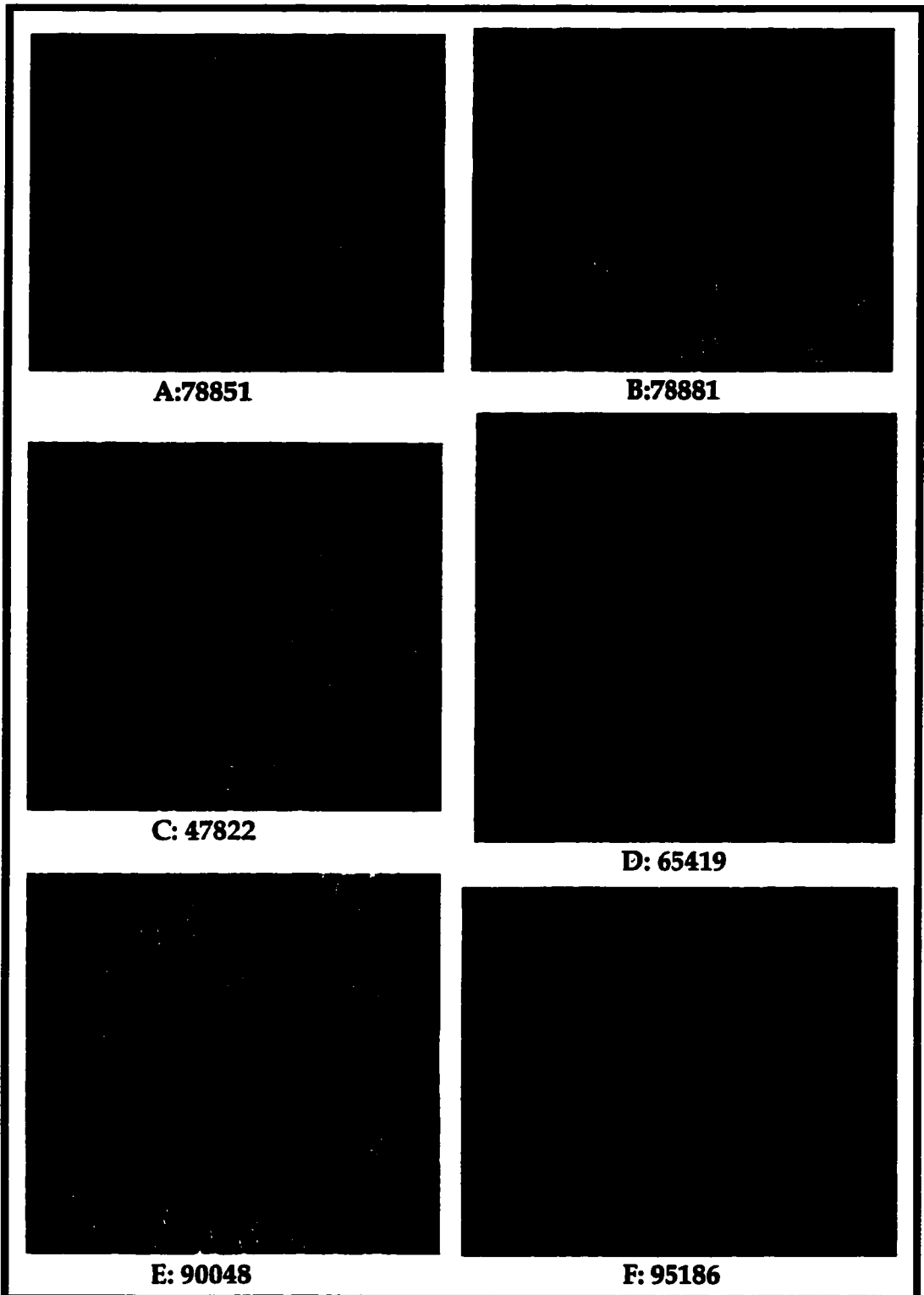


Figure 45A-F. Examples of U/L suture elements. 46A,B,E and F are from Punta San Jose. 46C, D are from Sucia Island.

produced by the cluster analysis of the U/L saddle ratio data and are labeled A-F, respectively (see Fig. 44). In all cases, these pairs of similarly looking patterns do not group closely together. This is especially so in the case of specimens 78851(A) and 78881(B).

Because in some cases, the lower level clusters do appear to have some meaning, it can be hypothesized that sutures are modified in predictable ways. Modification of the suture may be driven to some degree by adapting to changes in the shape and buoyancy of the phragmacone. Therefore, changes in cross-section shape over the life of the animal may also result in modifications to the suture. It may be that the mantle which secretes the septal suture can be stretched to a limited degree. Modifications of this kind could be the cause of the variations in the squareness and incision of the suture saddles and lobes. A natural extension of this idea would be the modification of the suture elements when the mantle that secretes the septum encounters ornamental ribs on the walls of the phragmacone. Ribs represent an expansion of shell space for the animal because the cavity beneath the rib is not filled with added shell material. The mantle would presumably have to mold its shape in order to attach to the cavity wall formed by a rib. The resulting distortion of the mantle lobes would cause an alteration in the shape of the septum. Differences in the depth of incision for suture elements may also be related to how firmly the posterior mantle is pressed onto the interior wall of the phragmacone during secretion of the septum. There are cases where the suture looks as if it were secreted by a modified mantle, in that there is bifurcation of secondary elements and notches in the folioles (see Fig. 45e).

In addition, there must be other factors that cannot be examined through a study of the septal suture pattern because it is only a 2-dimensional edge of a much more complex 3-dimensional feature. Until such time as a more complete method of suture analysis is used, it will be necessary to rely on the subjective analysis of the best computer available, the human brain.

While the simple analysis done for this study does not allow for the easy discrimination of baculitid species, it does suggest possible ways in which the suture pattern may vary for a given species. The specimens found at Punta San Jose have been grouped into two species, *Baculites rex* and *B. inornatus*. Aspects of U/L saddle morphology that were used to help in the grouping of specimens from Punta San Jose into these species include: 1) relative size of the main branches separated by the central lobule, 2) number and overall shape of minor elements that make up the main branches, 3) number and shape of the lateral branches, and 4) minor features of the lateral branches (see Fig. 43).

In the future, a multivariate approach to suture analysis such as a principal components analysis of simple measurements may be useful in describing the variation of suture patterns. However, it seems more likely that some form of shape analysis such as Fourier or Eigenshape analysis may be more profitable in the delineation of taxonomic groups based on shape characteristics of the suture. It may be possible to use a combination of measurements, ordinal data, and the presence and absence of features to easily group baculitids more effectively using suture morphology. In any case, the results of the suture analysis and the observational data used above to distinguish species suggest that characterizations of suture morphology such as squareness of the lobes and saddles and depth of incision are less important than features that stress the number and orientation of the major and minor branches of a suture element.

Questions that are not answered by this study of the septal suture are: 1) How broad is the range in variation for a particular suture pattern? 2) How does the suture pattern change through ontogeny? and 3) Is there a relationship between modifications in the suture pattern and changes in the cross-section? These problems can only be answered by a study that investigates a known species for which a large quantity of well-preserved specimens with a large size range are available.

BACULITID MORPHOLOGY AND BIOSTRATIGRAPHY

Baculitid species are currently defined using multiple morphological characters (cross-section shape, ornament and suture pattern). As noted before, the variation in all of these characters (e.g. ribs and cross-section) is considerable. This leads to the suspicion that current definitions of Pacific coast baculitid species may be somewhat arbitrary. Observation of the collections from Punta San Jose would suggest that baculitid species have multiple suture patterns when they are segregated using cross-section shape and ribbing as primary characters. The idea of a single species exhibiting multiple suture patterns would imply that the suture pattern of a given species evolves, or that the suture is modified ecophenotypically. Alternatively, it may be that other shape characteristic associated with a single suture pattern are ecophenotypic. If the suture pattern of a given species does evolve, there is the possibility that baculitid forms (subspecies or varieties) based primarily on suture morphology could provide a biostratigraphy that is capable of greater resolution in correlation.

The specimens collected from Punta San Jose have been grouped into two species (*Baculites inornatus* and *B. rex*) using the available morphological characters (see Fig. 6). The sequence of species found at Punta San Jose is similar to those proposed by Matsumoto (1960) and Ward (1978) for other areas of the Pacific coast region (see Fig. 46). The biostratigraphic pattern found at Punta San Jose does differ from these other biozonal schemes in several ways. Neither Ward (1978) nor Matsumoto (1960) show an overlap in the ranges of *Baculites rex* and *Baculites inornatus*. Matsumoto (1960) also shows additional co-occurring species that are not found at Punta San Jose. There are additional differences between the biostratigraphic pattern found at Punta San Jose and that of Ward (1978) for the Vancouver Island region. Most notable is the absence of either *Baculites occidentalis* or *B. anceps pacificus* at Punta San Jose.

International Stages	California Matsumoto, 1960		Vancouver Island Region Ward, 1978	Punta San Jose This paper
Maastrichtian	<i>B. rex</i>	<i>Eubaculites ootacodensis</i>	not present	not present
		<i>B. columna</i>		
		<i>B. lomaensis</i>		
Campanian	<i>B. inornatus</i>	<i>B. anceps pacificus</i>	<i>B. occidentalis</i>	<div style="border: 1px solid black; padding: 2px;"> <i>B. rex</i> </div> <div style="border: 1px solid black; padding: 2px;"> <i>B. inornatus</i> </div>
		<i>B. occidentalis</i>	<i>B. rex</i> <i>B. anceps pacificus</i>	
	<i>B. chicoensis</i>		<i>B. inornatus</i>	not present
			<i>B. chicoensis</i>	

Figure 46. Ranges of baculitid in California, the Nanaimo Group, and Punta San Jose (modified from Ward, 1978).

BACULITID EVOLUTION AT PUNTA SAN JOSE

As noted in the introduction, the zonal schemes for both the Western Interior and Pacific Coast regions seem to be based on the idea that baculitid species evolve gradually, from form to form through time. It is rare in either region for more than two species to be shown coexisting at one time. The distribution of species at Punta San Jose shows a similar pattern (see Fig. 6). However, interpreting the biostratigraphic pattern at Punta San Jose in terms of modern evolutionary theory is difficult. In order to test for either phyletic gradualism or alternative methods of evolutionary pattern, it is necessary to establish a time framework for the speciation event and to measure morphologic change in sequential species of the same lineage.

Estimates of the time for deposition of the section at Punta San Jose range from a maximum of 1.5MY based on the structure of the Sr isotopic signal and a minimum of 0.1MY based on estimates of depositional rates for similar siliciclastic shelf sequences. Estimates of species duration for baculitids from the Western Interior are 0.25MY to 1MY with an average duration of 0.54 MY (Kauffman, 1977). Given this range of species durations, the biostratigraphic pattern at Punta San Jose would seem to support the idea of a short depositional period, particularly as the section does not contain both the FAD and LAD for either species present. Given a relatively short period of deposition at Punta San Jose, it is tempting to suggest that the biostratigraphic pattern represents a speciation event compatible with the punctuated equilibrium evolutionary theory of Eldredge and Gould (1972). However, quantifying morphological change and evolutionary distance among the baculitids at Punta San Jose currently is not possible.

The process of discriminating species for biostratigraphic use implies nothing about the relatedness of the same species in an evolutionary sense. It is necessary to find some measurable morphological character(s) that can be used to establish evolutionary distance

among the taxa being studied. Cross-section shape and suture morphology are two aspects of baculitid morphology that seem likely to provide such a measure.

The analysis of suture morphology presented in this study has failed to provide a useful quantitative method for identifying baculitid species. Cross-section shape is difficult to use for such a measure. As presented before, eigenshape analysis of cross-section morphology at Punta San Jose shows a very general shift in morphology from more straight-sided to more ovoid shapes. However, this shape change is not statistically significant due to the large spread in the data. The shape analysis also suggests that this general shift may be the result of an increase in the range in shape variation above the 40 m level. This expansion in the range of cross-section shape corresponds to the first occurrence of the species, *Baculites rex*. Given a short period of time for the section at Punta San Jose, a shift in morphology of this kind would suggest a quick speciation event. However, a speciation event at this stratigraphic level would imply that *Baculites inornatus* and *B. rex* were in the same lineage. This idea has never been considered previously by either Matsumoto (1960) or Ward (1978) in their discussions of baculitid evolution. This would suggest that the appearance of *B. rex* at Punta San Jose is due to a migration event. This study does not support in any substantive way a relationship between these two species. Until a proper metric for measuring evolutionary distance between baculitid species is identified, any evolutionary relationship between these two or any other pair of baculitid species will continue to be subjective.

CHAPTER 4

CONCLUSIONS

Chronostratigraphic problems associated with upper Cretaceous sections of the Pacific Coast region were studied via complementary morphometric and chemostratigraphic analyses of fossil baculitid ammonites. A chemostratigraphic study of the section at Punta San Jose was based on the chemical analysis of well preserved fossil material. Specifically, the strontium isotopic ratio of fifteen samples was measured. Correlation with other upper Cretaceous sections for which Sr isotopic information is available suggests that the section at Punta San Jose is upper Campanian. The presence of both *Baculites inornatus* and *B. rex* at Punta San Jose places the top and base of their respective zones in the upper Campanian (see Fig. 46).

A review of species descriptions suggests that many of the characteristics used to describe North American baculitid species are highly variable. The morphometric analysis presented in this study focused on cross-section shape and elements of the septal suture. Fossil material used for this study was collected from Punta San Jose, Baja California and augmented by additional fossil material from sections at the Sucia Islands, Washington State. Cluster analysis of 191 cross-section shapes suggests that baculitid cross-section morphology is highly plastic and that there are not unique cross-sectional shapes for baculitid species. Observational data suggest that cross-section shape can be modified by non-lethal damage to the shell. Eigenshape analysis of the cross-section data set suggests that keeling of the cross-section is also not a species level characteristic but associated with a variety of cross-section shapes. Observational data also suggest that the presence or absence of ribs is not a species level characteristic for baculitids.

Cluster analysis of data for the U/L saddle element of the septal suture show that baculitid species cannot be discriminated based on simple x,y measurements. In addition,

none of the U/L saddle element data for specimens from Punta San Jose show any correlation with stratigraphic level or specimen size.

Despite the wide range of variation in both cross-section form and suture pattern, the baculitids from Punta San Jose can be lumped into two species, *Baculites inornatus* and *B. rex*. Species identifications are based on visual comparisons of the septal suture pattern and trends in cross-section form. The distribution of species at Punta San Jose is similar to those reported for baculitids from other Pacific coast sections.

Estimates for the time of deposition at Punta San Jose range from 0.1 to 1.5 MY. A shorter time period for deposition is suggested by the uniformity of sediments and lack of any depositional hiatus at Punta San Jose. These time estimates suggest that species durations at Punta San Jose may be comparable to those reported from previous studies of baculitids from the Western Interior. However, in no case is both the FAD and LAD present for either species found at Punta San Jose.

If a short time for deposition is assumed, it is possible but not certain that the biostratigraphic pattern at Punta San Jose represents a speciation event that fits the punctuated equilibrium model. However, an evolutionary relationship between the species *Baculites inornatus* and *B. rex* has never been seriously considered.

CITED REFERENCES

- Almgren, A. A. 1973. Upper Cretaceous foraminifera in southern California, *in* Cretaceous stratigraphy of the Santa Monica Mountains and Simi Hills: Society of Economic Paleontologists and Mineralogists, Pacific Section, Fall Field Trip Guidebook, p. 31-44.
- Anderson, F. M. 1958. Upper Cretaceous of the Pacific Coast: Geological Society of America Memoir 71, 378 pgs.
- Barrera, E. 1991. Global Environmental changes preceding the Cretaceous-Tertiary boundary: Early-late Maastrichtian transition: *Geology*, v. 22, p. 877-880.
- Bond, P. N. and W. B. Saunders. 1989. Sublethal injury and shell repair in Upper Mississippian ammonoids: *Paleobiology*, v. 15, p. 414-428.
- Bannon, J. L., Bottjer, D. J., Lund, S. P. and L. R. Saul. 1988. Campanian/-Maastrichtian stage boundary in southern California: Resolution and implications for large-scale depositional patterns: *Geology*, v. 17, p. 80-83.
- Bourgeois, J. and R. H. Dott Jr. 1985. Stratigraphy and sedimentology of Upper rocks in coastal southwest Oregon: Evidence for wrench-fault tectonics in a postulated accretionary terrane: *Geological Society of America Bulletin*, v. 96, p. 1007-1019.
- Boyajian, G. E. and T. M. Lutz. 1992. Evolution of biological complexity and its relationship to taxonomic longevity: *Geology*, v. 20, p. 983-986.
- Brandon, M. T., Cowan, D. S., and J. A. Vance. 1988. The Late Cretaceous San Juan thrust system, San Juan Islands, Washington: Geological Society of America Special Paper 221, 81p.
- Brinkman, R. 1929a. Statistisch-biostratigraphische Untersuchungen an mittel jurassischen Ammoniten über Artebegriff und Stammesentwicklung: *Abh. Gesell. Wiss. Göttingen Math. Phys. Kl.*, v. 13, n. 3, p. 1-249.
- Brinkman, R. 1929b. Monographie der Gattung *Kosmoceras*: *Abh. Gesell. Wiss. Göttingen Math. Phys. Kl.*, v. 13, n. 4, p. 1-124.
- Burnett, J. A., 1990. A new nannofossil zonal scheme for the boreal Campanian: *International Nannoplankton Association Newsletter*, v. 12, n. 3, p. 67-70.
- Cande, S. C. and D. V. Kent. 1992. A new geomagnetic polarity timescale for the Late Cretaceous and Cenozoic: *Journal of Geophysical Research*, v. 97, p. 13917-13951.
- Chave, A. D. 1984. Lower Paleogene-Upper Cretaceous magnetostratigraphy, Sites 525, 527, 528, 529, Deep-sea Drilling Project Leg 74, *in* Moore, T. C. and others, Initial Reports of the Deep Sea Drilling Project, v. 74: Washington D.C., U.S. Government Printing Office, p. 525-531.

- Chamberlain, J. A. jr. and G. E. G. Westermann. 1976. Hydrodynamic properties of cephalopod shell ornament: *Paleobiology*, v. 2, p. 316-331.
- Clapp, C. H. 1917. Sooke and Duncan map-areas, Vancouver Island: Geological Survey of Canada, Memoir 96, 445p.
- Clemens, S. C., Farrel, J. W., and L. P. Gromet. 1993. Synchronous changes in seawater strontium isotopic composition and global climate: *Nature*, v. 363, p. 607-609.
- Cobban, W. A. 1951. New species of Baculites from the Upper Cretaceous of Montana and South Dakota: *Journal of Paleontology*: v. 25, n. 6, p. 817-821.
- Cobban, W. A. 1958. Two new species of Baculites from the western interior region: *Journal of Paleontology*, v. 32, n. 4, p. 660-665.
- Cobban, W. A. 1962a. New Baculites from the Bearpaw shale and equivalent rocks of the Western Interior: *Journal of Paleontology*, v. 36, n. 1, p. 126-135.
- Cobban, W. A. 1962b. Baculites from the lower part of the Pierre Shale and equivalent rocks in the Western Interior: *Journal of Paleontology*, v. 36, n. 4, p. 704-718.
- Cobban, W. A. 1973. The late Cretaceous ammonite Baculites undatus Stephenson in Colorado and New Mexico: *U.S. Geological Survey Journal of Research*, v. 1, n. 4, p. 459-465.
- Cobban, W. A. 1974. Ammonites from the Navasink Formation at Atlantic Highlands, New Jersey: *U.S. Geological Survey Professional Paper* 845, 21p.
- Cobban, W. A. 1976. Ammonite record from the Pierre Shale of northeastern New Mexico: *New Mexico Geological Society Guidebook* 27, p. 165-169.
- Cobban, W. A. 1977. A new curved baculitid from the Upper Cretaceous of Wyoming: *U.S. Geological Survey Journal of Research*, v. 5, p. 457-462.
- Cobban, W. A. 1993. Diversity and distribution of Late Cretaceous ammonites, Western Interior, United States, *in* Caldwell, W. E. G., and E. G. Kaufmann, eds., *Evolution of the Western Interior Basin: Geological Association of Canada, Special Paper* 39, p. 435-451.
- Cobban, W. A. and W. J. Kennedy, 1991. Baculites thomi Reeside, 1927, an Upper Cretaceous ammonite in the Eastern Interior of the United States: *U.S. Geological Survey Bulletin* 1934-C, 8p.
- Cobban, W. A. and W. J. Kennedy, 1992a. Campanian ammonites from the Upper Cretaceous chalk of Lamar County, Texas: *Journal of Paleontology*, v. 66, n. 3, p. 440-454.
- Cobban, W. A. and W. J. Kennedy, 1992b. The last Western Interior Baculites from the Fox Hills Formation of South Dakota: *Journal of Paleontology*, v. 66, n. 4, p. 682-684.

- Cobban, W. A. and W. J. Kennedy, 1993. Middle Campanian ammonites and inoceramids from the Wolf City Sand in Northeastern Texas: *Journal of Paleontology*, v. 67, n. 1, p. 71-82.
- Dia, A. N., Cohen, A. S., O'Nions, R. K., and N. J. Shackleton. 1992. Seawater Sr isotopic variation over the past 300 kyr and influence of global climate cycles: *Nature*, v. 356, p. 786-788.
- Eldredge, N. and S. J. Gould. 1972. Punctuated Equilibria: an alternative to phyletic gradualism. *in* *Models in Paleobiology*, T. J. M. Schopf, ed. Freeman, Cooper, San Francisco, p. 82-115.
- Elias, M. K. 1933. Cephalopods of the Pierre Formation of Wallace County, Kansas, and adjacent area: *The University of Kansas Science Bulletin*, v. 21, n. 9, p. 289-363.
- Filmer, P. E. and J. L. Kirschvink. 1989. A paleomagnetic constraint on the Late Cretaceous paleoposition of northwestern Baja California, Mexico: *Journal of Geophysical Research*, v. 94, p. 7332-7342.
- Gastil, R. G., Phillips, R. P. and E. C. Allison. 1975. Reconnaissance geology of the State of Baja California: *Geological Society of America Memoir* 140, 170p.
- Henderson, G. M., Martel, D. J., O'Nions, R. K., and N. J. Shackleton. 1994. Evolution of seawater $^{87}\text{Sr}/^{86}\text{Sr}$ over the last 400 ka: the absence of glacial/interglacial cycles: *Earth and Planetary Science Letters*, v. 128, p. 643-651.
- Hengsbach, R. 1996. Ammonoid Pathology, *in* Landman, N. H., Tanabe, K. and R. A. Davis, eds., *Ammonoid Paleobiology: Topics in Geobiology*, v. 13, p. 581-605.
- Hicks, J. F., Obradovich, J. D., and L. Tauxe. 1995. A new calibration for the Late Cretaceous time scale: The $^{40}\text{Ar}/^{39}\text{Ar}$ isotope age for the C33r/C33n geomagnetic reversal from the Judith River Formation (Upper Cretaceous), Elk Basin, Wyoming, USA: *The Journal of Geology*, v. 103, p. 243-256.
- Hodell, D. A., Mueller, P. A., and J. R. Garrido. 1991. Variations in the strontium isotopic composition of seawater during the Neogene: *Geology*, v. 19, p. 24-27.
- Howarth, M.K. 1973. The stratigraphy and ammonite fauna of the Upper Liassic Grey Shales of the Yorkshire coast: *Bulletin of the British Museum of Natural History, Geology*, v. 24, p. 237-277.
- Howarth, R. J. and J. M. MacArthur. 1997. Statistics for Strontium Isotopic Stratigraphy: A Robust LOWESS Fit to the marine Sr-Isotopic curve for 0 to 206 Ma, with Look-up Table for Derivation of Numeric Age: *The Journal of Geology*, v. 105, p. 441-456.
- Huber, B. B. T., D. A. Hodell, and C. P. Hamilton, 1995. Middle-Late Cretaceous climate of the southern high latitudes: Stable isotopic evidence for minimal equator-to-pole thermal gradients: *Geological Society of America Bulletin*, v. 107, n. 10, p. 1164-1191.

- Ingersoll, R. V. 1979. Evolution of the Late Cretaceous forearc basin, northern and central California: *Geological Society of America Bulletin*, v. 90, p. 813-826.
- Jacobs, D. K. and J. A. Chamberlain 1996. Buoyancy and Hydrodynamics in Ammonoids, *in* Landman, N. H., Tanabe, K. and R. A. Davis, eds., *Ammonoid Paleobiology: Topics in Geobiology*, v. 13, p. 169-224.
- Jeletzky, J. A. 1971. Marine Cretaceous biotic provinces and paleogeography of Western and Arctic Canada: *Geological Survey of Canada Paper* 70-22, 92p.
- Kauffman, E. G. 1977. Evolutionary rates and biostratigraphy, *in* Kauffman, E. G. and Hazel, J. E., eds., *Concepts and methods of biostratigraphy*, Dowden, Hutchinson and Ross, Inc., p. 109-142.
- Kennedy, W. A. and W. A. Cobban, 1993a. Campanian ammonites from the Annona Chalk near Yancy, Arkansas: *Journal of Paleontology*, v. 67, n. 1, p. 83-97.
- Kennedy, W. A. and W. A. Cobban, 1993b. Ammonites from the Saratoga Chalk (Upper Cretaceous), Arkansas: *Journal of Paleontology*, n. 67, n. 3, p. 404-434.
- Kennedy, W. A. and W. A. Cobban, 1993c. Lower Campanian (Upper Cretaceous) ammonites from the Merchantville Formation of New Jersey, Maryland, and Delaware: *Journal of Paleontology*, v. 67, n. 5, p. 828-849.
- Kilmer, F. 1965. Late Cretaceous stratigraphy and paleontology, El Rosario, Northwestern Baja California, Mexico: *Geological Society of America Abstracts with Programs, Cordilleran Section*, p. 31-32.
- Klinger, H. C. and W. J. Kennedy. 1997. Cretaceous faunas from Zululand and Natal, South Africa: the ammonite family Baculitidae Gill, 1871 (excluding the genus Eubaculites): *Annals of the South African Museum*, v. 105, n.1. p. 1-206.
- Landman, N. H. and Waage, K. M. 1986. Shell abnormalities in scaphitid ammonites: *Lethaia*, v. 19, p. 211-224.
- Lohmann, G. P. and P. N. Sweitzer. 1988. On Eigenshape Analysis, *in* F. J. Rohlf and F. L. Bookstein, eds., *Proceedings of the Michigan Morphometrics Workshop*. University of Michigan Museum of Paleontology, Special Publication no. 2., p. 147-166.
- Lutz, T. M. and G. E. Boyajian. 1995. Fractal geometry of ammonoid sutures: *Paleobiology*, v. 21, p. 329-342.
- MacArthur, J. M., Thirwall, M. F., Chen, M., Gale, A. S. and W. J. Kennedy. 1993. Strontium isotope stratigraphy in the Late Cretaceous: Numerical calibration of the Sr isotope curve and intercontinental correlation for the Campanian: *Paleoceanography*, v. 8, n. 6, p. 859-873.
- MacArthur, J. M., Kennedy, W. J., Chen, M., Thirwall, M. F., and A. S. Gale. 1994. Strontium isotope stratigraphy for Late Cretaceous time: Direct numerical calibration of the Sr Isotope curve based on the US Western Interior: *Paleogeography, Paleoclimatology, Paleoecology*, v. 108, p. 95-119.

- MacArthur, J. M., Thirwall, M. F., A. S. Gale., Kennedy, Matthey, D., and A. R. Lord. 1995. Strontium isotope stratigraphy for the Late Cretaceous: A new curve based on the English Chalk, *in* Hailwood, E. A. and R. B. Kidd, eds., *High Resolution Stratigraphy: Geological Society Special Publication no. 70*, p. 195-209.
- Matsumoto, T. 1959. Zoning of the Upper Cretaceous in Japan and adjacent areas with special reference to world-wide correlation: *in* Kellum, L. B. and L. Benavides, eds., *The Cretaceous System, 20th International Geological Congress, Mexico, 1956*, v. II, p. 347-381.
- Matsumoto, T. 1960. Upper Cretaceous ammonites from California, Pt. 1 Introduction and Baculitidae: *Memoirs of the Faculty of Science, Kyushu University, Series D*, v. 8, n. 4, p. 91-171.
- Matsumoto T. and I. Obata. 1963. A monograph on the Baculitidae from Japan: *Memoirs of the Faculty of Science, Kyushu University, Series D*, v. 13, n. 1, p. 1-116.
- Meek, F. B. 1876. Descriptions and illustrations of fossils from Vancouver's and Suquia Islands, and other Northwestern localities: *in* Hayden, ed., *Bulletin of the U.S. Geological and Geographical Survey of the Territories*, v. 2, n. 4, p. 351-368.
- Morrison, J. O. and U. Brand. 1988. An evaluation of diagenesis and chemostratigraphy of Upper Cretaceous molluscs from the Canadian interior seaway: *Chemical Geology*, v. 72, p. 235-248.
- Morton, N. 1983. Pathologically deformed *Graphoceras* (Ammonitina) from the Jurassic of Skye, Scotland: *Paleontology (London)*, v. 26, p. 443-453.
- Nelson, B. K., MacLeod K. G. and P.D. Ward. 1991. Rapid change in strontium isotopic composition of sea water before the Cretaceous/Tertiary boundary: *Nature*, v. 351, n. 6328, p. 644-647.
- Muller, J. E. and J. A. Jeletzky. 1970. Geology of the Upper Cretaceous Nanaimo Group, Vancouver Island, and Gulf Islands, British Columbia: *Geological Survey of Canada Paper 69-25*, 77p.
- Nilsen, T. H. and P. L. Abbott. 1981. Paleogeography and sedimentology of Upper Cretaceous turbidites, San Diego, California: *American Association of Petroleum Geologists Bulletin*, v. 65, p. 1256-1284.
- Obradovich, J. D. 1993. A Cretaceous time scale, *in* Caldwell, W. G. E. and Kauffman, E. G., eds., *Evolution of the Western Interior Basin: Geological Association of Canada, Special paper 39*, p. 397-396.
- Perch-Nielsen, K. 1985. Mesozoic calcareous nannofossils, *in* Bolli, H. M., Saunders, J. B., and Perch-Nielsen, K., eds., *Plankton stratigraphy: Cambridge, United Kingdom, Cambridge University Press*, p. 329-426.
- Raup, D. M. 1967. Geometric analysis in shell coiling; coiling in ammonoids: *Journal of Paleontology*, v. 41, p. 43-65.

- Ray, T. H. 1990. Application of eigenshape analysis to second order leaf shape ontogeny in *Syngonium podophyllum* (Araceae), in F. J. Rohlf and F. L. Bookstein, eds., Proceedings of the Michigan Morphometrics Workshop. University of Michigan Museum of Paleontology, Special Publication no. 2., p. 201-212.
- Reeside, J. B. 1927. The cephalopods of the Eagle Sandstone and related formations in the Western Interior of the United States: U.S. Geological Survey Professional Paper 151, 87p.
- Richter, F. M. and K. K. Turekian. 1993. Simple models for the geochemical response of the ocean to climatic and tectonic forcing: Earth and Planetary Science Letters, v. 119, p. 121-131.
- Sadler, P. M. 1981. Sediment accumulation rates and the completeness of stratigraphic sections: Journal of Geology, v. 89, p. 569-584.
- Saunders, W. B. 1995. The ammonoid suture problem: relationship between shell- and septal thickness and suture complexity in Paleozoic ammonoids: Paleobiology, v. 21, p. 343-355.
- Saunders, W. B. and D. M. Work. 1996. Shell morphology and suture complexity in Upper Carboniferous ammonoids: Paleobiology, v. 22, p. 189-218.
- Saunders, W. B. and D. M. Work. 1997. Evolution of shell morphology and suture complexity in Paleozoic prolecanitids, the rootstock of Mesozoic ammonoids: Paleobiology, v. 23, p. 301-325.
- Sliter, W. V. 1973. Upper Cretaceous foraminifers from the Vancouver Island area, British Columbia, Canada: Journal of Foraminiferal Research, v. 3, n. 4, p. 167-186.
- Sliter, W. V. 1984. Cretaceous foraminiferans from La Jolla, California, in Abbot, P., ed., Upper Cretaceous depositional systems, southern California-Northern Baja California: Society of Economic Paleontologists and Mineralogists, Pacific Section, Book 36, p. 35-36.
- Sokal, R. R. and C. D. Michner. 1958. A statistical method for evaluating systematic relationships: University of Kansas Science Bulletin, v. 38, p. 1409-1438.
- Stoll, H. M. and D. P. Schrag. 1996. Evidence for Glacial Control of Rapid Sea Level Changes in the Early Cretaceous: Science, v. 272, p. 1771-1774.
- Sugarman, P. J., Miller, K. G., Bukry, D. and M. D. Feigenson. 1995. Uppermost Campanian-Maestrichtian strontium isotopic, biostratigraphic, and sequence stratigraphic framework of the New Jersey Coastal Plain: Geological Society of America Bulletin, v. 107, n. 1, p. 19-37.
- Vonhof, H. B. and J. Smit. 1997. High-resolution late Maastrichtian-early Danian oceanic $^{87}\text{Sr}/^{86}\text{Sr}$ record: Implications for Cretaceous-Tertiary boundary events: Geology, v. 25, n. 4, p. 347-350.

- Ward, P. D. 1978a. Baculitids from the Nanaimo Group, Vancouver Island, Canada and Washington State, USA: *Journal of Paleontology*, v. 52, p. 1143-1154.
- Ward, P. D. 1978b. Revisions in the stratigraphy and biochronology of the Upper Cretaceous Nanaimo Group, British Columbia and Washington State: *Canadian Journal of Earth Sciences*, v. 15, p. 405-423.
- Ward, P. D. 1980. Comparative shell shape distributions in Jurassic-Cretaceous ammonites and Jurassic-Tertiary nautilids: *Paleobiology*, v. 6, p. 32-43.
- Ward, P. D. 1987. The natural history of Nautilus. Allen & Unwin, London. 267pgs.
- Ward, P. D. 1990. A review of Maastrichtian ammonite ranges, in Sharpton, V. L., and Ward, P. D., eds., *Global catastrophes in Earth history; An interdisciplinary conference on impacts, volcanism, and mass mortality*: Geological Society of America Special Paper 247, p. 519-530.
- Ward, P. D. and J. Haggart. 1981. The Upper Cretaceous ammonite and inoceramid bivalve succession at Sand Creek, Colusa County, California, and its implications for the establishment of an Upper Cretaceous Great Valley Sequence ammonite zonation: *Newsletters on Stratigraphy*, v. 10, p. 140-147.
- Ward, P. D. and G. E. G. Westermann. 1985. Cephalopod paleoecology in Bottjer, D. J., Hickman, C. S., and P. D. Ward, eds., *Mollusks: notes for a short course*: University of Tennessee, Department of Geological Sciences, Studies in Geology v. 13, p. 215-229.
- Ward, P. D. , Verosub, K., and, J. Haggart. 1983. Marine magnetic anomaly 33-34 identified in the Upper Cretaceous of the Great Valley Sequence of California: *Geology*, v. 11, p. 90-93.
- Ward, P. D., Hurtado, J. M., Kirschvink, J. L., and K. L. Verosub. 1997. Measurements of the Cretaceous Paleolatitude of Vancouver Island: Consistent with the Baja-British Columbia Hypothesis: *Science*, v. 277, p. 1642-1645.
- Weiner S. and H. Lowenstam. 1980. Well preserved fossil mollusk shells: characterization of mild diagenetic processes, in P. Hare, ed., *Biogeochemistry of Amino Acids*, J. Wiley and Sons, pp. 95-114.
- Westermann, G. E. G. 1971. Form, structure and function of shell and siphuncle in coiled Mesozoic ammonoids: *Life Sciences Contributions of the Royal Ontario Museum*, v. 78, p. 1-39.
- Zahn, C. T. and R. Z. Roskies. 1972. Fourier descriptors for plane closed curves: *IEEE Trans. Comp.*, C21(3): 269-281.

APPENDIX A

SORTED EIGENSHAPE ANALYSIS SCORES

Scores for Punta San Jose Data set (n = 154) based on Correlations

Sp.#1	COR1	Sp.#2	COR2	Sp.#3	COR3	Sp.#4	COR4	Sp.#5	COR5
95048	0.986	94776	0.292	78907	0.256	78806	0.183	78922	0.164
78779	0.985	94616	0.208	78796	0.201	94775	0.183	78729	0.128
78808	0.985	95144	0.206	78750	0.2	95028	0.183	78916	0.116
78816	0.985	78834	0.202	78751	0.171	78986	0.18	78726	0.111
78799	0.984	78902	0.199	78714	0.171	95155	0.169	78706	0.105
95173	0.983	94778A	0.191	78906	0.17	95058	0.162	78994	0.105
78929	0.982	78849	0.188	78811	0.145	78994	0.158	78942	0.104
95163	0.982	78847	0.186	78765	0.144	78900	0.158	78768	0.101
95140	0.982	78914B	0.179	78752	0.139	78908A	0.151	78915	0.097
B5320	0.981	78940	0.173	78709	0.135	78875	0.141	78982	0.096
78937	0.981	78849	0.171	78986	0.122	78944	0.129	95170	0.094
95178	0.98	94775	0.157	78830	0.117	78737	0.12	78766	0.094
78960	0.98	78735	0.156	78763	0.113	78874	0.106	78743	0.091
78839A	0.98	78986	0.156	78940	0.107	78714	0.103	78852	0.09
78957	0.98	78969	0.154	78820	0.103	78995	0.102	78896	0.09
95134	0.98	95170	0.151	78878	0.101	78706	0.102	78944	0.085
78999B	0.98	78780	0.134	78896	0.099	95147	0.092	78839	0.084
78903	0.979	78706	0.133	79000	0.097	78972	0.088	78803	0.078
78839	0.979	95135	0.133	78895	0.097	78711	0.085	95147	0.078
78763	0.978	94777	0.123	78850	0.089	78843	0.076	78875	0.077
78815	0.978	78701	0.122	95179	0.088	78849	0.074	78780	0.076
78781	0.978	95035	0.121	78790	0.087	78703	0.074	78839A	0.075
78982	0.978	78874	0.121	95035	0.087	78752	0.068	78934	0.073
78895	0.978	78896	0.105	78994	0.087	78934	0.068	78729ii	0.073
95141	0.977	78803	0.104	78903	0.084	78849	0.066	78924	0.072
78904	0.977	95134	0.104	78956	0.083	78766	0.064	78907	0.07
78724	0.977	78951	0.104	94777	0.082	78726	0.063	78783	0.069
78733	0.977	78916	0.103	95163	0.081	78974	0.063	78811	0.069
78972	0.975	78934	0.099	78914	0.081	78830	0.061	95022	0.069
78745	0.975	95140	0.093	78982	0.079	78961	0.059	78995	0.069
95059	0.974	78900A	0.088	95070	0.077	78929	0.059	78719	0.067
78780	0.974	95140	0.087	78904	0.075	78963	0.059	78933	0.066
95147	0.974	78768	0.084	78992	0.074	78916	0.058	78878	0.066
78933	0.974	A85806	0.083	78720	0.068	95135	0.057	78840	0.064
78995	0.974	78839	0.077	78889	0.067	78796	0.051	95178	0.063
78766	0.973	78811	0.075	78728	0.062	78939	0.051	78796	0.062
78896	0.973	78937	0.073	78783	0.061	78960	0.05	78963	0.061
95022	0.973	78839A	0.073	78872	0.061	78909	0.046	78816	0.06
78783	0.973	78875	0.072	78743	0.06	78937	0.045	95141	0.059
78872	0.972	78878	0.067	78839	0.059	78937	0.045	78969	0.057
95035	0.972	95169	0.062	B5320	0.058	78852	0.044	78937	0.057
95140	0.972	78947	0.061	94775	0.058	94778A	0.04	95134	0.056
78851	0.972	78924	0.06	78779	0.057	94776	0.038	78751	0.053

Sp.#1	COR1	Sp.#2	COR2	Sp.#3	COR3	Sp.#4	COR4	Sp.#5	COR5
95179	0.972	78922	0.056	78805	0.056	95049	0.037	95179	0.052
78947	0.972	95070	0.055	78956	0.055	78840	0.035	78914	0.051
95049	0.971	78889	0.053	78733	0.053	78747	0.035	78843	0.051
78992	0.971	78963	0.047	78839A	0.052	78763	0.034	95140	0.05
78937	0.971	95163	0.046	95049	0.051	78700	0.033	78806	0.05
78882	0.971	78894	0.045	95134	0.051	78894	0.032	78718	0.05
78924	0.971	78779	0.045	78882	0.051	78895	0.031	78820	0.049
78805	0.971	78729ii	0.041	78721	0.05	78915	0.028	78973	0.048
78876	0.97	78851	0.036	78781	0.049	94616	0.028	78999	0.048
78889	0.97	78766	0.036	78799	0.046	94777	0.028	95140	0.047
79000	0.97	78806	0.034	78816	0.044	95179	0.024	78951	0.041
78969	0.97	95178	0.032	78947	0.043	78712	0.024	95048	0.04
78939	0.969	78816	0.03	78969	0.042	78924	0.023	95163	0.036
78894	0.969	95048	0.029	78957	0.042	78973	0.018	78747	0.035
78803	0.969	78939	0.027	78834	0.039	95134	0.017	78872	0.032
78914B	0.968	95141	0.027	78972	0.039	78851	0.017	78900	0.032
95169	0.968	78765	0.027	78747	0.038	78882	0.017	78720	0.028
78956	0.967	78913	0.024	78937	0.038	78765	0.016	78805	0.027
78768	0.967	B5320	0.023	78806	0.034	78745	0.015	78752	0.025
78908	0.967	78960	0.023	78745	0.033	78783	0.012	78986	0.022
78922	0.967	95187	0.023	78815	0.031	95170	0.011	78929	0.022
78840	0.967	78711	0.023	94616	0.029	78733	0.011	78815	0.021
78948	0.967	95064	0.023	78922	0.026	95141	0.01	78906	0.021
78872	0.967	78994	0.02	78902	0.026	78872	0.01	A85806	0.021
78951	0.966	78808	0.02	94776	0.025	78904	0.01	78889	0.019
78944	0.966	78900	0.018	78999B	0.021	95173	0.009	78960	0.018
A85806	0.966	95173	0.017	78913	0.013	95048	0.008	78739	0.017
78850	0.965	78799	0.016	78924	0.01	78808	0.008	78991	0.016
95070	0.965	78956	0.013	78914B	0.01	78815	0.008	78961	0.015
78729ii	0.964	78999B	0.009	78999	0.009	78908	0.005	78937	0.014
78909	0.964	78895	0.008	78916	0.009	95175	0.003	78914B	0.013
78974	0.964	95049	0.007	95140	0.009	78729	0.003	78947	0.012
95044A	0.963	95044A	0.007	78934	0.007	78903	0.002	78908	0.011
95135	0.963	78995	0.007	78874	0.005	95140	0.002	95035	0.01
78914	0.962	95059	0.005	78944	0.005	78969	0.001	78903	0.01
78913	0.962	78876	0.003	78711	0.003	78872	0	78847	0.007
78991	0.962	78972	-0.001	78803	0.002	95163	0	78909	0.006
78900A	0.962	78909	-0.002	78876	-0.003	78768	-0.002	78956	0.005
78916	0.962	78991	-0.002	78840	-0.006	78906	-0.003	94616	0
78721	0.961	78992	-0.003	95140	-0.006	78720	-0.006	95044A	-0.001
78820	0.961	78700	-0.004	95044A	-0.007	78922	-0.006	95064	-0.003
78875	0.961	78783	-0.004	78724	-0.008	78805	-0.007	78808	-0.003
78701	0.961	78908	-0.005	95144	-0.01	78878	-0.009	78799	-0.005
78728	0.961	78933	-0.01	78908	-0.011	78982	-0.01	95070	-0.005
78934	0.96	78815	-0.015	95048	-0.012	78743	-0.012	78750	-0.007
78811	0.96	78982	-0.019	95058	-0.012	78834	-0.012	78779	-0.009
78961	0.96	78843	-0.023	78701	-0.014	78889	-0.013	78763	-0.009
95175	0.96	78915	-0.023	78995	-0.014	78876	-0.013	78849	-0.011
78906	0.96	78872	-0.023	78900	-0.014	78781	-0.015	78830	-0.012
78765	0.959	78882	-0.026	78768	-0.015	78940	-0.016	95044B	-0.013
78806	0.959	78907	-0.028	95059	-0.019	78816	-0.018	95173	-0.013

Sp.#1	COR1	Sp.#2	COR2	Sp.#3	COR3	Sp.#4	COR4	Sp.#5	COR5
78830	0.959	95130	-0.028	78808	-0.019	95035	-0.019	78900A	-0.016
78878	0.958	78929	-0.03	78780	-0.021	78839A	-0.02	78851	-0.017
94616	0.958	78840	-0.031	78726	-0.023	78721	-0.021	78724	-0.017
78700	0.958	78957	-0.033	95173	-0.024	78947	-0.021	95155	-0.018
78963	0.957	78974	-0.034	78843	-0.028	78896	-0.022	78974	-0.019
78720	0.957	78796	-0.034	78894	-0.028	78839	-0.023	B5320	-0.019
78843	0.956	78948	-0.034	95147	-0.029	95140	-0.024	78790	-0.022
78994	0.956	78728	-0.035	78899	-0.029	95064	-0.025	79000	-0.023
95144	0.955	78721	-0.038	95141	-0.034	95022	-0.025	78939	-0.023
95187	0.955	78944	-0.038	95187	-0.035	78991	-0.03	78781	-0.025
78973	0.955	78745	-0.038	78974	-0.035	95187	-0.034	78957	-0.03
78796	0.954	78781	-0.041	78872	-0.039	78780	-0.034	95169	-0.031
78743	0.954	78763	-0.045	78991	-0.04	78914B	-0.036	95059	-0.032
78915	0.954	78914	-0.047	78929	-0.041	78779	-0.036	95049	-0.032
78852	0.953	78956	-0.049	78939	-0.046	78811	-0.038	78733	-0.033
78942	0.952	78820	-0.052	78973	-0.046	95130	-0.039	78904	-0.036
78739	0.952	78903	-0.055	78951	-0.048	78739	-0.041	78745	-0.036
95064	0.951	78724	-0.055	78937	-0.05	95070	-0.042	78895	-0.037
78874	0.951	78850	-0.058	95178	-0.05	78750	-0.042	78874	-0.039
78790	0.951	78942	-0.059	78851	-0.052	78951	-0.045	78940	-0.041
78986	0.95	78709	-0.06	78900A	-0.058	95044A	-0.045	95131	-0.045
78751	0.95	78733	-0.06	78948	-0.063	78999B	-0.047	78882	-0.047
78752	0.949	78906	-0.067	78737	-0.066	78820	-0.047	78992	-0.048
95170	0.949	78852	-0.067	95135	-0.066	78956	-0.047	95144	-0.054
95131	0.949	95175	-0.071	95028	-0.069	78799	-0.048	78721	-0.056
78711	0.948	78751	-0.074	78766	-0.072	B5320	-0.049	78849	-0.056
95130	0.948	79000	-0.075	78875	-0.073	78803	-0.05	78908A	-0.058
78849	0.948	95147	-0.078	78933	-0.078	95169	-0.05	78712	-0.06
78834	0.947	78830	-0.081	78942	-0.08	78933	-0.057	78894	-0.061
78712	0.947	78737	-0.081	95169	-0.082	78913	-0.057	78872	-0.065
78747	0.944	78719	-0.082	95155	-0.082	78701	-0.059	78850	-0.065
78750	0.942	78904	-0.086	95022	-0.083	78735	-0.059	78876	-0.066
78940	0.942	95022	-0.088	78729ii	-0.083	95044B	-0.06	78735	-0.069
95044B	0.942	95028	-0.089	78712	-0.084	79000	-0.06	78728	-0.07
78706	0.939	78805	-0.095	78847	-0.085	95178	-0.061	95187	-0.075
78900	0.939	78937	-0.103	78908A	-0.088	A85806	-0.061	78913	-0.079
95028	0.938	78790	-0.104	95175	-0.089	78948	-0.062	95028	-0.085
78847	0.937	78973	-0.114	78909	-0.09	78957	-0.068	94776	-0.085
78956	0.935	78872	-0.117	78700	-0.092	78992	-0.07	94775	-0.086
78709	0.935	95179	-0.119	A85806	-0.093	78907	-0.076	78701	-0.089
78735	0.933	78718	-0.121	78960	-0.097	78790	-0.083	78972	-0.089
78907	0.933	78743	-0.121	78739	-0.114	95144	-0.084	78709	-0.09
94776	0.932	78739	-0.13	95064	-0.116	78751	-0.091	78899	-0.098
94778A	0.929	78750	-0.131	78961	-0.118	78729ii	-0.092	78956	-0.106
78703	0.925	78703	-0.134	95044B	-0.123	95131	-0.094	78999B	-0.106
78737	0.925	95131	-0.139	78915	-0.128	78914	-0.098	78714	-0.107
78849	0.921	78720	-0.141	95130	-0.13	78724	-0.1	95130	-0.107
78999	0.92	78961	-0.163	78703	-0.132	78900A	-0.102	78765	-0.116
78726	0.917	95044B	-0.164	95170	-0.137	78850	-0.107	78948	-0.116
78908A	0.916	78999	-0.173	95131	-0.142	78942	-0.109	78737	-0.122
94775	0.914	78712	-0.18	94778A	-0.153	78728	-0.109	95135	-0.122

Sp.#1	COR1	Sp.#2	COR2	Sp.#3	COR3	Sp.#4	COR4	Sp.#5	COR5
78902	0.909	78752	-0.188	78963	-0.16	78847	-0.115	78711	-0.123
94777	0.903	78747	-0.197	78852	-0.169	95059	-0.119	78703	-0.126
95155	0.902	78714	-0.217	78735	-0.186	78999	-0.139	78700	-0.131
78719	0.902	95058	-0.22	78849	-0.191	78902	-0.167	78834	-0.142
78899	0.895	78908A	-0.274	78706	-0.196	78709	-0.176	95175	-0.145
78718	0.891	78899	-0.278	78729	-0.211	78899	-0.177	78902	-0.165
78714	0.885	78726	-0.286	78849	-0.224	78956	-0.211	94778A	-0.179
78729	0.873	95155	-0.289	78718	-0.249	78719	-0.228	94777	-0.185
95058	0.86	78729	-0.329	78719	-0.267	78718	-0.273	95058	-0.335

Scores from Punta San Jose Dataset (n = 154) based on Covariances

Sp.#1	COV1	Sp.#2	COV2	Sp.#3	COV3	Sp.#4	COV4	Sp.#5	COV5
78986	0.276	94776	0.061	78796	0.048	78718	0.052	78922	0.033
78805	0.262	94616	0.045	78907	0.047	78719	0.049	78994	0.032
78763	0.259	78834	0.045	78906	0.044	78956	0.034	78875	0.03
78743	0.255	78914B	0.044	78986	0.041	78999	0.032	78729	0.029
78906	0.254	94778A	0.043	78750	0.035	78942	0.029	78944	0.028
78768	0.253	78735	0.042	78751	0.035	78899	0.028	78766	0.027
78937	0.248	95144	0.042	78765	0.033	78914	0.028	78916	0.027
78876	0.246	78986	0.042	78811	0.033	78709	0.024	78706	0.025
78735	0.245	78902	0.041	78714	0.031	78751	0.023	78768	0.025
78780	0.245	78847	0.039	78763	0.03	95059	0.023	78852	0.025
78914B	0.242	78849	0.038	78752	0.03	78902	0.021	78995	0.024
78808	0.241	78849	0.038	78830	0.025	78847	0.021	78915	0.024
A85806	0.237	78940	0.038	78940	0.025	78907	0.021	78806	0.024
95134	0.236	78780	0.034	78896	0.024	78729ii	0.021	78726	0.024
78999B	0.236	95170	0.034	78994	0.023	78724	0.021	95147	0.023
95140	0.236	78969	0.032	78820	0.022	78790	0.019	78743	0.021
78816	0.236	95135	0.03	78895	0.02	78850	0.019	95170	0.021
78956	0.235	95035	0.027	78878	0.02	78900A	0.018	78963	0.019
78909	0.235	78701	0.027	95035	0.02	95178	0.018	78986	0.019
78781	0.234	94775	0.026	95179	0.019	78803	0.018	78840	0.018
78995	0.234	78803	0.025	78982	0.019	78728	0.016	78982	0.018
95140	0.233	78706	0.024	78956	0.019	95131	0.016	78934	0.018
78840	0.233	95134	0.024	95163	0.018	78933	0.016	78900	0.017
78765	0.233	78768	0.023	78709	0.018	A85806	0.015	78937	0.017
78799	0.232	78896	0.023	78903	0.018	78820	0.015	78843	0.016
78745	0.232	78916	0.023	78889	0.017	78780	0.014	78780	0.015
78803	0.232	78874	0.022	78790	0.017	78811	0.014	78924	0.015
B5320	0.232	95140	0.022	79000	0.017	78743	0.014	78942	0.014
78961	0.231	78951	0.021	78914	0.017	78922	0.014	78783	0.014
78766	0.231	95140	0.021	78743	0.016	78956	0.013	78896	0.014
78889	0.23	A85806	0.021	78805	0.015	95044B	0.013	95022	0.014
78806	0.229	78934	0.02	95070	0.015	78957	0.012	78973	0.013
95178	0.229	94777	0.019	78850	0.015	78896	0.012	78796	0.013
95135	0.228	78937	0.018	78839	0.014	78839	0.012	78803	0.013
78737	0.228	78900A	0.018	95134	0.014	78982	0.011	78839	0.013
78815	0.228	78839	0.017	78783	0.014	78951	0.011	95155	0.012
78982	0.228	78875	0.017	78872	0.014	78992	0.011	95141	0.012
78875	0.228	78839A	0.016	78904	0.014	79000	0.011	78839A	0.012
78701	0.227	78811	0.015	78992	0.013	95144	0.011	78961	0.011
78960	0.227	78922	0.013	78720	0.013	78768	0.01	95179	0.011
95035	0.227	78947	0.012	94775	0.012	95022	0.01	95134	0.011
78914	0.226	78878	0.012	78839A	0.012	78839A	0.01	78816	0.01
95187	0.226	95169	0.012	94777	0.012	78799	0.01	78969	0.01
78872	0.225	78924	0.012	95049	0.012	78729	0.009	95140	0.01
95163	0.225	78889	0.011	78806	0.012	95140	0.009	78933	0.01
95173	0.224	78963	0.011	B5320	0.012	B5320	0.009	95048	0.009
78796	0.224	95070	0.01	78733	0.011	78750	0.009	78960	0.009
95059	0.223	78729ii	0.009	78779	0.011	78816	0.009	78747	0.009
95058	0.223	78894	0.009	78969	0.011	95044A	0.009	78729ii	0.009

Sp.#1	COV1	Sp.#2	COV2	Sp.#3	COV3	Sp.#4	COV4	Sp.#5	COV5
78834	0.223	95163	0.009	78816	0.011	78739	0.009	78929	0.009
78896	0.223	78766	0.009	78781	0.01	95070	0.008	78752	0.009
95049	0.222	95178	0.008	78882	0.009	78914B	0.008	95178	0.009
78724	0.222	78779	0.008	78947	0.009	95169	0.007	78878	0.008
78929	0.22	78806	0.007	78728	0.009	78779	0.007	78811	0.008
78944	0.22	78851	0.007	78799	0.009	78906	0.006	95140	0.008
78933	0.22	95048	0.006	78834	0.008	78991	0.006	78872	0.006
78894	0.22	78816	0.006	78972	0.008	95064	0.006	78849	0.006
78839A	0.219	78960	0.006	78815	0.008	78805	0.006	78937	0.006
78733	0.219	95141	0.006	94616	0.008	78878	0.006	78909	0.006
78903	0.219	78939	0.005	78721	0.008	78735	0.006	78805	0.005
78974	0.219	95187	0.005	78922	0.008	78701	0.006	78720	0.005
78839	0.218	95064	0.005	78745	0.007	78720	0.005	95163	0.005
95044A	0.218	78913	0.004	78937	0.007	78889	0.005	78820	0.004
78940	0.218	B5320	0.004	78957	0.007	78948	0.004	78951	0.004
78790	0.217	78808	0.004	78747	0.006	78947	0.004	78815	0.004
78922	0.216	78994	0.003	78956	0.006	95035	0.004	78907	0.003
78916	0.215	95173	0.003	94776	0.006	95140	0.004	78739	0.003
78973	0.215	78765	0.003	78916	0.006	78969	0.004	78719	0.002
78994	0.215	78900	0.003	78934	0.004	78913	0.004	78914	0.002
78779	0.214	78799	0.003	78914B	0.004	78999B	0.003	78908	0.002
78963	0.214	78711	0.002	95140	0.004	95163	0.003	78908A	0.002
78852	0.214	78956	0.002	78944	0.004	78783	0.003	78974	0.001
78830	0.213	95044A	0.002	78924	0.003	95141	0.002	78906	0.001
78811	0.213	95059	0.001	78999B	0.003	78781	0.002	78991	0.001
95048	0.213	78999B	0.001	78874	0.002	78973	0.002	78889	0.001
95179	0.212	78995	0.001	78803	0.002	95170	0.002	78751	0.001
78752	0.212	78876	0	78902	0.002	95187	0.002	A85806	0.001
94616	0.212	78895	0	78913	0	78815	0.001	78947	0
78957	0.211	78909	-0.001	78900	-0.001	95179	0.001	95064	0
78895	0.211	95049	-0.001	78840	-0.001	95134	0.001	78808	0
95022	0.211	78991	-0.001	78999	-0.001	78924	0.001	78903	0
94778A	0.211	78992	-0.002	78711	-0.001	78903	0.001	78999	0
78783	0.211	78908	-0.002	78768	-0.001	78872	0.001	95028	-0.001
95147	0.211	78700	-0.002	95140	-0.001	78721	0.001	78830	-0.001
78850	0.21	78972	-0.002	95044A	-0.002	78908	0	94616	-0.001
78969	0.209	78933	-0.002	78995	-0.002	95130	0	78939	-0.001
78820	0.209	78783	-0.002	78908	-0.003	78915	0	78874	-0.001
78720	0.209	78915	-0.004	78876	-0.003	95048	0	78851	-0.002
78908	0.209	78843	-0.005	95048	-0.003	78940	0	78763	-0.002
78947	0.209	78982	-0.005	95144	-0.003	78876	-0.001	95173	-0.002
78882	0.208	78815	-0.005	78780	-0.004	78747	-0.002	78914B	-0.002
78934	0.208	78872	-0.006	78726	-0.004	78808	-0.002	95044A	-0.003
95131	0.208	95130	-0.006	78724	-0.005	78840	-0.003	95035	-0.003
78851	0.208	78907	-0.007	78843	-0.005	78726	-0.003	95044B	-0.004
95141	0.208	78948	-0.007	95147	-0.005	78733	-0.003	78849	-0.004
78849	0.207	78882	-0.007	78808	-0.005	78904	-0.003	78718	-0.004
78972	0.207	78929	-0.007	78701	-0.006	78852	-0.003	94775	-0.005
78991	0.206	78721	-0.008	95173	-0.006	95173	-0.003	78956	-0.005
78751	0.205	78840	-0.008	78894	-0.006	78872	-0.004	95049	-0.006
95044B	0.205	78957	-0.008	95059	-0.007	78745	-0.004	95070	-0.006

Sp.#1	COV1	Sp.#2	COV2	Sp.#3	COV3	Sp.#4	COV4	Sp.#5	COV5
95170	0.205	78728	-0.009	95141	-0.007	78916	-0.004	78779	-0.007
78904	0.205	78974	-0.009	78974	-0.008	78796	-0.004	78745	-0.007
78937	0.204	78796	-0.01	78929	-0.009	78851	-0.006	78712	-0.007
78843	0.204	78944	-0.01	78991	-0.009	78882	-0.006	78750	-0.007
78729ii	0.202	78956	-0.011	78939	-0.01	78937	-0.006	78799	-0.007
95070	0.202	78709	-0.011	95058	-0.01	78937	-0.007	78733	-0.007
95064	0.202	78781	-0.011	78951	-0.01	94616	-0.007	78847	-0.007
78924	0.201	78745	-0.011	95187	-0.01	78712	-0.007	78781	-0.008
78939	0.201	78942	-0.011	78872	-0.01	78763	-0.008	95169	-0.008
78948	0.201	78914	-0.012	78937	-0.011	78895	-0.008	78904	-0.008
78872	0.2	78820	-0.012	78899	-0.011	78766	-0.008	78895	-0.008
78915	0.2	78724	-0.013	78973	-0.011	78752	-0.009	78882	-0.009
94776	0.2	78903	-0.014	95178	-0.011	95049	-0.009	B5320	-0.01
78992	0.2	78852	-0.014	78851	-0.012	78834	-0.01	78900A	-0.01
78913	0.2	78850	-0.014	95028	-0.012	78960	-0.01	79000	-0.01
78942	0.2	95175	-0.015	78900A	-0.013	78934	-0.01	78894	-0.011
78847	0.199	78763	-0.015	78875	-0.013	95175	-0.01	78972	-0.012
78900A	0.199	78733	-0.015	78766	-0.015	78963	-0.01	78872	-0.012
78951	0.199	78719	-0.015	95135	-0.016	78843	-0.011	78957	-0.012
78728	0.197	79000	-0.016	78948	-0.016	78929	-0.011	78724	-0.012
95169	0.196	78751	-0.017	78942	-0.017	78909	-0.012	78721	-0.012
95130	0.196	95028	-0.017	78908A	-0.018	78894	-0.012	78790	-0.013
95144	0.196	95147	-0.017	78729ii	-0.018	78706	-0.013	95131	-0.013
95155	0.195	95022	-0.019	78737	-0.018	78961	-0.013	78714	-0.015
78956	0.194	78830	-0.02	95169	-0.018	78765	-0.013	78940	-0.015
79000	0.194	78904	-0.02	95155	-0.018	95147	-0.013	78703	-0.015
78999	0.193	78906	-0.021	78847	-0.019	78830	-0.013	95059	-0.016
78703	0.193	78718	-0.022	78933	-0.019	78939	-0.013	78992	-0.016
78878	0.192	78737	-0.023	78712	-0.019	78700	-0.014	78876	-0.017
78902	0.192	78937	-0.023	95022	-0.019	94777	-0.015	78737	-0.017
78719	0.191	78739	-0.025	95175	-0.02	78974	-0.015	94776	-0.017
95175	0.19	78790	-0.026	78700	-0.02	94776	-0.016	95144	-0.017
78900	0.19	78973	-0.026	78960	-0.021	78995	-0.018	78711	-0.018
78700	0.188	95179	-0.027	78909	-0.022	78849	-0.018	95187	-0.018
78739	0.187	78805	-0.027	78739	-0.023	78849	-0.019	95130	-0.02
78849	0.187	78750	-0.027	A85806	-0.024	78944	-0.021	78913	-0.02
78712	0.185	78703	-0.029	95064	-0.024	78874	-0.022	78735	-0.02
78747	0.182	78872	-0.029	78915	-0.026	78972	-0.023	78700	-0.02
78714	0.182	95131	-0.03	95170	-0.027	78703	-0.023	78728	-0.023
78711	0.181	78720	-0.031	95044B	-0.029	78714	-0.023	78850	-0.023
78750	0.18	78743	-0.033	95130	-0.029	78711	-0.023	95135	-0.023
78874	0.18	95044B	-0.035	78703	-0.03	94778A	-0.024	95175	-0.025
78721	0.179	78712	-0.036	78961	-0.03	78994	-0.024	78701	-0.026
78907	0.177	78999	-0.036	78706	-0.031	95135	-0.024	78709	-0.026
78718	0.176	78747	-0.039	95131	-0.034	78875	-0.026	78948	-0.026
78726	0.174	78961	-0.039	78963	-0.034	78900	-0.028	78899	-0.027
78729	0.174	78752	-0.044	94778A	-0.035	78908A	-0.028	78999B	-0.028
78899	0.174	78714	-0.048	78852	-0.036	95028	-0.034	78765	-0.029
78908A	0.172	78908A	-0.052	78849	-0.04	94775	-0.034	94777	-0.031
95028	0.167	78726	-0.054	78729	-0.043	95155	-0.035	94778A	-0.034
78706	0.165	78899	-0.054	78849	-0.044	78806	-0.037	78834	-0.035

Sp.#1	COV1	Sp.#2	COV2	Sp.#3	COV3	Sp.#4	COV4	Sp.#5	COV5
94775	0.165	95058	-0.063	78735	-0.052	78737	-0.039	78956	-0.036
94777	0.162	78729	-0.063	78718	-0.053	78986	-0.048	78902	-0.046
78709	0.161	95155	-0.064	78719	-0.06	95058	-0.07	95058	-0.069

Scores from Sucia Islands Data set (n = 37) based on Correlations

Sp.#1	COR1	Sp.#2	COR2	Sp.#3	COR3	Sp.#4	COR4	Sp.#5	COR5
13259	0.982	94615	0.256	15946A	0.171	94725	0.167	15946	0.128
94666	0.977	94629	0.159	65747B	0.129	94614	0.156	43037	0.114
16733	0.975	65747B	0.145	94635	0.113	14622	0.116	94635	0.098
94609	0.975	94675	0.135	15946B	0.108	65747A	0.073	94727	0.082
94612A	0.973	94726	0.122	65747A	0.107	16733	0.067	94610	0.081
94644	0.973	94610	0.107	94642	0.099	94613	0.061	94615	0.077
91645	0.972	94727	0.102	15946	0.081	65409	0.059	94665	0.065
12771	0.972	94666	0.074	15946C	0.074	94675	0.059	94609	0.062
47822	0.971	65396A	0.073	94665	0.071	15946B	0.058	15946C	0.057
15946B	0.971	94611	0.062	94650	0.062	91645	0.043	16733	0.055
94727	0.971	94650	0.05	94726	0.054	94638	0.038	47822	0.054
94638	0.969	94644	0.048	94612A	0.049	12771	0.037	94650	0.045
94610	0.969	65747A	0.036	94638	0.028	13259	0.02	94612A	0.042
94675	0.968	91645A	0.032	94727	0.024	94609	0.017	12771	0.029
94642	0.968	94725	0.031	94613	0.024	94644	0.016	94644	0.027
65396A	0.968	94638	0.021	94725	0.021	94642	0.016	94613	0.027
94650	0.967	94614	0.015	94666	0.016	94610	0.014	94726	0.022
94665	0.966	91645	0.013	13259	0.01	47822	0.013	94629	0.013
94613	0.964	94664	0.011	94644	0.001	15946	0.008	94675	0.007
94726	0.964	94635	0.004	65396A	0	65396A	0.006	94614	-0.006
94614	0.964	65396B	-0.017	94615	-0.014	94635	0.006	94725	-0.007
94629	0.962	94642	-0.023	94675	-0.018	94629	0.006	94638	-0.014
91645A	0.962	47822	-0.031	12771	-0.02	94726	-0.002	15946B	-0.014
65396B	0.961	94609	-0.032	16733	-0.021	65747B	-0.004	94611	-0.024
15946C	0.958	94613	-0.043	94610	-0.042	94727	-0.009	65747A	-0.025
65409	0.957	15946B	-0.054	94609	-0.045	94665	-0.012	94666	-0.026
15946	0.957	16733	-0.062	94611	-0.057	91645A	-0.026	65396A	-0.034
94635	0.956	15946C	-0.063	65409	-0.062	94615	-0.034	91645	-0.039
65747A	0.954	13259	-0.071	94664	-0.068	94666	-0.046	13259	-0.039
94725	0.954	94612A	-0.074	91645	-0.073	94650	-0.049	14622	-0.069
94611	0.95	65409	-0.098	47822	-0.084	15946A	-0.081	94664	-0.086
94664	0.946	94665	-0.128	65396B	-0.098	65396B	-0.09	94642	-0.088
15946A	0.946	12771	-0.129	14622	-0.112	94612A	-0.1	91645A	-0.108
65747B	0.942	15946A	-0.142	94629	-0.115	43037	-0.131	65396B	-0.115
14622	0.941	15946	-0.161	94614	-0.123	15946C	-0.134	65409	-0.121
94615	0.94	43037	-0.176	91645A	-0.124	94664	-0.173	65747B	-0.133
43037	0.931	14622	-0.194	43037	-0.167	94611	-0.176	15946A	-0.141

Scores for Sucia Islands Data set (n = 37) based on Covariances

Sp.#1	COV1	Sp.#2	COV2	Sp.#3	COV3	Sp.#4	COV4	Sp.#5	COV5
47822	0.214	94615	0.05	15946A	0.04	94725	0.033	15946A	0.03
94609	0.212	94629	0.03	65747B	0.025	65747A	0.022	65747B	0.025
91645A	0.209	94675	0.028	15946C	0.021	94614	0.019	91645A	0.024
91645	0.208	65747B	0.027	65747A	0.018	14622	0.018	65396B	0.021
16733	0.207	94610	0.023	94635	0.017	16733	0.015	65409	0.02
94727	0.204	94726	0.022	94642	0.017	15946B	0.014	14622	0.017
94612A	0.203	94727	0.022	94612A	0.016	94675	0.011	94642	0.016
14622	0.202	65396A	0.016	15946B	0.016	94613	0.01	91645	0.01
15946A	0.202	94666	0.014	15946	0.014	15946	0.009	65747A	0.009
65396A	0.199	94611	0.012	94665	0.014	94638	0.008	94664	0.009
65396B	0.199	94644	0.01	94650	0.012	94635	0.008	13259	0.008
94610	0.197	94650	0.009	94726	0.011	12771	0.006	65396A	0.006
13259	0.196	91645A	0.008	94666	0.006	65747B	0.006	15946B	0.005
15946	0.195	65747A	0.007	94727	0.006	94642	0.005	94638	0.005
65747A	0.195	94725	0.006	94638	0.004	91645	0.005	94666	0.004
94638	0.193	94638	0.005	65396A	0.002	94644	0.004	94725	0.004
94665	0.193	94614	0.004	94613	0.002	94665	0.003	94614	0.004
94675	0.193	91645	0.004	94615	0.001	94726	0.003	94675	0.002
15946C	0.189	94664	0.002	94644	0.001	13259	0.003	94611	0.001
12771	0.189	94635	0.001	13259	0	65409	0.003	94629	-0.002
94666	0.186	65396B	-0.002	94611	-0.001	94727	0.002	94613	-0.004
94644	0.185	94642	-0.005	94664	-0.003	94609	0.002	94726	-0.004
94725	0.184	94613	-0.006	94725	-0.005	94610	0.002	94644	-0.005
94650	0.182	47822	-0.006	12771	-0.006	65396A	0	12771	-0.006
94615	0.182	94609	-0.007	94675	-0.006	47822	-0.002	94650	-0.009
65747B	0.182	15946B	-0.01	94610	-0.008	94650	-0.003	16733	-0.011
94642	0.179	15946C	-0.012	16733	-0.009	94629	-0.005	94609	-0.012
94611	0.179	16733	-0.013	94609	-0.012	94615	-0.006	94635	-0.012
94629	0.178	13259	-0.014	65409	-0.012	94666	-0.008	94612A	-0.013
94726	0.178	94612A	-0.015	65396B	-0.014	15946A	-0.013	15946C	-0.014
15946B	0.177	65409	-0.017	47822	-0.019	94612A	-0.017	47822	-0.015
94614	0.173	94665	-0.025	91645	-0.019	91645A	-0.017	94665	-0.015
65409	0.169	12771	-0.025	94629	-0.019	15946C	-0.021	94610	-0.015
43037	0.167	43037	-0.029	43037	-0.022	65396B	-0.029	94615	-0.016
94613	0.165	15946A	-0.032	91645A	-0.024	43037	-0.029	94727	-0.017
94664	0.162	15946	-0.033	94614	-0.027	94664	-0.03	43037	-0.022
94635	0.159	14622	-0.042	14622	-0.033	94611	-0.033	15946	-0.027

Scores from Combined Data set (n=191) using Correlations

Sp.#1	COR1	Sp.#2	COR2	Sp.#3	COR3	Sp.#4	COR4	Sp.#5	COR5
95048	0.986	78729	0.373	78907	0.259	15946	0.197	78922	0.16
78779	0.986	78899	0.314	78750	0.206	78986	0.191	94635	0.146
78816	0.985	95155	0.311	78796	0.188	78806	0.185	78942	0.127
78808	0.985	78726	0.304	78714	0.179	78994	0.183	78907	0.116
78799	0.984	78908A	0.291	78751	0.176	78900	0.156	15946C	0.114
95140	0.983	78747	0.22	78906	0.167	94775	0.156	78768	0.109
78937	0.983	78752	0.219	78709	0.164	78944	0.146	78896	0.108
95163	0.983	78712	0.219	78765	0.157	95028	0.14	78803	0.107
95134	0.983	78999	0.211	94629	0.143	14622	0.14	78982	0.107
95173	0.982	78714	0.207	78811	0.135	78875	0.139	78916	0.104
13259	0.982	95058	0.207	78752	0.132	95155	0.13	78839	0.103
78839A	0.981	95044B	0.206	78763	0.112	78995	0.112	78811	0.101
78960	0.981	98761	0.194	78850	0.112	78908A	0.106	78719	0.097
B5320	0.98	78720	0.184	78830	0.108	16733	0.101	78751	0.093
78839	0.98	78739	0.181	79000	0.105	94665	0.101	78780	0.093
95178	0.98	78703	0.168	78790	0.104	95147	0.101	78718	0.092
78999B	0.979	78973	0.158	78940	0.104	78706	0.098	78914	0.092
78929	0.979	95179	0.156	78820	0.101	78796	0.094	78729ii	0.091
95141	0.978	95131	0.154	78895	0.097	78916	0.09	78839A	0.091
78895	0.978	78743	0.151	94615	0.094	78934	0.089	78743	0.09
78957	0.978	78718	0.15	94610	0.092	12771	0.088	78729	0.086
78982	0.977	78750	0.148	78956	0.089	78752	0.087	78878	0.078
78780	0.976	78872	0.142	78986	0.089	78726	0.087	95178	0.078
78815	0.976	78805	0.142	94777	0.088	78714	0.087	95170	0.077
78896	0.976	78937	0.136	78992	0.086	78874	0.083	78999	0.076
78781	0.976	95028	0.126	78728	0.085	78843	0.081	78820	0.07
78903	0.975	95147	0.125	78878	0.084	78766	0.07	78783	0.07
78969	0.975	78719	0.125	78896	0.083	78830	0.069	78924	0.07
78733	0.975	95022	0.122	95179	0.083	15946B	0.069	78816	0.07
78724	0.975	78852	0.118	78956	0.083	78737	0.068	78969	0.07
78763	0.975	95175	0.114	78904	0.083	94613	0.066	15946A	0.069
78851	0.974	78790	0.113	78903	0.082	65747A	0.066	15946	0.069
78933	0.974	78830	0.111	78914	0.08	95058	0.065	78915	0.068
95140	0.974	78737	0.111	95035	0.078	78972	0.061	78766	0.068
78972	0.974	78904	0.11	95070	0.077	94614	0.056	78933	0.067
95035	0.974	78751	0.108	95163	0.073	78963	0.055	78994	0.066
78995	0.974	78942	0.103	78720	0.07	78929	0.054	78796	0.066
78766	0.973	78903	0.103	94609	0.067	78937	0.051	95140	0.065
78914B	0.973	79000	0.101	78902	0.066	78974	0.051	94612A	0.064
95059	0.973	78906	0.095	B5320	0.066	78840	0.05	78726	0.064
78745	0.973	78914	0.092	78982	0.065	94725	0.047	78706	0.063
12771	0.973	78733	0.088	78889	0.065	78937	0.047	95134	0.062
78904	0.973	78840	0.083	94675	0.065	78747	0.046	95022	0.06
78924	0.972	78763	0.082	78733	0.064	95179	0.045	78852	0.06
78783	0.972	78820	0.081	78779	0.062	78763	0.044	94665	0.058
78872	0.971	78721	0.078	78872	0.062	78711	0.042	78934	0.056
78889	0.971	78929	0.077	94614	0.06	43037	0.041	78951	0.056
78947	0.971	78781	0.076	78721	0.06	78924	0.04	95140	0.054
95049	0.971	78956	0.076	78743	0.059	78922	0.04	95141	0.052

Sp.#1	COR1	Sp.#2	COR2	Sp.#3	COR3	Sp.#4	COR4	Sp.#5	COR5
95147	0.97	78724	0.076	78805	0.059	94612A	0.04	95179	0.05
78939	0.97	78745	0.072	47822	0.058	95134	0.039	78840	0.044
78803	0.97	78796	0.072	94611	0.057	78960	0.039	95163	0.044
16733	0.969	78957	0.07	78994	0.056	98761	0.038	65747A	0.044
78922	0.969	78944	0.069	78957	0.054	78849	0.038	94650	0.043
78894	0.969	78709	0.068	78882	0.053	78852	0.038	78937	0.042
78882	0.969	78850	0.067	78834	0.052	78939	0.037	78889	0.04
78951	0.969	78907	0.064	78781	0.052	78783	0.036	95147	0.039
A85806	0.969	78915	0.063	91645A	0.05	94616	0.036	78944	0.039
78992	0.969	78815	0.063	78783	0.049	94635	0.035	78847	0.039
78768	0.969	78882	0.063	95049	0.049	95049	0.035	78914B	0.039
95022	0.969	78948	0.061	78799	0.048	78895	0.033	95048	0.037
95169	0.969	78974	0.06	78839	0.048	78909	0.03	78906	0.036
47822	0.968	950130	0.06	94727	0.047	78878	0.029	78995	0.035
78956	0.968	78991	0.06	94775	0.042	78872	0.029	78973	0.035
78937	0.967	78872	0.057	78999B	0.042	78982	0.029	78875	0.034
94609	0.967	78982	0.057	78947	0.041	78906	0.026	95035	0.034
78876	0.967	78843	0.056	78972	0.041	78969	0.024	78805	0.034
78908	0.967	78876	0.052	78839A	0.04	78915	0.024	78956	0.033
79000	0.967	78728	0.052	78747	0.039	94642	0.024	A85806	0.032
95135	0.967	43037	0.046	78745	0.039	78768	0.023	78947	0.031
95179	0.967	78992	0.043	43037	0.039	78849	0.021	78843	0.03
95070	0.966	78900	0.041	16733	0.039	94644	0.02	78720	0.027
78805	0.966	78700	0.04	95134	0.038	78896	0.02	78963	0.027
78916	0.965	95044A	0.039	78816	0.037	95170	0.019	78872	0.025
94616	0.965	95187	0.037	78815	0.035	95163	0.019	78815	0.025
78944	0.965	95059	0.037	78913	0.033	94609	0.019	78991	0.024
78701	0.965	78909	0.037	91645	0.032	95140	0.018	94609	0.022
78900A	0.965	78783	0.037	78937	0.031	94776	0.018	15946B	0.022
78948	0.965	78908	0.036	94644	0.031	95141	0.017	95044A	0.021
78934	0.964	78972	0.035	78969	0.026	65409	0.016	94638	0.021
78840	0.964	78933	0.033	95058	0.025	95048	0.016	94727	0.021
78850	0.964	95064	0.033	78999	0.023	47822	0.015	78903	0.02
78872	0.963	78995	0.03	65747A	0.023	78743	0.014	78750	0.02
78729ii	0.963	78999B	0.026	94776	0.022	95135	0.014	78799	0.019
91645	0.963	78994	0.026	94726	0.018	13259	0.014	78900A	0.018
78974	0.963	95173	0.024	78899	0.018	78903	0.013	78739	0.016
78909	0.963	78895	0.024	94635	0.016	78973	0.012	95070	0.013
78875	0.962	78808	0.024	94616	0.015	78894	0.012	78908	0.012
78811	0.962	78913	0.023	78711	0.013	78720	0.011	78779	0.011
94612A	0.961	95049	0.023	78724	0.009	78815	0.011	95059	0.01
95044A	0.961	78806	0.023	78806	0.007	94610	0.011	78752	0.009
78878	0.961	78799	0.018	94725	0.005	78839	0.009	78724	0.009
78913	0.96	95048	0.017	78922	0.004	78882	0.008	78747	0.007
78728	0.96	78729ii	0.016	78876	0.002	78839A	0.008	78806	0.007
95144	0.96	B5320	0.014	95059	0.002	78904	0.008	94616	0.005
78991	0.96	78956	0.014	78914B	0.002	78703	0.008	B5320	0.004
78765	0.959	78960	0.013	78701	0.001	15946C	0.008	95064	0.003
78721	0.959	78816	0.01	14622	0.001	78851	0.006	78790	0.003
78963	0.958	95178	0.009	95044A	-0.001	78733	0.004	78929	0.002
78820	0.958	78766	0.008	78924	-0.002	78908	0.004	79000	0.001

Sp.#1	COR1	Sp.#2	COR2	Sp.#3	COR3	Sp.#4	COR4	Sp.#5	COR5
65396B	0.958	95141	0.008	94664	-0.002	78745	0.004	94644	-0.001
78914	0.958	78711	0.007	95140	-0.002	78816	0.004	78937	-0.001
78700	0.958	78765	0.006	78874	-0.003	78808	0.003	78957	-0.001
78806	0.958	78939	0.002	95144	-0.004	78765	0.002	78960	-0.002
91645A	0.958	78894	0	78803	-0.006	78811	0.002	13259	-0.002
78906	0.957	78947	-0.001	78934	-0.012	78805	0.001	94611	-0.003
94665	0.957	78963	-0.006	94638	-0.013	95173	0.001	94664	-0.004
95175	0.956	78851	-0.008	78908	-0.013	78889	0	95144	-0.005
78830	0.955	95163	-0.01	95140	-0.014	95035	-0.003	78986	-0.006
78994	0.955	78889	-0.01	94650	-0.015	15946A	-0.005	78763	-0.006
98761	0.955	78779	-0.012	78916	-0.016	78729	-0.005	78900	-0.006
78843	0.955	78875	-0.015	94666	-0.017	65747B	-0.006	95044B	-0.006
78986	0.954	95070	-0.021	12771	-0.018	94727	-0.008	78808	-0.007
15946	0.954	95169	-0.022	78808	-0.019	78940	-0.009	78940	-0.008
94638	0.954	78922	-0.023	78944	-0.02	94777	-0.01	12771	-0.009
78874	0.953	14622	-0.025	95173	-0.02	95140	-0.01	43037	-0.01
78834	0.953	78924	-0.025	95048	-0.021	78947	-0.012	78992	-0.013
94614	0.953	78839A	-0.027	65396A	-0.022	78780	-0.014	95173	-0.014
15946B	0.953	78937	-0.028	78840	-0.022	78820	-0.015	95169	-0.015
78849	0.953	78839	-0.029	78894	-0.023	78781	-0.015	78781	-0.015
95187	0.953	78768	-0.037	95187	-0.025	94650	-0.015	78830	-0.017
65409	0.952	78811	-0.039	78872	-0.025	78712	-0.016	94610	-0.023
78915	0.952	95140	-0.041	78726	-0.03	95022	-0.017	78909	-0.024
95170	0.952	78878	-0.046	78780	-0.032	78750	-0.017	78850	-0.025
78796	0.952	78803	-0.049	78768	-0.033	94726	-0.018	78851	-0.026
94642	0.95	78900A	-0.049	78995	-0.035	91645	-0.021	94675	-0.026
78852	0.95	95140	-0.051	78843	-0.036	78907	-0.023	16733	-0.027
78720	0.95	12771	-0.056	78948	-0.038	78700	-0.024	78709	-0.027
95064	0.95	A85806	-0.057	78974	-0.038	78914B	-0.025	95049	-0.029
94644	0.95	95134	-0.06	95141	-0.04	78803	-0.025	78895	-0.029
78973	0.95	78951	-0.062	78991	-0.04	78721	-0.027	78733	-0.03
78743	0.949	78934	-0.064	78900	-0.041	95070	-0.029	94666	-0.031
78942	0.949	78874	-0.064	65747B	-0.041	94638	-0.03	98761	-0.032
94666	0.949	78916	-0.067	65409	-0.043	78991	-0.032	94615	-0.033
78711	0.948	94664	-0.071	78973	-0.044	78779	-0.032	78849	-0.034
15946C	0.948	78706	-0.072	78900A	-0.044	78956	-0.032	78728	-0.035
78790	0.948	95035	-0.072	95147	-0.045	78872	-0.034	78904	-0.035
78940	0.948	78896	-0.074	13259	-0.048	78876	-0.035	78745	-0.035
94610	0.947	78780	-0.077	95178	-0.049	94778A	-0.037	65747B	-0.036
94613	0.947	47822	-0.078	65396B	-0.049	65396A	-0.038	78721	-0.036
78751	0.946	13259	-0.081	78929	-0.05	78951	-0.038	94642	-0.037
950130	0.946	15946	-0.082	78939	-0.052	78799	-0.04	78956	-0.037
78739	0.945	65396B	-0.083	94613	-0.053	94666	-0.041	94726	-0.038
95131	0.945	65409	-0.088	78851	-0.055	78933	-0.045	95131	-0.04
43037	0.945	78701	-0.091	95175	-0.057	95064	-0.045	78939	-0.041
94727	0.945	16733	-0.096	78951	-0.057	B5320	-0.047	47822	-0.042
94664	0.944	95170	-0.097	15946	-0.06	78751	-0.048	78974	-0.044
94650	0.944	95135	-0.098	15946B	-0.06	95178	-0.049	94629	-0.044
94675	0.943	15946A	-0.098	78737	-0.061	79000	-0.05	78882	-0.044
94776	0.942	78986	-0.104	95135	-0.061	95044A	-0.051	91645A	-0.047
78752	0.942	94609	-0.105	94612A	-0.064	78834	-0.051	78899	-0.048

Sp.#1	COR1	Sp.#2	COR2	Sp.#3	COR3	Sp.#4	COR4	Sp.#5	COR5
15946A	0.942	94775	-0.115	78937	-0.066	94675	-0.056	94613	-0.049
14622	0.942	91645A	-0.116	78712	-0.067	78739	-0.056	91645	-0.05
78706	0.941	78969	-0.116	95169	-0.071	95175	-0.06	94725	-0.051
65396A	0.941	94777	-0.117	78700	-0.073	78957	-0.066	78874	-0.052
94629	0.941	78849	-0.121	15946C	-0.074	78914	-0.067	78913	-0.052
78847	0.941	94665	-0.122	95028	-0.075	8580-6	-0.067	78876	-0.054
78735	0.939	91645	-0.123	78847	-0.076	95187	-0.068	95187	-0.055
78712	0.939	15946C	-0.123	78942	-0.076	78992	-0.07	78701	-0.056
78900	0.938	78735	-0.13	95155	-0.077	78999B	-0.072	78735	-0.061
94635	0.937	94612A	-0.131	78933	-0.081	95169	-0.073	78894	-0.063
78747	0.937	94614	-0.137	78908A	-0.082	78913	-0.074	78872	-0.065
78750	0.937	78914B	-0.138	94665	-0.084	78790	-0.074	65396A	-0.069
94725	0.936	94778A	-0.139	78729ii	-0.089	78729ii	-0.081	94776	-0.069
95044B	0.935	78847	-0.139	95022	-0.089	94611	-0.081	78999B	-0.077
95028	0.935	78940	-0.148	78766	-0.09	95044B	-0.083	78849	-0.079
78709	0.934	95144	-0.152	A85806	-0.094	78942	-0.084	78902	-0.082
94778A	0.933	78849	-0.155	78909	-0.095	950130	-0.087	78712	-0.083
78956	0.932	94613	-0.159	78739	-0.096	65396B	-0.088	95155	-0.089
78907	0.93	15946B	-0.16	78875	-0.098	78701	-0.088	78765	-0.093
65747A	0.928	78834	-0.162	950130	-0.103	95144	-0.092	78948	-0.094
94611	0.928	94638	-0.172	78960	-0.104	78735	-0.101	65396B	-0.094
78849	0.928	94611	-0.174	95044B	-0.105	78948	-0.102	950130	-0.098
94726	0.927	78902	-0.174	95064	-0.113	78724	-0.104	78972	-0.103
78737	0.922	94616	-0.175	78703	-0.116	91645A	-0.104	78834	-0.11
78703	0.919	94642	-0.181	95131	-0.117	78900A	-0.105	94775	-0.111
94775	0.919	94725	-0.181	98761	-0.117	78850	-0.109	65409	-0.118
78902	0.915	94635	-0.19	94642	-0.119	94615	-0.11	78908A	-0.125
78999	0.913	94629	-0.203	78915	-0.137	94629	-0.111	95135	-0.129
94777	0.909	94650	-0.203	94778A	-0.139	78728	-0.115	78711	-0.13
78908A	0.908	94610	-0.215	95170	-0.156	78999	-0.12	78714	-0.133
78726	0.908	94644	-0.217	78963	-0.172	78847	-0.121	95028	-0.138
94615	0.907	94675	-0.22	78735	-0.174	95131	-0.129	78700	-0.138
78719	0.898	94666	-0.223	78852	-0.178	95059	-0.13	14622	-0.141
65747B	0.896	65747A	-0.224	78849	-0.202	94664	-0.135	95175	-0.145
95155	0.892	65396A	-0.231	78729	-0.21	78709	-0.17	78703	-0.159
78718	0.886	94727	-0.236	15946A	-0.216	78902	-0.204	94614	-0.16
78899	0.883	94776	-0.258	78718	-0.217	78899	-0.205	78737	-0.161
78714	0.88	94726	-0.295	78706	-0.225	78956	-0.224	94777	-0.172
78729	0.86	94615	-0.302	78849	-0.228	78719	-0.242	94778A	-0.174
95058	0.855	65747B	-0.347	78719	-0.24	78718	-0.277	95058	-0.382

Scores from the Combined Data set (n=191) using Covariances

Sp.#1	COV1	Sp.#2	COV2	Sp.#3	COV3	Sp.#4	COV4	Sp.#5	COV5
78986	0.277	78729	0.072	78907	0.048	78986	0.052	78922	0.033
78805	0.261	95155	0.067	78796	0.046	78806	0.044	78942	0.029
78763	0.258	78899	0.06	78906	0.044	15946	0.042	78768	0.029
78906	0.254	78726	0.057	78765	0.037	78994	0.041	78719	0.029
78768	0.254	95058	0.056	78750	0.037	78875	0.037	78803	0.027
78743	0.254	78908A	0.054	78751	0.036	78944	0.034	78718	0.027
78937	0.248	78752	0.049	78714	0.035	78900	0.032	78780	0.024
78735	0.247	98761	0.045	78986	0.034	78995	0.029	78743	0.023
78780	0.246	78714	0.044	78811	0.031	95155	0.027	78914	0.023
78876	0.245	95044B	0.043	78763	0.03	14622	0.024	78982	0.023
78914B	0.243	78999	0.043	78752	0.03	78706	0.024	78839	0.022
78808	0.241	78747	0.042	78830	0.025	94665	0.023	78896	0.022
A85806	0.238	78712	0.042	78940	0.024	78916	0.023	78907	0.021
95140	0.237	78743	0.04	94629	0.023	95147	0.023	78729ii	0.021
78999B	0.236	78720	0.039	78820	0.022	94775	0.023	94635	0.021
95134	0.236	78805	0.038	78709	0.022	95028	0.022	15946C	0.021
78816	0.236	78739	0.034	78895	0.021	78766	0.022	78751	0.02
78956	0.235	78703	0.034	78896	0.02	78934	0.021	78811	0.02
78909	0.235	95179	0.034	78790	0.02	16733	0.019	78999	0.02
78995	0.234	78973	0.034	78850	0.02	78843	0.018	95178	0.02
78781	0.234	95131	0.033	95179	0.019	78963	0.018	78839A	0.019
95140	0.234	78872	0.033	94610	0.019	78726	0.017	78729	0.019
78765	0.233	78937	0.028	78956	0.019	78908A	0.017	78916	0.019
78803	0.233	78750	0.028	78878	0.018	78796	0.017	95170	0.016
78799	0.232	78737	0.028	78903	0.018	12771	0.017	78820	0.015
B5320	0.232	78718	0.027	78994	0.018	78937	0.016	78933	0.015
78745	0.232	95147	0.026	79000	0.018	78752	0.015	95140	0.015
78840	0.232	78790	0.026	95035	0.018	78874	0.015	15946A	0.015
78766	0.231	78906	0.026	95163	0.017	78852	0.015	78816	0.015
78889	0.23	95022	0.025	78914	0.017	78840	0.014	78766	0.014
95178	0.23	78830	0.025	78982	0.016	65747A	0.014	95022	0.014
98761	0.23	78852	0.024	94615	0.016	15946B	0.014	78915	0.014
78806	0.229	78751	0.023	78889	0.016	78849	0.013	78852	0.014
95135	0.229	78719	0.023	78743	0.016	78737	0.013	78969	0.013
78982	0.228	78904	0.023	78904	0.016	78922	0.013	78924	0.013
95035	0.228	78763	0.022	78992	0.015	78929	0.013	78783	0.013
78737	0.228	95028	0.022	95070	0.015	98761	0.012	95134	0.013
78875	0.228	78903	0.022	94609	0.015	78960	0.012	95140	0.012
78960	0.227	78914	0.021	78805	0.015	78974	0.011	94612A	0.012
78815	0.227	95175	0.021	B5320	0.014	94612A	0.011	78951	0.012
78701	0.227	79000	0.02	94777	0.014	78830	0.011	78878	0.012
95187	0.226	78733	0.019	78720	0.014	95170	0.011	78847	0.011
78914	0.225	78942	0.019	78872	0.014	78768	0.011	78914B	0.01
78872	0.225	78840	0.019	78728	0.013	78915	0.011	78726	0.01
95163	0.225	78781	0.018	78733	0.013	94613	0.011	95141	0.01
95173	0.224	78820	0.017	78779	0.012	95134	0.01	78796	0.01
78834	0.224	78796	0.017	47822	0.012	78924	0.01	A85806	0.01
78896	0.223	78745	0.017	78839	0.012	78909	0.009	78889	0.009
95059	0.223	78929	0.016	94675	0.012	78972	0.009	78840	0.009

Sp.#1	COV1	Sp.#2	COV2	Sp.#3	COV3	Sp.#4	COV4	Sp.#5	COV5
78796	0.223	78724	0.016	95134	0.012	78849	0.008	78937	0.009
95058	0.222	78944	0.015	95049	0.012	95179	0.008	78706	0.009
95049	0.222	78956	0.015	78783	0.012	94635	0.008	78805	0.009
78724	0.221	78850	0.014	94727	0.011	78783	0.008	95179	0.009
78894	0.22	78721	0.014	94775	0.011	78937	0.008	78973	0.009
78933	0.22	78957	0.014	94614	0.011	94616	0.007	78994	0.009
78839A	0.22	78974	0.013	16733	0.011	78982	0.007	78906	0.008
78944	0.22	78815	0.013	78956	0.011	78747	0.007	95163	0.008
78974	0.219	78882	0.013	78781	0.01	15946A	0.007	94665	0.008
78929	0.219	78907	0.012	78882	0.01	78939	0.007	78956	0.008
78940	0.219	78948	0.012	78839A	0.01	78714	0.007	78934	0.008
78839	0.218	78915	0.012	78834	0.01	94725	0.007	78900A	0.007
78903	0.218	78982	0.012	78799	0.01	78763	0.007	95044A	0.007
78733	0.218	78709	0.011	94611	0.009	78729	0.007	95048	0.007
95044A	0.218	78872	0.011	78745	0.009	94642	0.006	94650	0.007
78790	0.217	950130	0.011	78721	0.009	78969	0.006	95059	0.007
78922	0.217	78876	0.011	78972	0.009	95141	0.006	15946	0.007
78916	0.215	78843	0.011	78957	0.009	15946C	0.006	95035	0.006
78994	0.215	78991	0.011	78816	0.009	95048	0.005	78815	0.006
78779	0.215	78728	0.01	78947	0.008	78872	0.005	78947	0.006
78963	0.214	78909	0.008	78969	0.008	43037	0.005	78739	0.006
78973	0.214	43037	0.008	78902	0.008	78896	0.005	78991	0.006
94616	0.214	78992	0.008	78815	0.008	95140	0.005	95064	0.005
78811	0.213	78908	0.007	43037	0.007	78878	0.005	78724	0.005
47822	0.213	78700	0.007	94644	0.007	94614	0.004	78720	0.005
78852	0.213	95044A	0.007	91645A	0.007	95049	0.004	78995	0.005
95048	0.213	78972	0.007	78806	0.007	78973	0.004	78875	0.005
78830	0.212	78783	0.007	78999B	0.007	78711	0.004	95147	0.005
94778A	0.212	95187	0.007	65747A	0.007	13259	0.004	78799	0.005
78895	0.211	78900	0.007	78747	0.006	78743	0.004	78944	0.004
78783	0.211	95059	0.006	94776	0.006	78839A	0.003	78843	0.004
95179	0.211	78933	0.006	78937	0.006	95163	0.003	95044B	0.004
95022	0.21	78995	0.006	94616	0.005	94644	0.003	65747A	0.004
78957	0.21	95049	0.005	91645	0.005	78895	0.003	78963	0.004
94609	0.21	78994	0.005	94635	0.005	78839	0.003	95070	0.003
78969	0.21	95064	0.005	78913	0.004	78815	0.002	78903	0.003
78850	0.21	78999B	0.005	94726	0.004	78816	0.002	94727	0.003
95147	0.21	78895	0.005	78922	0.003	78851	0.002	94638	0.003
78752	0.21	78808	0.005	94725	0.002	94609	0.002	78779	0.003
78947	0.209	78913	0.004	14622	0.002	78908	0.001	78872	0.003
78820	0.209	95173	0.004	78711	0.002	94776	0.001	78908	0.002
95141	0.209	78806	0.004	78914B	0.002	78906	0.001	94609	0.002
78908	0.209	78956	0.003	78934	0.001	78720	0.001	95144	0.002
78720	0.208	78799	0.003	78999	0.001	65409	0.001	94664	0.002
78934	0.208	95048	0.002	78916	0.001	78808	0.001	78750	0.002
91645A	0.208	B5320	0.002	95058	0.001	78780	0.001	78790	0.002
78849	0.208	78765	0.002	78924	0.001	78894	0.001	B5320	0.002
78851	0.208	78816	0.001	95140	0.001	95135	0.001	78957	0.001
95131	0.207	78729ii	0.001	78874	0.001	78811	0	79000	0
78972	0.207	78711	0.001	78803	0	47822	0	15946B	0
78882	0.207	78960	0.001	78944	0	95058	0	78747	0

Sp.#1	COV1	Sp.#2	COV2	Sp.#3	COV3	Sp.#4	COV4	Sp.#5	COV5
95170	0.206	95141	0.001	95044A	-0.001	95140	0	95169	0
16733	0.206	78766	0	94650	-0.002	95022	0	94611	0
91645	0.206	95178	0	78876	-0.002	95173	0	78992	-0.001
78751	0.205	78894	-0.001	95144	-0.002	78903	0	78937	-0.001
78991	0.205	78939	-0.001	12771	-0.002	78703	0	94616	-0.001
78904	0.204	78947	-0.002	78724	-0.002	94610	-0.001	78960	-0.001
78937	0.204	78851	-0.002	95140	-0.003	78889	-0.001	78929	-0.001
78843	0.204	78963	-0.003	94664	-0.003	78805	-0.001	78808	-0.001
95044B	0.204	78779	-0.003	94638	-0.003	65747B	-0.001	78752	-0.001
78729ii	0.202	95163	-0.003	78908	-0.003	78745	-0.002	78956	-0.001
78924	0.202	78889	-0.003	78701	-0.003	78882	-0.002	13259	-0.002
95070	0.202	95070	-0.005	78899	-0.004	78904	-0.002	94644	-0.002
78939	0.202	14622	-0.005	95048	-0.004	78733	-0.002	78709	-0.002
94776	0.202	78875	-0.006	94666	-0.004	94650	-0.002	43037	-0.002
14622	0.201	78922	-0.006	78840	-0.004	95035	-0.002	78899	-0.002
78948	0.201	95169	-0.006	95059	-0.004	78803	-0.003	95173	-0.003
95064	0.201	78924	-0.006	65396A	-0.005	94727	-0.003	95131	-0.003
94612A	0.201	78839	-0.008	95173	-0.005	78947	-0.003	78781	-0.003
78872	0.2	78839A	-0.008	78894	-0.005	78712	-0.004	78763	-0.004
78915	0.2	78878	-0.009	78900	-0.005	78951	-0.005	78806	-0.004
78942	0.2	78937	-0.009	78808	-0.005	78991	-0.005	78940	-0.004
15946A	0.2	78811	-0.009	78995	-0.005	78820	-0.005	78850	-0.004
78992	0.2	12771	-0.011	78726	-0.005	94726	-0.005	12771	-0.005
78900A	0.199	78768	-0.012	78843	-0.006	78914B	-0.005	78900	-0.005
78951	0.199	78900A	-0.012	78768	-0.006	78781	-0.006	78728	-0.005
78913	0.199	95140	-0.012	15946	-0.006	78933	-0.006	94666	-0.006
78847	0.199	94664	-0.013	78780	-0.007	78940	-0.006	94615	-0.006
94727	0.198	78874	-0.013	95147	-0.007	94638	-0.006	94675	-0.006
65396B	0.198	78951	-0.014	65747B	-0.007	95064	-0.007	78721	-0.006
95144	0.197	95140	-0.014	94613	-0.007	78700	-0.007	78909	-0.007
78728	0.197	78803	-0.014	65409	-0.008	78739	-0.008	94629	-0.007
13259	0.196	78934	-0.015	78872	-0.008	95178	-0.008	78733	-0.007
95169	0.196	78706	-0.015	95141	-0.008	78872	-0.008	78851	-0.007
950130	0.196	78916	-0.016	78974	-0.009	94666	-0.008	78849	-0.007
15946	0.195	A85806	-0.016	95187	-0.009	78765	-0.008	94610	-0.007
95155	0.194	65409	-0.016	15946B	-0.009	91645	-0.008	78904	-0.008
78956	0.194	95134	-0.016	13259	-0.009	78721	-0.008	98761	-0.008
79000	0.193	15946	-0.017	78929	-0.01	94777	-0.008	78830	-0.008
78902	0.193	13259	-0.017	78991	-0.01	78750	-0.008	94642	-0.008
65396A	0.193	47822	-0.017	78939	-0.011	95070	-0.009	78895	-0.008
78878	0.192	78896	-0.018	78973	-0.011	78907	-0.009	94726	-0.008
94610	0.192	65396B	-0.018	94612A	-0.011	78779	-0.009	91645A	-0.008
78703	0.192	95035	-0.018	78900A	-0.011	94778A	-0.009	95049	-0.008
78999	0.192	94777	-0.02	94665	-0.012	65396A	-0.009	78745	-0.008
94665	0.191	94775	-0.021	95028	-0.012	95044A	-0.01	65747B	-0.009
78719	0.191	16733	-0.021	78951	-0.012	78956	-0.01	95187	-0.009
65747A	0.19	78701	-0.022	78851	-0.012	78799	-0.011	78913	-0.01
94638	0.19	78780	-0.022	78948	-0.012	78729ii	-0.011	78882	-0.01
95175	0.189	94609	-0.023	95178	-0.012	A85806	-0.012	78939	-0.01
12771	0.189	15946A	-0.023	65396B	-0.013	78942	-0.012	94613	-0.011
78849	0.189	95170	-0.023	15946C	-0.013	78876	-0.012	78986	-0.011

Sp.#1	COV1	Sp.#2	COV2	Sp.#3	COV3	Sp.#4	COV4	Sp.#5	COV5
78900	0.189	94614	-0.024	78937	-0.014	95169	-0.013	47822	-0.011
94675	0.188	95135	-0.024	95135	-0.015	B5320	-0.013	78902	-0.011
78700	0.188	91645	-0.026	95175	-0.015	78751	-0.013	78701	-0.011
15946C	0.187	15946C	-0.026	95169	-0.016	79000	-0.013	16733	-0.011
78739	0.186	91645A	-0.026	78908A	-0.016	94675	-0.014	78876	-0.011
78712	0.184	78969	-0.026	78712	-0.016	95175	-0.014	78874	-0.012
78711	0.182	94665	-0.026	95155	-0.016	78914	-0.016	78872	-0.012
94725	0.181	94613	-0.027	78737	-0.016	78834	-0.016	91645	-0.012
78714	0.181	94612A	-0.028	78700	-0.017	95044B	-0.016	78735	-0.012
94666	0.181	78849	-0.029	78847	-0.018	94611	-0.016	78974	-0.012
78747	0.181	15946B	-0.03	78875	-0.018	78957	-0.016	94725	-0.013
78874	0.18	78847	-0.031	78942	-0.018	78913	-0.017	78712	-0.014
94644	0.18	78986	-0.031	78766	-0.019	95187	-0.017	78894	-0.015
78750	0.179	94635	-0.032	78933	-0.02	950130	-0.018	65396A	-0.015
78721	0.178	95144	-0.033	78729ii	-0.02	95144	-0.018	78849	-0.016
94650	0.178	94611	-0.033	95022	-0.02	78992	-0.018	78999B	-0.016
78907	0.177	78849	-0.033	78739	-0.021	65396B	-0.019	950130	-0.016
94642	0.175	94778A	-0.034	94642	-0.021	78900A	-0.02	78948	-0.016
78718	0.175	94642	-0.034	78960	-0.023	78999B	-0.021	94776	-0.017
94611	0.175	94638	-0.035	78909	-0.024	78790	-0.021	65396B	-0.017
94615	0.175	78940	-0.035	A85806	-0.025	94664	-0.022	65409	-0.021
94629	0.174	94725	-0.035	950130	-0.025	78847	-0.022	95155	-0.022
15946B	0.174	78914B	-0.036	95064	-0.025	78948	-0.023	78972	-0.023
78899	0.173	78735	-0.037	95044B	-0.026	78701	-0.023	94775	-0.023
65747B	0.173	78902	-0.038	78703	-0.027	78735	-0.023	78908A	-0.024
78726	0.172	94629	-0.038	78915	-0.028	78724	-0.024	78765	-0.025
78729	0.172	78834	-0.039	98761	-0.029	94615	-0.024	95028	-0.025
78908A	0.171	94650	-0.039	95131	-0.031	78999	-0.024	95175	-0.025
94726	0.171	94616	-0.04	95170	-0.032	94629	-0.025	78834	-0.025
94614	0.17	94644	-0.042	94778A	-0.033	95131	-0.026	78700	-0.025
43037	0.17	94666	-0.043	78706	-0.036	91645A	-0.026	78711	-0.027
65409	0.168	94610	-0.044	78963	-0.036	78728	-0.027	78714	-0.029
95028	0.167	94675	-0.044	78852	-0.038	78850	-0.028	95135	-0.031
78706	0.166	65747A	-0.046	78849	-0.042	95059	-0.029	78703	-0.031
94775	0.165	65396A	-0.048	78729	-0.043	78709	-0.034	94614	-0.031
94777	0.163	94727	-0.05	78849	-0.045	78899	-0.041	94777	-0.031
94613	0.162	94726	-0.055	15946A	-0.045	78719	-0.042	14622	-0.035
94664	0.161	94776	-0.056	78718	-0.05	78902	-0.046	94778A	-0.037
78709	0.16	94615	-0.059	78735	-0.051	78718	-0.046	78737	-0.042
94635	0.156	65747B	-0.068	78719	-0.058	78956	-0.049	95058	-0.105

Scores from Combined Data set (n = 144) based on Covariances

Sp.#1	COV1	Sp.#2	COV2	Sp.#3	COV3	Sp.#4	COV4	Sp.#5	COV5
78937ii	0.248	98761	0.046	78956	0.041	78994	0.037	78737	0.043
78780	0.246	78720	0.041	94629	0.034	78806	0.029	78765	0.036
78876	0.245	78703	0.039	78751	0.033	78811	0.028	94614	0.033
78914B	0.243	78973	0.037	78850	0.033	78751	0.026	78972	0.026
78808	0.241	78739	0.036	78765	0.032	78982	0.026	95135	0.025
A85806	0.238	95179	0.035	78790	0.029	78896	0.026	78703	0.025
95140ii	0.237	95131	0.033	78728	0.028	15946	0.025	78711	0.025
78816	0.236	78872	0.033	91645A	0.025	95179	0.024	78806	0.023
95134	0.236	78737	0.033	78914	0.022	78944	0.022	78874	0.022
78999B	0.236	78937	0.03	78992	0.021	78839	0.021	16733	0.02
78909	0.235	95147	0.027	79000	0.021	78830	0.021	78894	0.017
95140	0.234	95022	0.027	78999B	0.021	78878	0.02	94725	0.017
78995	0.234	78903	0.026	78811	0.02	78783	0.018	47822	0.016
78781	0.234	78840	0.025	78957	0.019	95134	0.017	78830	0.016
78803	0.233	78751	0.025	78940	0.019	94635	0.017	78940	0.016
78765	0.233	78790	0.025	95070	0.017	78934	0.017	65409	0.015
78799	0.232	78830	0.025	78820	0.017	78900	0.016	78895	0.015
78840	0.232	78914	0.024	78721	0.017	78839A	0.016	94610	0.014
78745	0.232	78904	0.023	B5320	0.017	78820	0.016	78700	0.013
B5320	0.232	79000	0.022	94675	0.016	78872	0.016	78904	0.012
78766	0.231	78942	0.021	95059	0.016	78889	0.015	94613	0.012
95178	0.23	78781	0.021	78799	0.015	94609	0.015	78994	0.011
78889	0.23	78956	0.02	78724	0.015	78903	0.014	78900	0.011
78806	0.229	78733	0.02	78701	0.015	95163	0.014	95049	0.011
98761	0.229	78745	0.019	78913	0.015	16733	0.014	78999B	0.011
95135	0.229	78876	0.019	95144	0.014	78995	0.014	65396A	0.011
78875	0.228	78929	0.019	78904	0.014	78816	0.013	78745	0.011
95035	0.228	78991	0.019	78889	0.013	95147	0.013	12771	0.011
78982	0.228	78820	0.018	94664	0.013	65747A	0.013	78974	0.01
78737	0.227	78957	0.017	94610	0.013	78720	0.013	78944	0.01
78960	0.227	95187	0.017	78781	0.013	78914	0.013	78882	0.01
78815	0.227	78724	0.017	78779	0.012	78969	0.012	78733	0.009
78701	0.227	78882	0.016	78895	0.012	78803	0.012	78875	0.008
95187	0.226	78815	0.016	78903	0.012	78875	0.012	94644	0.008
78914	0.225	78944	0.015	95035	0.012	95049	0.012	95130	0.007
95163	0.225	78721	0.015	78733	0.011	94665	0.011	94629	0.007
78872	0.224	78915	0.015	78830	0.011	78895	0.011	78843	0.007
95173	0.224	95130	0.015	78720	0.011	78924	0.011	78939	0.007
95059	0.223	78948	0.014	78896	0.01	95035	0.011	94616	0.007
78896	0.223	78982	0.014	47822	0.01	95140	0.011	78872ii	0.007
95049	0.222	78850	0.014	94727	0.01	78843	0.009	78995	0.007
78933	0.221	78872ii	0.014	94609	0.01	78815	0.009	78781	0.006
78724	0.221	78974	0.014	78948	0.01	78937	0.008	78815	0.006
78894	0.22	78992	0.013	95049	0.009	78940	0.007	94675	0.006
78944	0.22	95044A	0.012	95044A	0.009	95070	0.006	15946	0.006
78839A	0.22	78843	0.012	78900A	0.009	12771	0.006	78728	0.006
78940	0.219	78909	0.012	78745	0.009	78780	0.006	78721	0.006
78974	0.219	78700	0.011	95179	0.008	78904	0.006	91645	0.005
78839	0.219	78900	0.011	78878	0.008	78721	0.005	78872	0.005

Sp.#1	COV1	Sp.#2	COV2	Sp.#3	COV3	Sp.#4	COV4	Sp.#5	COV5
78929	0.219	78728	0.011	78882	0.008	78947	0.005	65747A	0.005
78903	0.218	78972	0.01	95163	0.007	78733	0.005	98761	0.005
78733	0.218	95059	0.01	94614	0.006	15946C	0.005	65747B	0.004
78790	0.217	78994	0.009	78947	0.006	95140ii	0.005	95173	0.004
95044A	0.217	78908	0.009	78876	0.006	94616	0.005	78909	0.004
78779	0.215	95064	0.009	95187	0.006	78766	0.005	78850	0.004
78994	0.215	78808	0.009	78815	0.005	94610	0.005	78948	0.003
78973	0.214	78783	0.009	78839	0.005	78937ii	0.005	78929	0.003
78811	0.214	78913	0.009	91645	0.005	78765	0.005	78889	0.002
94616	0.214	78999B	0.009	94638	0.005	78840	0.005	94666	0.002
95048	0.213	78806	0.008	78982	0.005	94727	0.004	78937	0.002
47822	0.213	95173	0.008	94644	0.005	94612A	0.004	94642	0.002
78830	0.212	78995	0.008	78914B	0.004	79000	0.003	B5320	0.002
78895	0.211	78729ii	0.007	78839A	0.004	78973	0.003	65396B	0.002
95179	0.211	95048	0.007	78872	0.004	94644	0.003	78876	0.002
78783	0.211	78765	0.007	65396B	0.003	78882	0.003	79000	0.001
78969	0.21	78895	0.007	94666	0.003	78799	0.003	94665	0.001
94609	0.21	B5320	0.006	65396A	0.003	15946B	0.002	15946B	0.001
95147	0.21	78933	0.006	78816	0.003	78781	0.002	78720	0.001
78957	0.21	78947	0.005	78783	0.001	78779	0.002	78903	0.001
95022	0.21	78799	0.005	78803	0.001	95048	0.002	13259	0
95141	0.209	95049	0.005	95134	0	78790	0.002	95147	0
91645A	0.209	78816	0.003	78711	0	78874	0.002	94727	0
78934	0.209	78960	0.003	78969	0	78745	0.001	78779	0
78820	0.209	78894	0.003	94616	0	47822	0.001	78783	0
78908	0.209	78766	0.002	78847	-0.001	78929	0.001	78992	0
78850	0.209	78711	0.002	78972	-0.001	78914B	0.001	78934	0
78947	0.209	78939	0.002	95178	-0.001	95141	0	78878	0
78851	0.208	95141	0.002	95169	-0.002	94638	0	95179	0
78972	0.207	95178	0.001	78937	-0.002	78942	0	95163	0
95131	0.207	78889	0	78872ii	-0.002	78908	-0.001	78913	0
78720	0.207	78851	0	95140ii	-0.002	78972	-0.002	78851	0
91645	0.207	78875	-0.001	95140	-0.002	78957	-0.002	91645A	-0.001
78882	0.207	95163	-0.001	95173	-0.003	B5320	-0.002	78960	-0.001
16733	0.206	78779	-0.001	94725	-0.003	94725	-0.002	78808	-0.001
95170	0.206	95169	-0.002	65409	-0.003	94650	-0.002	95044A	-0.002
78991	0.205	95070	-0.003	94650	-0.003	95178	-0.003	95035	-0.002
78751	0.205	78924	-0.005	94635	-0.003	78992	-0.003	94609	-0.002
78843	0.204	78839	-0.005	95131	-0.004	95044A	-0.004	78790	-0.003
78904	0.204	78937ii	-0.006	78894	-0.004	94613	-0.005	95070	-0.003
78937	0.203	78811	-0.006	16733	-0.004	78850	-0.005	95187	-0.003
95070	0.202	78839A	-0.006	95130	-0.004	95173	-0.005	78908	-0.003
78939	0.202	95140ii	-0.008	78908	-0.004	94629	-0.006	78811	-0.003
78924	0.202	78874	-0.008	78991	-0.005	78974	-0.006	95134	-0.003
78729ii	0.202	78803	-0.009	78942	-0.006	78939	-0.006	78820	-0.004
95064	0.201	78900A	-0.009	78780	-0.006	78808	-0.006	78840	-0.004
94612A	0.201	78878	-0.01	78700	-0.006	94614	-0.007	78957	-0.004
78951	0.2	78951	-0.011	78951	-0.006	95022	-0.007	94612A	-0.005
78872ii	0.2	95140	-0.011	78808	-0.007	13259	-0.007	95141	-0.005
78847	0.2	12771	-0.011	65747A	-0.007	78951	-0.008	78947	-0.005
78948	0.2	94664	-0.012	78729ii	-0.007	78933	-0.008	95048	-0.005

Sp.#1	COV1	Sp.#2	COV2	Sp.#3	COV3	Sp.#4	COV4	Sp.#5	COV5
78992	0.2	95035	-0.013	65747B	-0.007	94675	-0.008	78751	-0.005
78942	0.199	95134	-0.014	78924	-0.008	78960	-0.008	78799	-0.006
78913	0.199	A85806	-0.014	78874	-0.008	78991	-0.009	78701	-0.006
78900A	0.199	65409	-0.014	95064	-0.009	78711	-0.009	78924	-0.007
78915	0.199	78780	-0.015	78739	-0.009	78729ii	-0.009	94650	-0.007
94727	0.198	13259	-0.015	95135	-0.009	95170	-0.009	78914B	-0.007
65396B	0.198	65396B	-0.015	95048	-0.009	78894	-0.01	78766	-0.008
95144	0.197	78934	-0.016	A85806	-0.01	91645	-0.01	95140	-0.009
78728	0.197	78896	-0.017	13259	-0.01	78915	-0.011	78969	-0.009
95169	0.196	78701	-0.018	78939	-0.012	78913	-0.011	78937ii	-0.009
95130	0.196	15946	-0.018	78851	-0.012	78739	-0.011	78816	-0.01
13259	0.196	47822	-0.018	78933	-0.012	78851	-0.012	95144	-0.01
15946	0.195	95170	-0.019	78973	-0.013	95144	-0.012	95169	-0.01
65396A	0.194	95135	-0.02	95141	-0.013	78724	-0.013	94664	-0.01
78956	0.194	78969	-0.022	94613	-0.014	78728	-0.014	94638	-0.01
94610	0.193	16733	-0.022	12771	-0.014	65409	-0.014	95131	-0.01
79000	0.193	91645A	-0.023	15946C	-0.014	94666	-0.014	78982	-0.011
78703	0.192	94614	-0.023	78934	-0.014	91645A	-0.015	78991	-0.011
78878	0.192	94609	-0.025	94612A	-0.015	78900A	-0.015	78896	-0.011
94665	0.191	95144	-0.025	95022	-0.016	78876	-0.016	78724	-0.012
94638	0.19	78847	-0.026	78840	-0.016	65747B	-0.016	78739	-0.012
65747A	0.19	91645	-0.026	78929	-0.017	78909	-0.016	78956	-0.013
12771	0.19	94665	-0.026	15946B	-0.017	95059	-0.017	95140ii	-0.013
78900	0.189	94613	-0.026	78974	-0.017	94642	-0.017	78839A	-0.014
94675	0.189	15946C	-0.027	94642	-0.018	78999B	-0.017	95064	-0.014
78700	0.188	94612A	-0.029	78994	-0.02	94664	-0.017	78973	-0.014
15946C	0.187	15946B	-0.03	78843	-0.02	78872ii	-0.018	78839	-0.015
78739	0.185	78940	-0.032	78737	-0.021	98761	-0.019	78915	-0.015
94725	0.181	94635	-0.032	78937ii	-0.021	65396A	-0.019	94635	-0.016
94666	0.181	78914B	-0.032	78960	-0.023	95064	-0.019	95059	-0.017
78711	0.181	94642	-0.033	78703	-0.023	95169	-0.019	95022	-0.017
78874	0.18	94725	-0.034	78806	-0.023	78701	-0.021	78900A	-0.019
94644	0.18	94638	-0.035	95147	-0.024	A85806	-0.022	78951	-0.019
78721	0.178	94629	-0.036	94665	-0.024	95187	-0.024	95178	-0.02
94650	0.178	94616	-0.038	78944	-0.025	95135	-0.024	A85806	-0.02
94642	0.176	94650	-0.04	78909	-0.027	78956	-0.025	15946C	-0.021
94629	0.175	94644	-0.041	78900	-0.027	78700	-0.025	95170	-0.022
65747B	0.174	94610	-0.042	78995	-0.027	78847	-0.025	78780	-0.022
15946B	0.174	94666	-0.043	95170	-0.031	78737	-0.025	78803	-0.024
94614	0.171	94675	-0.044	78766	-0.032	78948	-0.027	78933	-0.025
65409	0.168	65747A	-0.046	98761	-0.033	65396B	-0.032	78847	-0.025
94613	0.163	65396A	-0.047	78915	-0.035	78703	-0.033	78914	-0.026
94664	0.161	94727	-0.049	15946	-0.036	95130	-0.035	78729ii	-0.03
94635	0.157	65747B	-0.067	78875	-0.039	95131	-0.038	78942	-0.035

APPENDIX B

Statistics for Suture Data

Basic Statistics for Combined Dataset U/L Suture Ratios:

	R1	R2	R3	R4	R5
NO. OF CASES	88	88	88	85	88
MINIMUM	0.773	0.767	0.604	0.235	0.349
MAXIMUM	1.345	1.307	1.083	0.718	0.781
MEAN	0.981	0.925	0.796	0.521	0.575
VARIANCE	0.007	0.008	0.007	0.007	0.006
STD. DEVIATION	0.084	0.087	0.082	0.083	0.078

	R6	R7	R8	R9	R10
NO. OF CASES	88	88	88	88	88
MINIMUM	0.314	0.923	0.871	0.504	0.231
MAXIMUM	0.663	1.996	1.645	1.009	0.495
MEAN	0.460	1.267	1.153	0.674	0.401
VARIANCE	0.003	0.037	0.026	0.005	0.002
STD. DEVIATION	0.052	0.191	0.160	0.073	0.049

	R11	R12	R13	R14	R15
NO. OF CASES	88	88	85	88	88
MINIMUM	0.556	0.794	0.173	0.483	0.703
MAXIMUM	0.736	1.026	0.394	0.744	0.877
MEAN	0.647	0.910	0.285	0.636	0.808
VARIANCE	0.002	0.002	0.002	0.002	0.001
STD. DEVIATION	0.041	0.041	0.050	0.043	0.035

	R16	R17	R18	R19	R20
NO. OF CASES	87	88	88	88	88
MINIMUM	0.170	0.467	0.672	0.304	0.486
MAXIMUM	0.548	0.812	0.893	0.618	0.809
MEAN	0.358	0.658	0.802	0.444	0.662
VARIANCE	0.005	0.004	0.002	0.005	0.004
STD. DEVIATION	0.070	0.063	0.040	0.070	0.067

	R21	R22	R23	R24	R25
NO. OF CASES	88	88	88	88	88
MINIMUM	0.802	0.271	0.293	0.224	0.399
MAXIMUM	1.012	0.477	0.601	0.559	0.707
MEAN	0.923	0.378	0.441	0.395	0.559
VARIANCE	0.002	0.002	0.003	0.003	0.003
STD. DEVIATION	0.043	0.046	0.054	0.057	0.054

	R26	R27	R28	R29	R30
NO. OF CASES	88	88	88	88	88
MINIMUM	0.246	0.137	1.308	1.023	0.768
MAXIMUM	0.676	0.226	3.527	3.119	1.655
MEAN	0.472	0.085	1.993	1.827	1.150
VARIANCE	0.005	0.007	0.145	0.189	0.029
STD. DEVIATION	0.073	0.081	0.380	0.435	0.169

	R31	R32	R33	R34	R35
NO. OF CASES	88	88	88	85	85
MINIMUM	0.670	0.492	0.470	0.432	0.409
MAXIMUM	1.670	0.983	1.077	3.047	3.742
MEAN	1.135	0.702	0.693	1.544	1.256
VARIANCE	0.045	0.009	0.011	0.279	0.291
STD. DEVIATION	0.211	0.097	0.103	0.528	0.539

	R36	R37	R38	R39	R40
NO. OF CASES	88	88	88	88	88
MINIMUM	0.318	0.293	0.283	0.264	0.794
MAXIMUM	1.100	1.148	0.598	0.610	1.026
MEAN	0.732	0.712	0.457	0.461	0.910
VARIANCE	0.023	0.026	0.004	0.005	0.002
STD. DEVIATION	0.151	0.162	0.065	0.070	0.041

	R41	R42	R43	R44	R45
NO. OF CASES	88	88	85	88	88
MINIMUM	0.074	0.561	0.786	0.479	0.403
MAXIMUM	0.295	1.332	1.813	0.647	0.765
MEAN	0.142	0.811	1.126	0.579	0.623
VARIANCE	0.002	0.014	0.036	0.001	0.006
STD. DEVIATION	0.040	0.118	0.189	0.037	0.077

	R46	R47
NO. OF CASES	85	88
MINIMUM	0.254	0.879
MAXIMUM	0.738	1.292
MEAN	0.534	1.099
VARIANCE	0.008	0.009
STD. DEVIATION	0.087	0.095

CORRELATION MATRIX FOR U/L SUTURE RATIOS FROM PSJ:

	R1	R2	R3	R4	R5
R1	1.000				
R2	0.868	1.000			
R3	0.641	0.743	1.000		
R4	0.202	0.276	-0.010	1.000	
R5	0.322	0.388	0.324	0.439	1.000
R6	0.553	0.648	0.763	0.115	0.328
R7	0.477	0.423	0.444	-0.419	-0.204
R8	0.420	0.461	0.469	-0.256	-0.113
R9	0.336	0.342	0.398	-0.075	0.108
R10	-0.098	-0.206	-0.109	-0.318	-0.144
R11	-0.063	-0.075	-0.082	-0.075	-0.149
R12	-0.143	-0.017	-0.214	0.235	-0.121
R13	-0.100	-0.223	-0.138	-0.303	0.025
R14	-0.214	-0.244	-0.060	-0.196	0.166
R15	-0.241	-0.153	-0.255	0.133	-0.077
R16	-0.039	-0.136	0.020	-0.383	-0.079
R17	0.097	-0.033	-0.010	-0.219	0.126
R18	-0.054	-0.076	-0.013	-0.334	-0.209
R19	-0.032	-0.202	-0.070	-0.403	-0.262
R20	0.069	0.005	-0.046	-0.237	-0.129
R21	-0.006	-0.047	-0.142	-0.229	-0.167
R22	0.076	0.182	0.105	0.044	0.015
R23	0.129	0.149	0.149	-0.197	-0.048
R24	0.056	0.038	0.191	-0.197	-0.085
R25	-0.129	-0.149	-0.149	0.197	0.048
R26	0.071	0.001	0.008	-0.111	0.063
R27	0.140	-0.009	0.028	-0.306	-0.145
R28	0.128	0.172	-0.016	0.641	0.387
R29	0.054	0.158	-0.027	0.595	0.365
R30	0.057	0.180	-0.002	0.615	0.463
R31	-0.018	0.104	-0.019	0.572	0.357
R32	-0.022	0.052	0.241	0.359	0.453
R33	-0.054	0.060	0.210	0.479	0.434
R34	-0.050	0.053	-0.105	0.757	0.268
R35	-0.067	0.031	-0.131	0.670	0.257
R36	-0.026	0.045	-0.084	0.632	0.681
R37	-0.126	-0.014	-0.084	0.584	0.591
R38	-0.006	0.071	0.145	0.465	0.436
R39	-0.055	0.044	0.057	0.571	0.439
R40	-0.143	-0.017	-0.214	0.235	-0.121
R41	0.204	0.180	0.184	-0.256	-0.510
R42	0.044	0.037	0.189	-0.362	-0.776
R43	0.044	0.016	0.281	-0.682	0.325
R44	-0.058	-0.066	-0.251	0.184	0.031
R45	-0.213	-0.232	-0.129	0.286	0.803
R46	-0.287	-0.146	-0.320	0.875	0.269
R47	0.153	-0.013	0.042	-0.297	-0.137

	R1	R2	R3	R4	R5
HT	-0.248	-0.185	-0.299	0.103	-0.042
LV	-0.129	-0.120	-0.223	0.185	0.051

	R6	R7	R8	R9	R10
R6	1.000				
R7	0.373	1.000			
R8	0.383	0.819	1.000		
R9	0.358	0.209	0.079	1.000	
R10	-0.030	-0.013	-0.198	-0.208	1.000
R11	0.033	-0.133	-0.205	-0.091	0.572
R12	-0.135	-0.169	0.137	-0.439	0.040
R13	-0.013	0.072	-0.205	0.024	0.639
R14	0.006	-0.152	-0.240	0.022	0.514
R15	-0.028	-0.133	0.004	-0.146	0.291
R16	0.116	0.320	-0.127	0.140	0.343
R17	0.089	0.158	-0.169	0.229	0.192
R18	0.197	0.263	0.002	0.124	0.159
R19	-0.032	0.249	-0.273	0.258	0.375
R20	0.036	0.210	-0.168	0.255	0.155
R21	0.009	0.035	-0.295	0.317	0.081
R22	-0.026	-0.242	-0.069	0.101	-0.114
R23	0.065	0.236	0.149	-0.229	0.012
R24	-0.125	0.149	0.123	-0.161	-0.204
R25	-0.065	-0.236	-0.149	0.229	-0.012
R26	0.026	-0.001	-0.121	0.560	-0.060
R27	0.072	0.409	-0.182	0.211	0.317
R28	-0.060	-0.609	-0.383	0.125	-0.637
R29	-0.071	-0.614	-0.180	-0.198	-0.297
R30	-0.063	-0.716	-0.486	0.039	-0.370
R31	-0.088	-0.700	-0.343	-0.156	-0.183
R32	0.105	-0.707	-0.604	0.170	-0.083
R33	0.049	-0.714	-0.428	-0.065	-0.096
R34	-0.109	-0.653	-0.382	-0.080	-0.482
R35	-0.197	-0.638	-0.301	-0.134	-0.325
R36	-0.093	-0.756	-0.556	-0.040	-0.273
R37	-0.140	-0.770	-0.488	-0.125	-0.173
R38	0.276	-0.726	-0.592	0.090	-0.108
R39	0.164	-0.786	-0.541	-0.003	-0.070
R40	-0.135	-0.169	0.137	-0.439	0.040
R41	0.108	0.470	0.410	0.134	-0.033
R42	0.312	0.460	0.393	0.105	0.112
R43	0.132	0.246	0.160	0.166	0.166
R44	0.432	-0.053	-0.074	-0.014	0.105
R45	-0.069	-0.473	-0.410	-0.085	-0.014
R46	-0.163	-0.624	-0.448	-0.231	-0.257
R47	0.084	0.412	-0.159	0.210	0.323
HT	-0.331	-0.276	-0.044	-0.244	-0.157
LV	-0.142	-0.113	0.152	-0.226	-0.279

	R11	R12	R13	R14	R15
R11	1.000				
R12	0.220	1.000			
R13	0.261	-0.145	1.000		
R14	0.690	-0.059	0.365	1.000	
R15	0.385	0.581	0.162	0.322	1.000
R16	0.093	-0.424	0.425	0.245	-0.086
R17	0.231	-0.365	0.215	0.365	-0.059
R18	0.196	-0.007	0.223	0.241	0.270
R19	0.209	-0.505	0.387	0.226	-0.216
R20	0.302	-0.307	0.154	0.230	-0.039
R21	0.226	-0.290	0.093	0.171	-0.065
R22	-0.048	-0.057	-0.262	-0.210	-0.287
R23	0.028	-0.129	-0.171	0.043	-0.255
R24	-0.208	0.068	-0.172	-0.196	-0.551
R25	-0.028	0.129	0.171	-0.043	0.255
R26	0.029	-0.320	0.085	0.278	-0.114
R27	0.106	-0.515	0.459	0.140	-0.226
R28	-0.264	0.058	-0.483	-0.282	-0.172
R29	-0.088	0.428	-0.355	-0.168	0.142
R30	-0.324	0.081	-0.340	-0.284	-0.114
R31	-0.105	0.315	-0.267	-0.152	0.058
R32	0.029	-0.259	-0.140	0.139	-0.200
R33	0.019	0.147	-0.206	0.056	0.001
R34	-0.151	0.236	-0.667	-0.229	0.012
R35	-0.047	0.376	-0.348	-0.152	0.119
R36	-0.222	0.058	-0.185	-0.118	-0.061
R37	-0.095	0.202	-0.153	0.018	0.072
R38	0.064	-0.094	-0.156	0.066	-0.184
R39	0.102	0.087	-0.167	0.065	0.030
R40	0.220	1.000	-0.145	-0.059	0.581
R41	0.023	-0.001	-0.103	-0.204	0.024
R42	0.150	0.018	-0.041	-0.177	0.042
R43	-0.049	-0.299	0.317	0.291	-0.230
R44	0.168	0.086	0.182	0.094	0.302
R45	-0.098	-0.115	0.175	0.351	0.028
R46	-0.024	0.300	-0.242	-0.078	0.263
R47	0.114	-0.467	0.473	0.170	-0.180
HT	-0.141	0.455	-0.159	-0.211	0.023
LV	-0.308	0.386	-0.118	-0.277	0.198

	R16	R17	R18	R19	R20
R16	1.000				
R17	0.617	1.000			
R18	0.507	0.513	1.000		
R19	0.797	0.635	0.457	1.000	
R20	0.566	0.758	0.537	0.717	1.000

	R16	R17	R18	R19	R20
R21	0.490	0.577	0.566	0.639	0.708
R22	-0.260	-0.275	-0.445	-0.192	-0.082
R23	0.102	0.107	0.223	0.091	0.056
R24	-0.062	-0.051	0.041	-0.001	-0.088
R25	-0.102	-0.107	-0.223	-0.091	-0.056
R26	0.096	0.194	0.290	0.210	0.222
R27	0.762	0.541	0.450	0.862	0.615
R28	-0.495	-0.173	-0.345	-0.433	-0.202
R29	-0.771	-0.486	-0.482	-0.837	-0.567
R30	-0.461	-0.269	-0.402	-0.452	-0.315
R31	-0.640	-0.556	-0.546	-0.673	-0.699
R32	-0.210	-0.046	-0.290	-0.150	-0.137
R33	-0.476	-0.330	-0.451	-0.484	-0.435
R34	-0.513	-0.260	-0.375	-0.459	-0.258
R35	-0.800	-0.436	-0.450	-0.647	-0.412
R36	-0.369	-0.128	-0.400	-0.397	-0.275
R37	-0.517	-0.438	-0.499	-0.547	-0.490
R38	-0.222	-0.054	-0.211	-0.190	-0.146
R39	-0.397	-0.242	-0.460	-0.388	-0.327
R40	-0.424	-0.365	-0.007	-0.505	-0.307
R41	0.055	-0.016	0.114	0.161	0.170
R42	0.134	-0.101	0.279	0.201	0.126
R43	0.268	0.294	0.148	0.193	0.114
R44	0.138	0.140	0.314	0.048	0.104
R45	0.012	0.172	-0.161	-0.129	-0.130
R46	-0.330	-0.256	-0.293	-0.366	-0.261
R47	0.744	0.507	0.457	0.818	0.576
HT	-0.393	-0.363	-0.209	-0.413	-0.281
LV	-0.379	-0.224	-0.029	-0.470	-0.329

	R21	R22	R23	R24	R25
R21	1.000				
R22	-0.052	1.000			
R23	0.143	-0.069	1.000		
R24	-0.051	-0.204	0.298	1.000	
R25	-0.143	0.069	-1.000	-0.298	1.000
R26	0.352	-0.151	0.031	0.017	-0.031
R27	0.534	-0.318	0.170	0.045	-0.170
R28	-0.090	0.303	-0.153	0.024	0.153
R29	-0.475	0.296	-0.155	-0.039	0.155
R30	-0.162	0.369	-0.171	-0.029	0.171
R31	-0.450	0.308	-0.157	-0.034	0.157
R32	-0.049	0.338	-0.097	-0.053	0.097
R33	-0.450	0.304	-0.178	-0.001	0.178
R34	-0.169	0.246	-0.118	-0.035	0.118
R35	-0.387	0.228	-0.200	-0.030	0.200
R36	-0.190	0.236	-0.216	-0.081	0.216
R37	-0.362	0.260	-0.235	-0.098	0.235

	R21	R22	R23	R24	R25
R38	-0.000	0.324	-0.100	-0.072	0.100
R39	-0.214	0.354	-0.247	-0.231	0.247
R40	-0.290	-0.057	-0.129	0.068	0.129
R41	0.055	0.009	0.073	0.006	-0.073
R42	0.107	-0.038	0.088	0.014	-0.088
R43	0.098	-0.016	0.144	0.210	-0.144
R44	0.207	-0.192	-0.103	-0.447	0.103
R45	-0.135	-0.120	-0.153	-0.109	0.153
R46	-0.218	-0.004	-0.270	-0.229	0.270
R47	0.465	-0.314	0.147	0.023	-0.147
HT	-0.266	0.310	-0.100	0.084	0.100
LV	-0.361	-0.164	-0.112	0.138	0.112

	R26	R27	R28	R29	R30
R26	1.000				
R27	0.185	1.000			
R28	0.067	-0.468	1.000		
R29	-0.151	-0.793	0.738	1.000	
R30	-0.013	-0.475	0.880	0.783	1.000
R31	-0.152	-0.669	0.690	0.891	0.833
R32	0.084	-0.257	0.648	0.526	0.751
R33	-0.115	-0.556	0.653	0.769	0.774
R34	-0.084	-0.534	0.852	0.729	0.797
R35	-0.090	-0.656	0.750	0.886	0.738
R36	-0.040	-0.420	0.804	0.733	0.906
R37	-0.048	-0.554	0.693	0.807	0.830
R38	0.041	-0.293	0.679	0.558	0.751
R39	-0.101	-0.480	0.688	0.716	0.787
R40	-0.320	-0.515	0.058	0.428	0.081
R41	-0.229	0.126	-0.220	-0.267	-0.325
R42	-0.093	0.161	-0.411	-0.373	-0.490
R43	0.165	0.184	-0.295	-0.299	-0.243
R44	0.033	0.071	-0.069	-0.069	-0.100
R45	0.078	-0.134	0.283	0.264	0.355
R46	-0.150	-0.350	0.541	0.538	0.551
R47	0.168	0.961	-0.460	-0.752	-0.477
HT	-0.167	-0.395	0.174	0.383	0.210
LV	-0.186	-0.428	0.188	0.359	0.151

	R31	R32	R33	R34	R35
R31	1.000				
R32	0.644	1.000			
R33	0.835	0.869	1.000		
R34	0.706	0.569	0.658	1.000	
R35	0.792	0.517	0.726	0.783	1.000
R36	0.770	0.743	0.767	0.732	0.705
R37	0.876	0.712	0.838	0.687	0.774

	R31	R32	R33	R34	R35
R38	0.654	0.885	0.791	0.623	0.521
R39	0.801	0.843	0.874	0.697	0.662
R40	0.315	-0.259	0.147	0.236	0.376
R41	-0.322	-0.322	-0.319	-0.204	-0.250
R42	-0.393	-0.372	-0.374	-0.327	-0.351
R43	-0.279	0.007	-0.121	-0.531	-0.455
R44	-0.102	-0.182	-0.223	-0.024	-0.106
R45	0.294	0.437	0.409	0.239	0.244
R46	0.557	0.347	0.481	0.745	0.671
R47	-0.645	-0.258	-0.522	-0.526	-0.624
HT	0.288	-0.034	0.168	0.208	0.371
LV	0.209	-0.187	0.049	0.203	0.298

	R36	R37	R38	R39	R40
R36	1.000				
R37	0.904	1.000			
R38	0.746	0.681	1.000		
R39	0.797	0.812	0.920	1.000	
R40	0.058	0.202	-0.094	0.087	1.000
R41	-0.505	-0.488	-0.345	-0.335	-0.001
R42	-0.721	-0.654	-0.264	-0.321	0.018
R43	-0.093	-0.121	-0.110	-0.219	-0.299
R44	-0.032	-0.097	0.210	0.160	0.086
R45	0.676	0.620	0.402	0.422	-0.115
R46	0.616	0.623	0.436	0.568	0.300
R47	-0.420	-0.530	-0.295	-0.470	-0.467
HT	0.201	0.285	0.023	0.097	0.455
LV	0.170	0.160	-0.088	-0.013	0.386

	R41	R42	R43	R44	R45
R41	1.000				
R42	0.597	1.000			
R43	-0.111	-0.231	1.000		
R44	-0.093	0.211	-0.204	1.000	
R45	-0.638	-0.845	0.328	0.068	1.000
R46	-0.354	-0.378	-0.693	0.202	0.384
R47	0.147	0.169	0.182	0.069	-0.123
HT	-0.219	-0.187	-0.121	-0.095	0.070
LV	0.006	-0.144	-0.129	0.104	0.126

	R46	R47	HT	LV
R46	1.000			
R47	-0.346	1.000		
HT	0.234	-0.358	1.000	
LV	0.231	-0.381	0.170	1.000

FREQUENCY TABLE

	R1	R2	R3	R4	R5
R1	77				
R2	77	77			
R3	77	77	77		
R4	74	74	74	74	
R5	77	77	77	74	77
R6	77	77	77	74	77
R7	77	77	77	74	77
R8	77	77	77	74	77
R9	77	77	77	74	77
R10	77	77	77	74	77
R11	77	77	77	74	77
R12	77	77	77	74	77
R13	74	74	74	74	74
R14	77	77	77	74	77
R15	77	77	77	74	77
R16	76	76	76	74	76
R17	77	77	77	74	77
R18	77	77	77	74	77
R19	77	77	77	74	77
R20	77	77	77	74	77
R21	77	77	77	74	77
R22	77	77	77	74	77
R23	77	77	77	74	77
R24	77	77	77	74	77
R25	77	77	77	74	77
R26	77	77	77	74	77
R27	77	77	77	74	77
R28	77	77	77	74	77
R29	77	77	77	74	77
R30	77	77	77	74	77
R31	77	77	77	74	77
R32	77	77	77	74	77
R33	77	77	77	74	77
R34	74	74	74	74	74
R35	74	74	74	74	74
R36	77	77	77	74	77
R37	77	77	77	74	77
R38	77	77	77	74	77
R39	77	77	77	74	77
R40	77	77	77	74	77

	R1	R2	R3	R4	R5
R41	77	77	77	74	77
R42	77	77	77	74	77
R43	74	74	74	74	74
R44	77	77	77	74	77
R45	77	77	77	74	77
R46	74	74	74	74	74
R47	77	77	77	74	77
HT	71	71	71	68	71
LV	72	72	72	69	72
	R6	R7	R8	R9	R10
R6	77				
R7	77	77			
R8	77	77	77		
R9	77	77	77	77	
R10	77	77	77	77	77
R11	77	77	77	77	77
R12	77	77	77	77	77
R13	74	74	74	74	74
R14	77	77	77	77	77
R15	77	77	77	77	77
R16	76	76	76	76	76
R17	77	77	77	77	77
R18	77	77	77	77	77
R19	77	77	77	77	77
R20	77	77	77	77	77
R21	77	77	77	77	77
R22	77	77	77	77	77
R23	77	77	77	77	77
R24	77	77	77	77	77
R25	77	77	77	77	77
R26	77	77	77	77	77
R27	77	77	77	77	77
R28	77	77	77	77	77
R29	77	77	77	77	77
R30	77	77	77	77	77
R31	77	77	77	77	77
R32	77	77	77	77	77
R33	77	77	77	77	77
R34	74	74	74	74	74
R35	74	74	74	74	74
R36	77	77	77	77	77
R37	77	77	77	77	77
R38	77	77	77	77	77
R39	77	77	77	77	77
R40	77	77	77	77	77
R41	77	77	77	77	77
R42	77	77	77	77	77

	R6	R7	R8	R9	R10
R43	74	74	74	74	74
R44	77	77	77	77	77
R45	77	77	77	77	77
R46	74	74	74	74	74
R47	77	77	77	77	77
HT	71	71	71	71	71
LV	72	72	72	72	72
	R11	R12	R13	R14	R15
R11	77				
R12	77	77			
R13	74	74	74		
R14	77	77	74	77	
R15	77	77	74	77	77
R16	76	76	74	76	76
R17	77	77	74	77	77
R18	77	77	74	77	77
R19	77	77	74	77	77
R20	77	77	74	77	77
R21	77	77	74	77	77
R22	77	77	74	77	77
R23	77	77	74	77	77
R24	77	77	74	77	77
R25	77	77	74	77	77
R26	77	77	74	77	77
R27	77	77	74	77	77
R28	77	77	74	77	77
R29	77	77	74	77	77
R30	77	77	74	77	77
R31	77	77	74	77	77
R32	77	77	74	77	77
R33	77	77	74	77	77
R34	74	74	74	74	74
R35	74	74	74	74	74
R36	77	77	74	77	77
R37	77	77	74	77	77
R38	77	77	74	77	77
R39	77	77	74	77	77
R40	77	77	74	77	77
R41	77	77	74	77	77
R42	77	77	74	77	77
R43	74	74	74	74	74
R44	77	77	74	77	77
R45	77	77	74	77	77
R46	74	74	74	74	74
R47	77	77	74	77	77
HT	71	71	68	71	71
LV	72	72	69	72	72

	R16	R17	R18	R19	R20
R16	76				
R17	76	77			
R18	76	77	77		
R19	76	77	77	77	
R20	76	77	77	77	77
R21	76	77	77	77	77
R22	76	77	77	77	77
R23	76	77	77	77	77
R24	76	77	77	77	77
R25	76	77	77	77	77
R26	76	77	77	77	77
R27	76	77	77	77	77
R28	76	77	77	77	77
R29	76	77	77	77	77
R30	76	77	77	77	77
R31	76	77	77	77	77
R32	76	77	77	77	77
R33	76	77	77	77	77
R34	74	74	74	74	74
R35	74	74	74	74	74
R36	76	77	77	77	77
R37	76	77	77	77	77
R38	76	77	77	77	77
R39	76	77	77	77	77
R40	76	77	77	77	77
R41	76	77	77	77	77
R42	76	77	77	77	77
R43	74	74	74	74	74
R44	76	77	77	77	77
R45	76	77	77	77	77
R46	74	74	74	74	74
R47	76	77	77	77	77
HT	70	71	71	71	71
LV	71	72	72	72	72

	R21	R22	R23	R24	R25
R21	77				
R22	77	77			
R23	77	77	77		
R24	77	77	77	77	
R25	77	77	77	77	77
R26	77	77	77	77	77
R27	77	77	77	77	77
R28	77	77	77	77	77
R29	77	77	77	77	77
R30	77	77	77	77	77
R31	77	77	77	77	77
R32	77	77	77	77	77

	R21	R22	R23	R24	R25
R33	77	77	77	77	77
R34	74	74	74	74	74
R35	74	74	74	74	74
R36	77	77	77	77	77
R37	77	77	77	77	77
R38	77	77	77	77	77
R39	77	77	77	77	77
R40	77	77	77	77	77
R41	77	77	77	77	77
R42	77	77	77	77	77
R43	74	74	74	74	74
R44	77	77	77	77	77
R45	77	77	77	77	77
R46	74	74	74	74	74
R47	77	77	77	77	77
HT	71	71	71	71	71
LV	72	72	72	72	72

	R26	R27	R28	R29	R30
R26	77				
R27	77	77			
R28	77	77	77		
R29	77	77	77	77	
R30	77	77	77	77	77
R31	77	77	77	77	77
R32	77	77	77	77	77
R33	77	77	77	77	77
R34	74	74	74	74	74
R35	74	74	74	74	74
R36	77	77	77	77	77
R37	77	77	77	77	77
R38	77	77	77	77	77
R39	77	77	77	77	77
R40	77	77	77	77	77
R41	77	77	77	77	77
R42	77	77	77	77	77
R43	74	74	74	74	74
R44	77	77	77	77	77
R45	77	77	77	77	77
R46	74	74	74	74	74
R47	77	77	77	77	77
HT	71	71	71	71	71
LV	72	72	72	72	72

	R31	R32	R33	R34	R35
R31	77				
R32	77	77			
R33	77	77	77		
R34	74	74	74	74	
R35	74	74	74	74	74
R36	77	77	77	74	74
R37	77	77	77	74	74
R38	77	77	77	74	74
R39	77	77	77	74	74
R40	77	77	77	74	74
R41	77	77	77	74	74
R42	77	77	77	74	74
R43	74	74	74	74	74
R44	77	77	77	74	74
R45	77	77	77	74	74
R46	74	74	74	74	74
R47	77	77	77	74	74
HT	71	71	71	68	68
LV	72	72	72	69	69

	R36	R37	R38	R39	R40
R36	77				
R37	77	77			
R38	77	77	77		
R39	77	77	77	77	
R40	77	77	77	77	77
R41	77	77	77	77	77
R42	77	77	77	77	77
R43	74	74	74	74	74
R44	77	77	77	77	77
R45	77	77	77	77	77
R46	74	74	74	74	74
R47	77	77	77	77	77
HT	71	71	71	71	71
LV	72	72	72	72	72

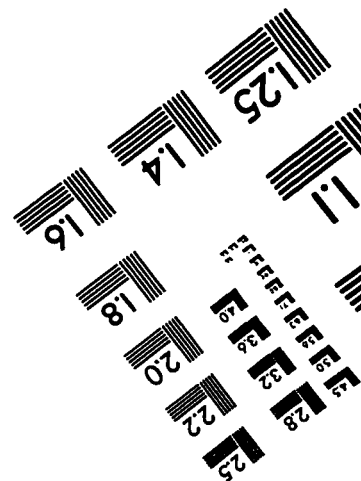
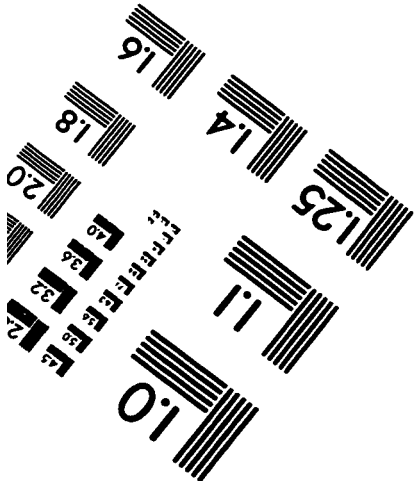
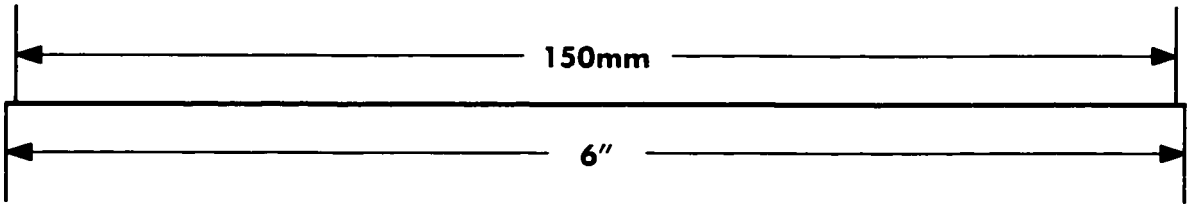
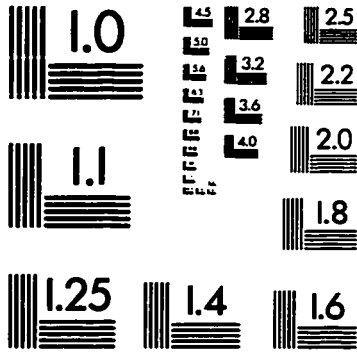
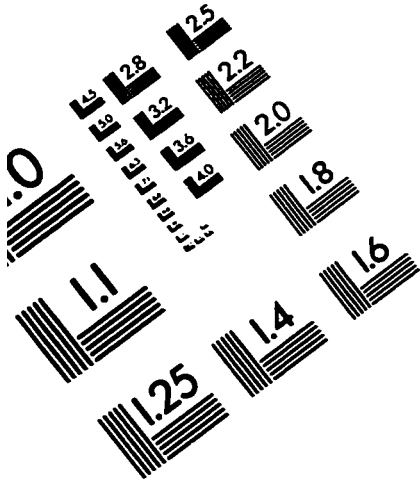
	R41	R42	R43	R44	R45
R41	77				
R42	77	77			
R43	74	74	74		
R44	77	77	74	77	
R45	77	77	74	77	77
R46	74	74	74	74	74
R47	77	77	74	77	77
HT	71	71	68	71	71
LV	72	72	69	72	72

	R46	R47	HT	LV
R46	74			
R47	74	77		
HT	68	71	71	
LV	69	72	68	72

VITA

David H. Backus received a Bachelor of Arts degree in geology from Haverford College in Haverford, PA in 1982. Before beginning graduate school in 1990, he worked in the Museum of Comparative Zoology at Harvard University as an Assistant Curator of Mollusks and as Research Assistant to Dr. Stephen J. Gould. He received his Master of Science degree in geology at the University of Washington in 1994.

IMAGE EVALUATION TEST TARGET (QA-3)



APPLIED IMAGE . Inc
1653 East Main Street
Rochester, NY 14609 USA
Phone: 716/482-0300
Fax: 716/288-5989

© 1993, Applied Image, Inc., All Rights Reserved